personal buildup for

Force Motors Ltd.

MTZ worldwide 1/2011, as epaper released on 16.12.2010
http://www.mtz-worldwide.com

content:

www.MTZonline.com

MTZ WORLDWIDE

01 January 2011 | Volume 72

SIMULATION of the Compressor Performance of Exhaust Gas Turbochargers

ACTIVE High-EGR Concept

OPTIMIZATION Criteria for Ignition Timing Calibration of Advanced SI Engines

OPTIMIZED MIXTURE FORMATION
THROUGH INNOVATIVE INJECTION TECHNOLOGY

CONTENTS

COVER STORY

OPTIMIZED MIXTURE FORMATION THROUGH INNOVATIVE INJECTION TECHNOLOGY

4, 10 I Denso presents its fourth-generation diesel common rail system for passenger cars, trucks and off-road applications. The automotive supplier has increased fuel injection pressures in cars to 2500 bar, and pressures of up to 3000 bar are being examined for commercial vehicle applications. L'Orange has developed a new heavy oil common rail injection system designed for an increase in pressure to 1800 bar. A special feature of this system is the storage volume integrated into individual reservoirs in the injectors.

COVER FIGURE © Denso **FIGURE ABOVE** © Delphi

NEW IMPETUS

Dear Reader,

We can now look back on an exciting 2010. Not only because the economy showed a surprisingly strong upward trend in many areas, but also because considerable technical changes were underway. In powertrain engineering in particular, the industry was in an almost experimental mood. And not without reason, as the policy of electromobility has become more embedded in the customer's perception, thus increasing the pressure to respond.

Now, following an initial stormy reaction by the industry, the hype is starting to ease off. With the same seriousness but with more care, electrification is now being applied to the powertrain. And a reassessment of the internal combustion engine is taking place. As far as electric drive systems and internal combustion engines are concerned, it is no longer a question of either/or. Instead, the focus is on further optimising the internal combustion engine, the drive system that currently makes more sense both technically and economically, while at the same time using the benefits of electrification and establishing an efficient overall system step by step.

This is resulting in many new ideas, many different philosophies for powertrain configurations and a great need for communication among developers. These are three aspects that we welcome, as they produce extremely exciting discussions and valuable material for our technical magazines and conferences. Our industry is picking up momentum once again, and we are starting the New Year with a good deal of confidence and expectation that we will once again see innovative solutions for the drivetrain of the future.

A personal exchange of ideas remains a vitally important aspect for us, as it ensures that we maintain a broad horizon and identify key issues. I had the pleasure of meeting some of you in person last year. And I am looking forward to further interesting meetings and constructive discussions. We will have an ideal opportunity for this right at the beginning of the year: at the MTZ Conference "The Drivetrain of Tomorrow", which will take place on 25 and 26 January in Wolfsburg.

I wish you a relaxing New Year and all the best for 2011.

Ihr

RUBEN DANISCH, Vice Editor-in-Chief
Wiesbaden, 3 December 2010

3000 BAR COMMON RAIL SYSTEM

As a breakthrough technology to reverse the trend of increasingly complex systems, Denso successfully developed the 4th generation common rail system. This paper describes the potential of the system and discusses the possibility of meeting the future requirements of diesel engines.

AUTHORS

YUKIHIRO SHINOHARA
is General Manager Diesel Injection Product Division at the Denso Corporation in Kariya (Japan).

KATSUHIKO TAKEUCHI
is Senior Manager Diesel System Development Center Diesel Injection Engineering Dept. 1 at the Denso Corporation in Kariya (Japan).

DR. OLAF ERIK HERRMANN
is Project Leader Advanced Diesel Engineering at the Denso Automotive Deutschland GmbH in Wegberg (Germany).

DR. HERMANN JOSEF LAUMEN
is Senior Technical Specialist Diesel Injection Systems at the FEV Motorentechnik GmbH in Aachen (Germany).

CHALLENGES FOR DIESEL DEVELOPMENT

Powertrain solutions for future mobility have a major role to play in global environment protection and energy saving. The development of gasoline direct injection, gasoline hybrid and other CO_2 reduction technologies was rapidly accelerated, particularly in the last few years. Highly efficient diesel engines have become popular for passenger car applications and are the indispensable powertrain in the fields of logistics, construction and agriculture sectors that underpin today's society. However, in order to comply with the increasingly stringent emissions regulations, diesel systems have become larger and more complicated, including aftertreatment systems such as De-NO_x Cat.

The history of diesel engine development is that of development of technologies to comply with emission regulations, whilst simultaneously adding value for the end customers. In order to meet these regulations, diesel power train technologies have become more advanced. However, at present the industry does not have a single, well-established approach for every kinds of application, and instead is trying to implement various approaches like those shown in ❶.

DENSO'S APPROACH

Denso considers two concepts to be essential to reduce emissions in compliance with the regulations, to enhance fuel efficiency and add value for the end customers.

: Maximize the potential of the fuel injection system and realize a pressure of 3000 bar
: Accurate and fully flexible injection patterns over product lifetime: Robust accurate multiple injection quantities over the product lifetime via the world's first closed-loop control: "intelligent Accuracy Refinement Technology"

To realize this approach, Denso developed the 4th generation common rail system, shown in ❷. To achieve 3000 bar injection pressure, the injector with solenoid-control achieves zero static leakage, which also improves fuel economy and FIE robustness. To achieve a closed-loop fuel injection control, the injector has a built-in pressure sensor to detect the fuel injection rate directly. Realizing the above concepts, the 4th generation common rail system contributes to the achievement of Euro 6 and Tier 4f regulations without a DeNO_x catalyst, which is a key for simplifying diesel systems in various applications.

As also shown in ②, 3000 bar and i-Art are the first steps towards significant re-simplification of the diesel engine: known as the "diesel revolution". Denso's 4th generation solenoid system, capable of 2500 bar, will be released in 2013 and with up to 3000 bar in 2015. Denso will be releasing i-Art in 2012. Mass production of the 3000 bar system and i-Art is a further step towards increased usage of closed loop combustion control algorithms. The

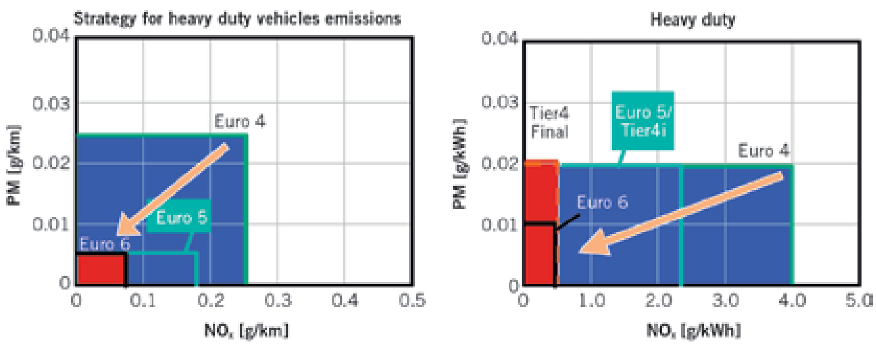

	Injection	Air/EGR	Aftertreatment
Euro 4/5	1800 to 2000 bar	TCI, VNT, HP-EGR	DOC, DPF
Euro 6	2000 to 3000 bar	TCI, 1 or 2 stage TC, HP or LP-EGR	DOC, DPF, SCR, LNT

❶ Emission strategies for diesel engines

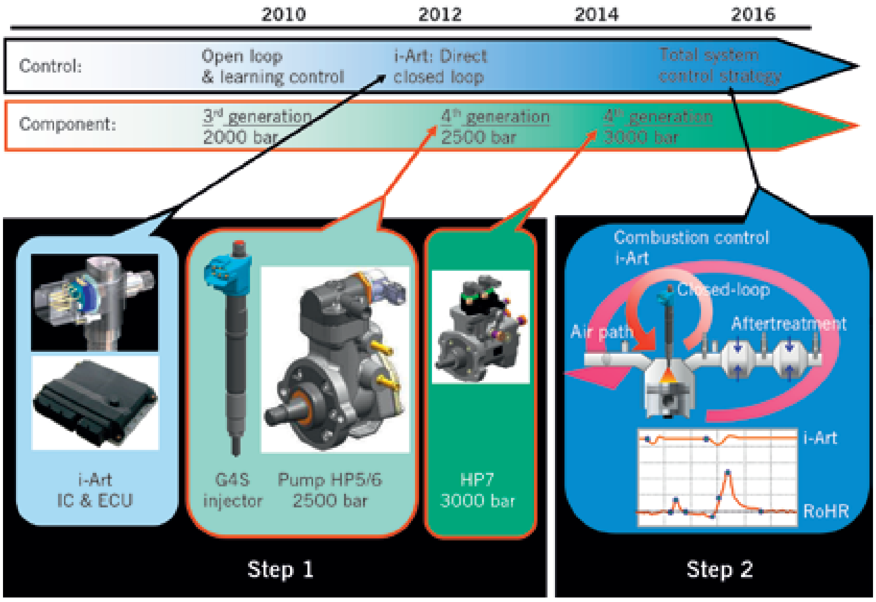

❷ Denso 4th generation common rail system

so-called "total system strategy" will be the second phase of the diesel revolution. This will help to drastically re-simplify the diesel engine, in order to ensure it remains attractive through these two revolutions.[1]

CONCEPT OF 3000 BAR COMMON RAIL SYSTEM

Since the first mass produced Common Rail Systems (1200 bar in 1995), the injection pressure has been continuously increased. ❸ shows the benefit of stronger penetration of the spray vapour phase and the improved spray-to-air mixing. This in combination with combustion optimization leads to improved air utilization (less rich areas during combustion), ③. To achieve an engine-out NO_x level as required for Tier 4f/Euro 6, EGR rates above 40 % will be required. To maintain a relative A/F-ratio e. g. of 1.5 at 30 kW/L, the boost pressure then has to be increased up to 5 bar (absolute).

It is well established that increased boost pressure and, thus, cylinder charge density leads to less penetration and less air utilization. This explains the result in ③, in which fuel consumption and soot emissions increase dramatically with increased EGR and boost, even though the relative A/F-ratio has been kept constant. An increase in injection pressure up to 3000 bar helps to increase spray penetration and air utilisation, leading to a reduction in smoke emissions, in this case, by 40 %. Also, the injection duration and, thus, the combustion duration is shortened resulting in significantly improved fuel consumption – 800 bar injection pressure increase leads to a 5 % reduction in indicated fuel consumption.

❹ shows the improvement achieved by additional nozzle geometry optimization at the Tier 4f NO_x level (red). The base NO_x level of 1.2 g/kWh, which would require a NO_x aftertreatment efficiency of 70 % to achieve Tier 4f emission level, is shown in blue.

One reason for the PM improvement is an adjusted nozzle flow rate – increased injection pressure allows the reduction of the nozzle flow without disadvantages in fuel consumption. In this case, at the Tier 4f NO_x level and base relative air-fuel ratio ($\lambda \sim 1.5$) in the C100 mode, a reasonable soot level below 100 mg/kWh was achieved with an eight-hole nozzle. Further, in C100, an additional 30 % soot reduction could be achieved with post injection, after optimization of the post injection parameters.

From today's point of view, the efficient G4S 3000 bar system can contribute significantly to achieve Euro 6 or Tier 4f without $DeNO_x$ system, along with excellent fuel consumption. In combination with FEV's AHDCS combustion [3], an excellent part load soot level can also be achieved, leading to very low DPF soot loading levels for many applications. This will reduce the need for active regeneration to a minimum. In such a case, a simplified, more robust and more efficient diesel system will be attractive for the end users too.

If today's common approach of using an SCR system is selected, shown in ④ (blue lines), the usage of injection pres-

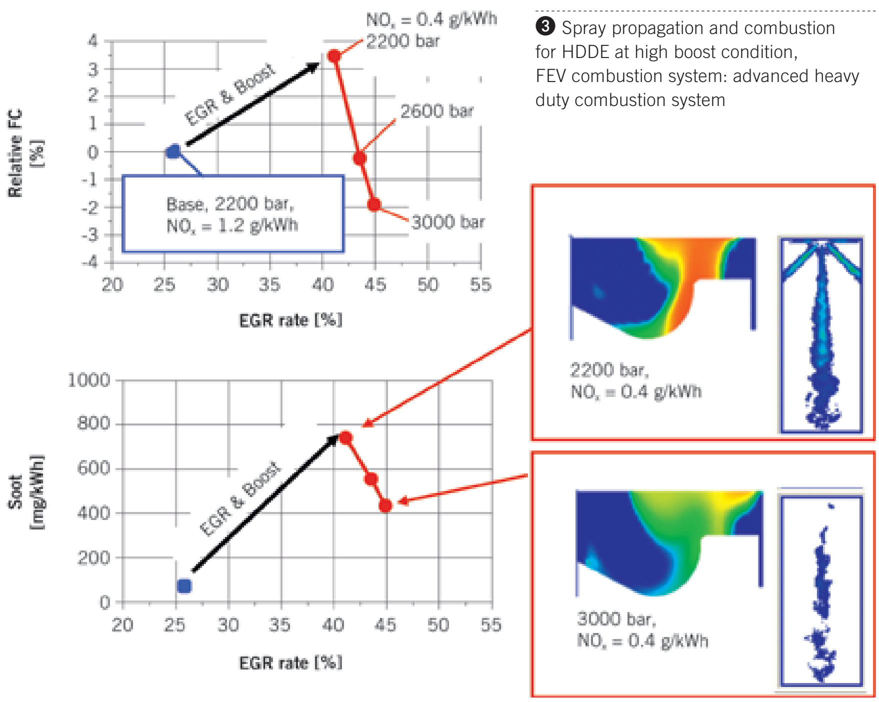

❸ Spray propagation and combustion for HDDE at high boost condition, FEV combustion system: advanced heavy duty combustion system

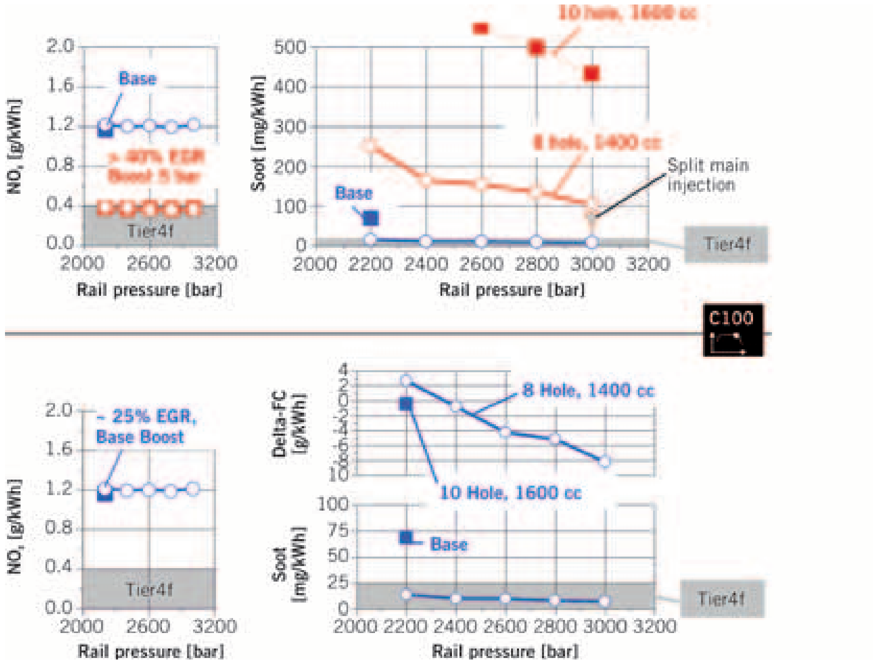

❹ Nozzle geometry tuning and injection pressure impact, 2.2 l single cylinder with AHDCS combustion

sures above 2500 bar, in combination with a reduced hydraulic flow nozzle, helps to significantly reduce soot emissions and improve fuel consumption. Therefore, increasing the injection pressure up to 3000 bar, even for a conventional low boost concept, will have additional fuel consumption benefits and/or offers further options to reduce NO_x levels and, thereby, reduces $DeNO_x$ efficiency requirements and urea consumption.

CONCEPT OF I-ART SYSTEM

Similar to heavy duty engines, various efforts have been made to increase common rail system pressure, and develop high-EGR and combustion technologies for passenger car diesel engines. In ❺, the complex technical challenge of reducing engine-out NO_x emissions, using conventional fuel-efficient combustion is summarized. To control soot, noise and NO_x, advanced multiple injection patterns are important to achieve lowest NO_x levels. There is a strong relationship between NO_x, CO and oxygen content in the exhaust gas (or in the engine intake). This relationship becomes stronger for Euro 6 applications without $DeNO_x$ system. Therefore, it is necessary not only to apply advanced injection patterns but also to ensure the accuracy of lambda (rel. air-fuel ratio) for the engine lifetime. This is determined by the supplied fresh air and in particular the injected fuel quantities over the whole engine map area.

In the future, Denso will adopt a very different approach to ensure the injection accuracy, even with multiple injections through a completely autonomous closed-loop injection control, i-Art. ❻ shows the i-Art injector, which has a built-in pressure sensor connected to the high pressure path. It detects the injection pressure trace during the injection event. In this way, the fuel injection rate can be detected, which is fed back to the ECU for comparison with the injection rate model values. Each injector has a memory chip that stores individual differences for each injector, in order to correct the injection model. This system structure, thus, enables high accuracy injection compensation throughout the lifetime of the engine.

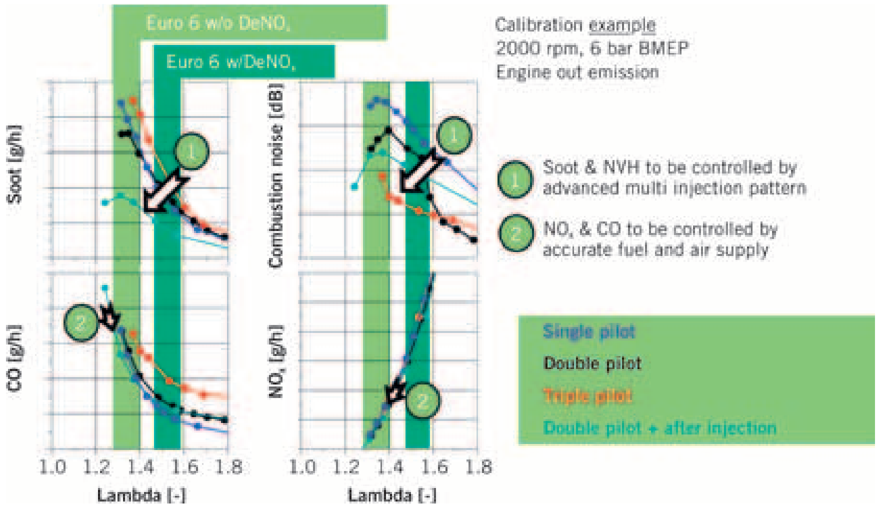

❺ Challenge of low NO_x Combustion, Passenger Car Diesel

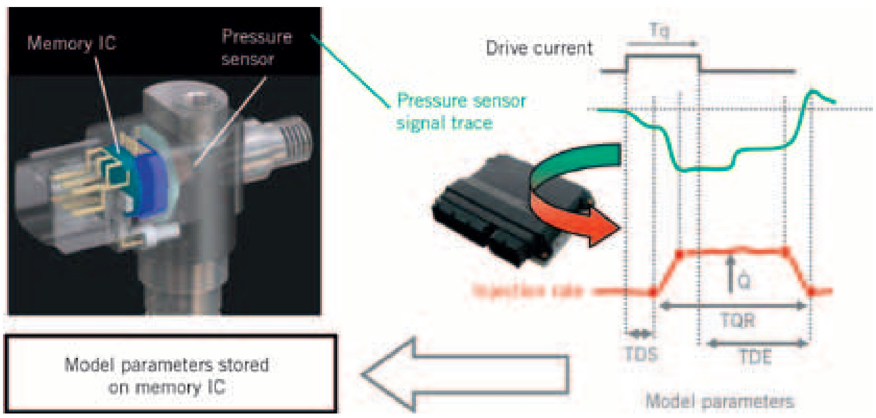

❻ Closed loop with i-Art

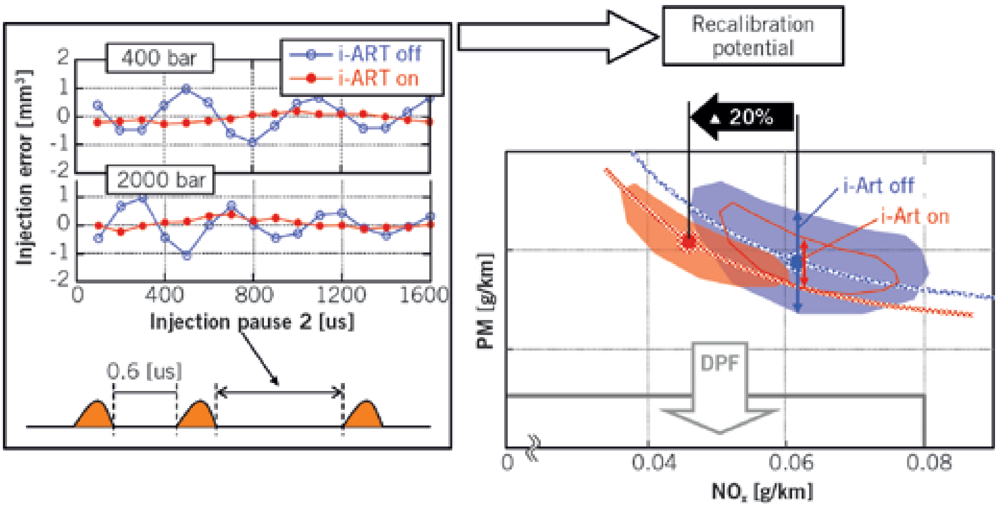

❼ Accuracy and emission potential with i-Art, recalibration-study, 1.6 t, 2.2 l

The accurate control of fuel injection quantities over the engine's lifetime not only achieves flexibility in emissions calibration, but also substantially reduces calibration efforts through flexible and accurate injections. In addition, its memory function is applied for OBD. It also elminates the need for end-of-line QR-Code programming. i-Art provides a wide variety of benefits. Denso will apply the i-Art system to all applications of 4th generation common rail system in the near future.

As shown in ❼, the application of beneficial complex injection patterns such as triple pilot injection can be freely calibrated without fuel quantity variances when changing injection intervals. Finally with i-Art an accuracy of better than 0.3 mm³ can be achieved for pilot injection quantities. This is independent of the calibrated intervals and rail pressures. This not only allows the calibration of more and smaller pilot quantities, but also the various post injection strategies needed for soot reduction or aftertreatment.

A potential scenario of simplification of a diesel system with NO_x aftertreatment is shown in ⑦. The increased injection quantity accuracy achieved by i-Art reduces the NO_x level by approximately 20 %, and as a result, either the SCR system can be dimensioned approximately 20 % smaller, or the ammonia trap catalyst can be eliminated. As just described, the use of i-Art offers the possibility of a simple, competitive and attractive diesel system [2].

CONCLUSION

This paper describes the innovations of Denso's new 4th generation diesel common rail system as a contributor to CO_2 emission reduction and a greener society. Closed loop injection control and ultra high efficient injection pressure generation are the features that help to meet future requirements for low emissions and excellent fuel efficiency. Ultra high injection pressure for heavy duty diesel engines has a significant potential to improve fuel consumption – an 800 bar injection pressure increase from 2200 bar to 3000 bar, on a single cylinder engine, delivers a 5 % fuel consumption benefit. Also, the potential to achieve Tier 4f or Euro 6 without complex NO_x aftertreatment could be demonstrated.

i-Art, the world's first closed-loop injection control for production applications, allows free calibration of the optimum injection patterns and strategies in the full engine map range. Beside this, there is potential to reduce emissions and reduce the engineering margins for NO_x and PM. Further, i-Art enables a reduction of at least 20 % in NO_x emissions. Thus, i-Art not only helps to re-simplify the diesel power train for passenger car and heavy duty applications but also helps in CO_2 reduction.

REFERENCES

[1] Miyaki, M.; Takeuchi, K.; Ishizuka, K.; Sasaki, S.: The Breakthrough of Common Rail System: Closed-loop Control Strategy Using Injector with Built-in Pressure Sensor. Wiener Motorensymposium 2009

[2] Wang, X.; Kikutani, T.; Takeuchi, K.; Nakane, N.: Development towards "Diesel Revolution" using ultra high pressure CRS with closed loop control system for heavy duty engine. Fisita, 2010

[3] Herrmann, O. E.; Ruhkamp, L.; Körfer, T.; Pischinger, S.; Schönfeld, S.: Possibilities for Optimization of Injection Parameters to improve Engine Performance of Heavy Duty and Industrial Engines. 11. Tagung "Der Arbeitsprozess des Verbrennungsmotors", 2007

THANKS

The Authors would like to thank Max Nakagawa, Denso Automotive Deutschland GmbH, and Vinod Rajamani, Lehrstuhl für Verbrennungskraftmaschinen, RWTH Aachen University, for their support.

NEW HEAVY FUEL OIL INJECTION SYSTEM

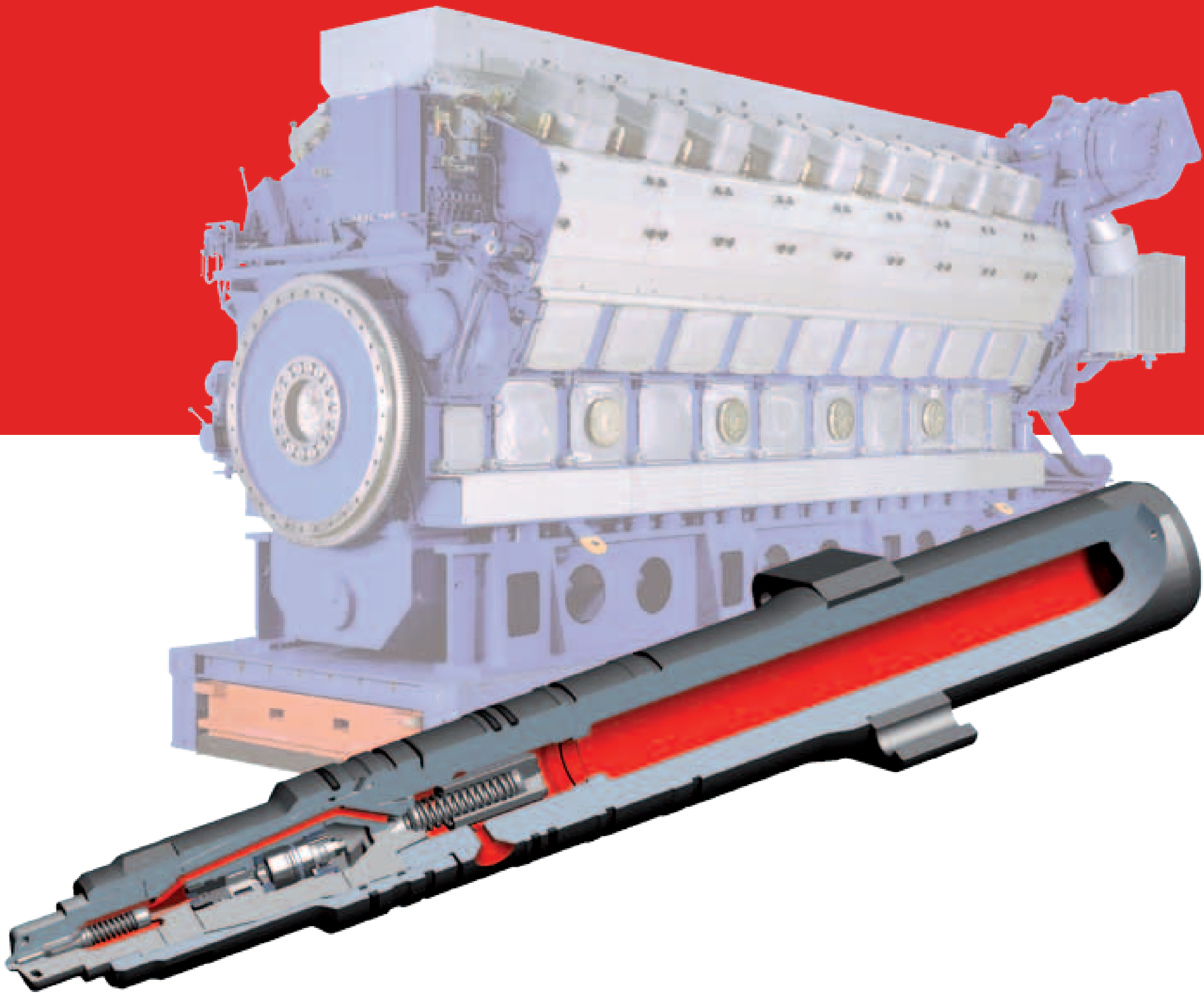

In 2001 Wärtsilä and L'Orange launched the first common rail injection system for heavy fuel oil applications on the Wärtsilä W32 engine. This common rail system is very complex and relatively slow, compared to the marine diesel common rail systems. The second generation of heavy fuel oil common rail systems will be improved regarding functionality, costs, lifetime and maintainability [1].

AUTHORS

CLEMENS SENGHAAS
is Director Research & Development at L'Orange GmbH in Stuttgart (Germany).

HARTMUT SCHNEIDER
is Senior Manager responsible for Advanced Development at L'Orange GmbH in Stuttgart (Germany).

STEFFEN REINHARD
is Test and Project Engineer in the Development Department at L'Orange GmbH in Stuttgart (Germany).

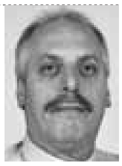

DAVE JAY
is Manager Fuel Injection Equipment at Wärtsilä in Vaasa (Finland).

KENNETH EHRSTRÖM
is Project Manager for the W32CR-Injection System at Wärtsilä in Vaasa (Finland).

CHALLENGES FOR MARINE APPLICATIONS

Apart from the well-known requirements such as the reduction of fuel consumption, and of costs, as well as the increase of TBO-times, the focus of the development of large engines still is on reduction of emissions. As far as marine applications are concerned, this is mainly valid for the reduction of nitrogen oxides. The driving forces in this context are Marpol-Exhaust-Emission-Regulation [2] with IMO Tier 2, a reduction by 20 % by 2011, and then IMO Tier 3, with a reduction by 80 % by 2016.

It will be a great challenge to reach IMO Tier 3 without any exhaust after-treatment only by making engine modifications. High potential arises from the further development of the fuel injection system. One successful way for the medium-speed engines is the common rail system. L'Orange and Wärtsilä jointly develop a second generation HFO fuel injection system for the Wärtsilä W32 Common Rail engine. Today, PLN injection systems or common rail systems of the first generation are used on this engine.

INJECTION SYSTEM

The reduction of NO_x emissions as well as of particulate emissions requires multiple injections, higher system pressure and better repeat accuracy. Additionally the system must be robust and suitable for operation on diesel and on all common heavy fuel oils with viscosities up to 700 cst at 50 °C. This means fuel temperatures of up to 150 °C.

One of the targets of development is a maximum system pressure of 1800 bar. In the first step, it will be only 1500 bar for the Tier 2-applications, design and qualification will however already be made for 1800 bar. The chosen fuel injection system, ❶, is based on a concept for Diesel applications which is in serial production on the MTU series 4000 since 2007. It consists of one or, if necessary for redundancy, of two high-pressure pumps for pressure generation, of one distributor rail with outlets to the injectors and of the injectors themselves. In contrast to HFO common rail systems existing up to now, the accumulator volume is now integrated no longer in the rail but, for reasons of performance in the injector.

On the distributor rail you will also find the pressure sensors, the circulation valve, which is necessary for heavy fuel oil operation during engine standby operation, and the safety valve (PDSV – Pressure Drop Safety Valve). The tasks of the safety valve are to avoid too high system pressures, to offer a limp-home function and the possibility to stop the engine with compressed air [3]. These components are approved L'Orange standard components, i.e. further developments only have to be adjusted to the special requirements of the respective engine type. Thus, development costs and times can be reduced considerably.

For safety reasons, all lines are double-walled. Detectors to find leakages or locations of leakages are integrated in the rail connection cast housings. The high pressure pump is based on the well-known standard high pressure pump of L'Orange [4]. The pump lubricated by engine oil is available in in-line version with two and also with four cylinders depending on the

❶ Layout fuel injection system

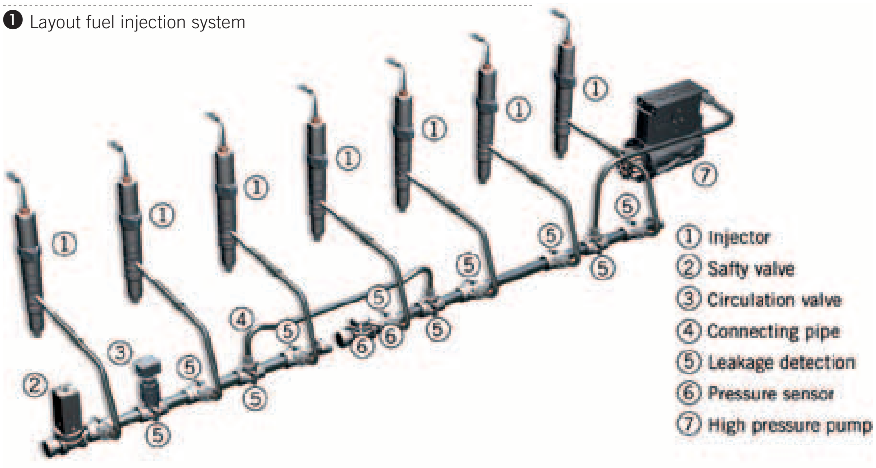

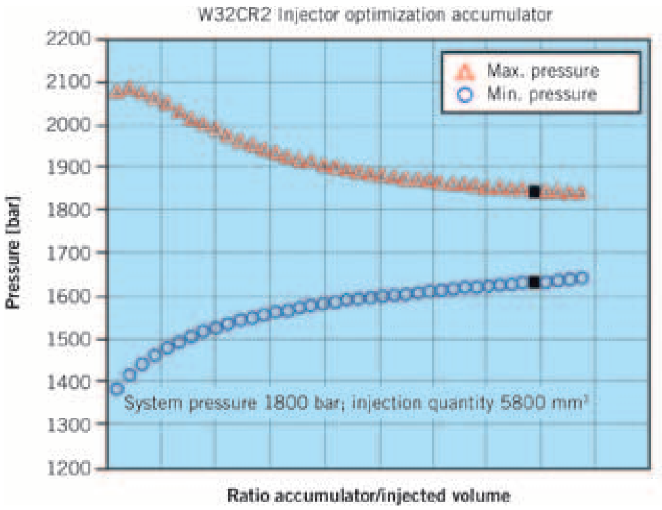

❷ Influence of accumulator size on pressure waves

delivery rate which is required. To achieve best possible efficiency, the pump has suction throttle control. In contrast to the pump which is used for diesel applications, the HFO pump has an additional segregation of fuel and engine oil in order to avoid lacquering. The delivery rates at 1800 bar are 29.5 l/min at nominal speed for the four-cylinder pump during HFO operation and 25.5 l/min during diesel operation.

The novelty of the fuel injection system mainly comes from the injector. As already described, this injection system does not have the accumulator-rail or any external accumulator any more but an accumulator which is now integrated in the injector. Thus, pressure peaks as well as pressure drops during injection can be reduced drastically. This has a positive effect on the stress the components are exposed to. It means that with the same design and the same kind of materials used, higher system pressures can be realised. On the other hand, a much more stable operation in the case of multiple injections can be guaranteed by avoiding strong pressure fluctuations and thus fluctuations in delivery quantities.

To further improve quantity stability and switching speed of the injector, the inertia of the system has been reduced by placing pilot valve and solenoid close to the nozzle. Solenoid and nozzle are cooled via an additional engine oil cooling circuit for operation on fuel temperatures of up to 150 °C. By specific selection of materials and coatings of movable parts, operation on the required types of fuel is guaranteed.

Due to the fact that the accumulator volume is now integrated in the injector, the flow fuse had to be integrated into the injector which had been on the line to the injector before. Thus, discharging of the whole accumulator volume into the combustion chamber can be avoided in case of its activation in order to prevent permanent injection.

Apart from the advantages already described, the single-circuit injector in contrast to the two-circuit injector which is used today in the W32CR is much less complex and therefore offers considerable advantages regarding product costs and robustness.

DEVELOPMENT RESULTS

Extensive 1-D-hydraulic simulations were already made at the first design stage. Thus, the great variety of possible injector design versions could be reduced considerably already in an early development phase. The main focus is placed on the determination of an optimum accumulator size in the injector regarding damping of pressure waves, ❷, and manufacturability as well as regarding available space. The results of calculations were confirmed later on by function tests.

Despite extensive investigations at the preliminary stage of development (simulation and component testing), detailed hydraulic adjustment of the injector will also be necessary in the future.

Component tests at the L'Orange test rig enables us to provide proof of all functions requested from the injection system with all its components, such as the standby process, emergency stop and limp-home operation with the focus on injector functions.

By tests with different accumulator volumes in the injector considering different kinds of throttles and borehole cross-sections, the optimum solution regarding damping characteristics and available space

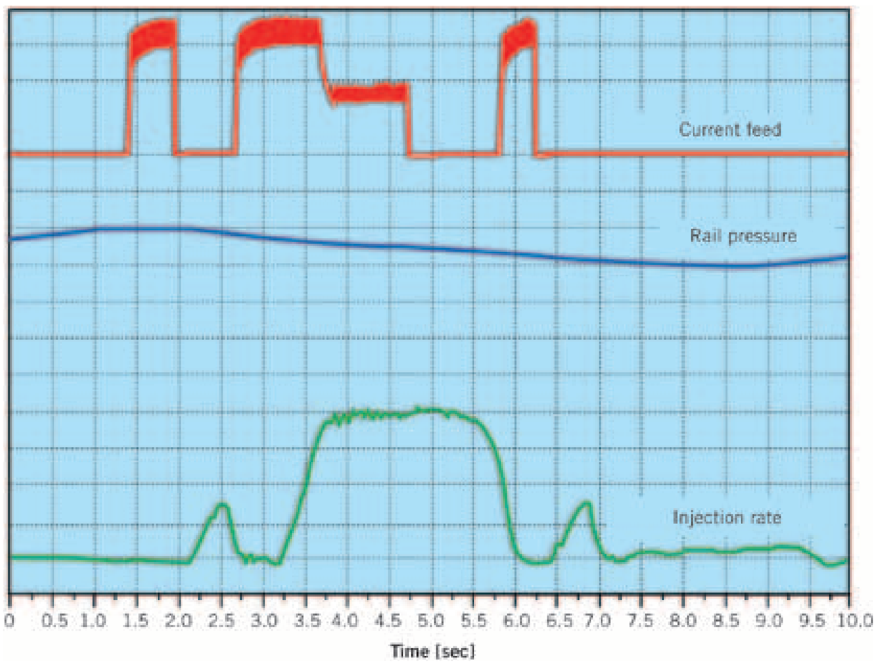

❸ Injection rate with mutiple injection

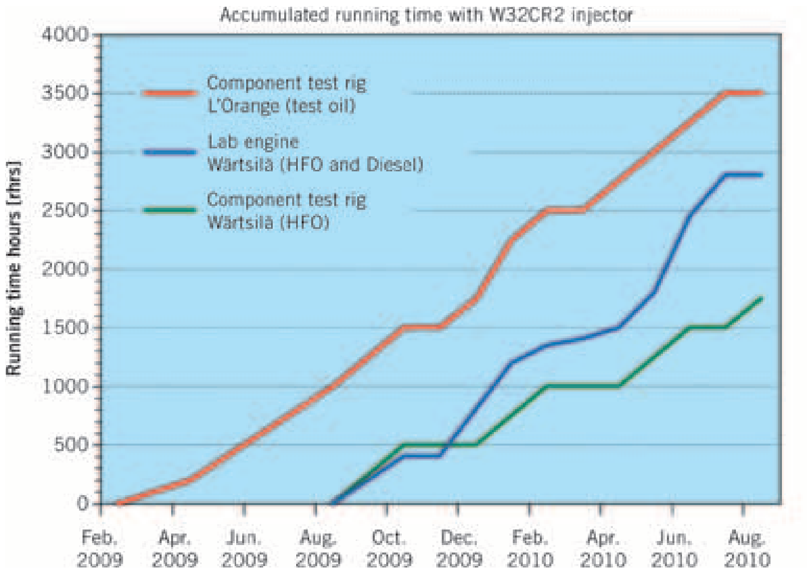

❹ Accumulated running time

determined by simulation could finally be confirmed. This showed that the injector concept with integrated accumulator is the way to success for the required performance data.

This is also what we can see from the test results regarding multiple injection capability, ❸. Both for pilot injection and for post injection, the quantities and distances to main injection are below the values required in the performance specifications. The variance of injection quantities for shot-to-shot and injector-to-injector could be reduced considerably compared with the system of the first generation.

In addition to the function tests, durability and leak-tightness were proved by tests on several test rigs. The L'Orange qualification process requires successful endurance tests for at least 1000 hrs considering the real engine load profile before giving release for engine tests. Additional overload tests with overpressure are also part of the qualification. The endurance tests were made on test rigs at L'Orange with test oil and on a similar test rig at Wärtsilä with Heavy Fuel Oil and Diesel, ❹.

Full functionality was still there after all these tests. All hydraulic values were even within the tolerances required for new parts, and all sealing points were still o.k. The inspection revealed most of the key components to be in excellent condition.

The control pin which releases the hydraulic pressure acting on top of the nozzle needle after solenoid activation, showed the largest wear. This is highly influenced by the selected testing conditions being more severe than the future field operation environment. The filtration has been only 30 microns (45 microns absolute) to promote maximum abrasive wear, and the testing pressure is 300 bar over the engine operation requirements. Tests on the engine with 10 microns (24 microns absolute) filtration showed excellent results, ❺, and therefore emphasize the importance of correct filtration on the final operational applications.

ENGINE RESULTS

The first engine tests with CR2 equipment started as injector tests on a current Wärtsilä 7L32CR engine in August 2009. One advantage with the new injector is excellent control of small injection quantities. This can be noticed as very stable injections at idle conditions and also with multiple injections.

With CR2 equipment specific fuel consumption can be reduced up to 3 % at same NO_x Tier 2 level as compared to CR1, ❻. One reason is the improved heat release. This can be achieved already with single injection events and 1500 bar rail pressure levels, with further potential improvement in the future with 1800 bar rail pressure utilisation.

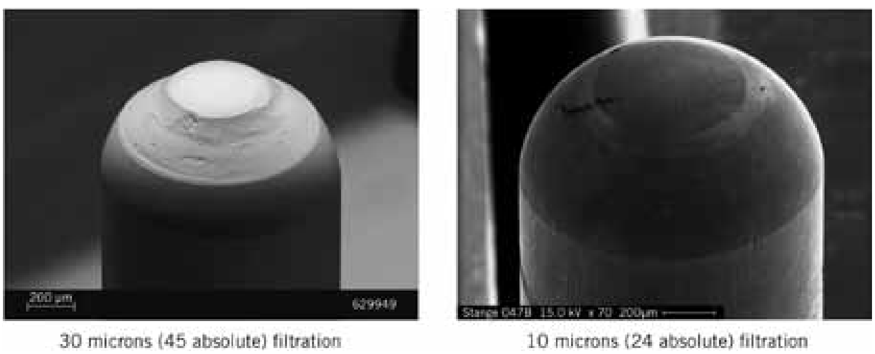

❺ Comparison of pilot valve pin after 500 hrs with different filtration

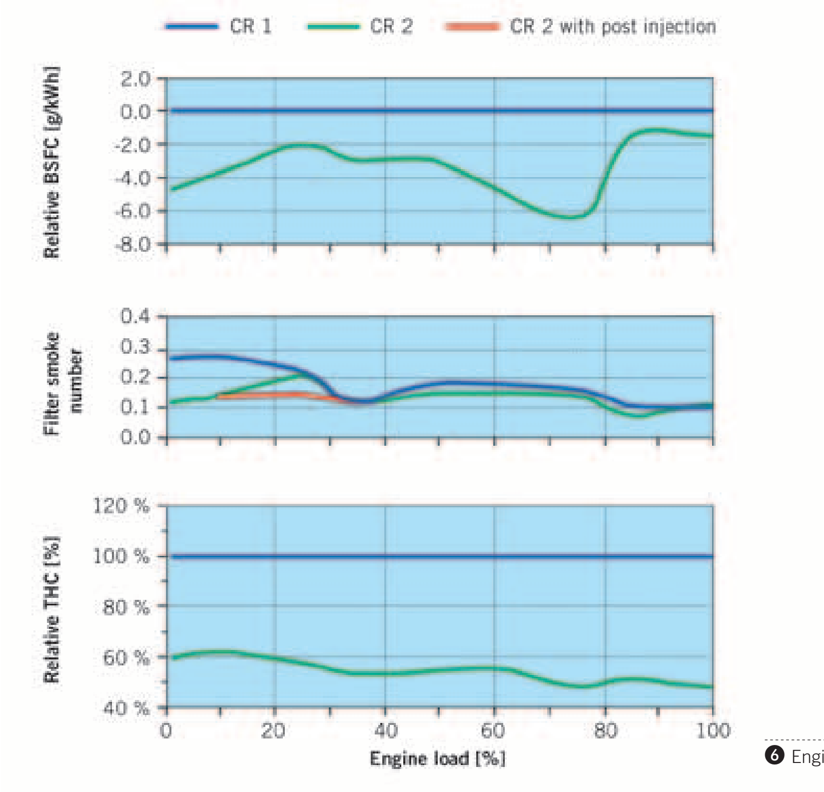

❻ Engine results

It also has been possible to reduce the already low smoke values that were achieved with CR1. The biggest improvement can be seen at very low load but there are improvements over the whole load range. This has given more possibilities to further optimise other load points with respect to emission and fuel consumption reductions. Similar to the fuel consumption there is potential for improvement with 1800 bar rail pressure.

Characteristic for the CR2 injectors is also that the total HC emissions are reduce remarkably. The THC emissions are up to 50 % lower compared to CR1 thanks to the smaller sac volume used.

The CR2 injectors have given the possibility to fully utilise multiple injections. A great part of the testing time has therefore been used for that mapping work. Post injections are good for smoke reduction at low loads since it increases the temperature in the combustion chamber during soot oxidation process. For this reason there is further potential regarding fuel consumption and smoke with multiple injection.

CONCLUSION

The results of the present development show the big potential of the new L'Orange fuel injection system. It is mainly the accumulator being integrated in the injector, the location of the pilot valve close to the nozzle and an optimised nozzle design which mark a distinctive progress over the HFO CR injection systems which are on the market today. Apart from functionality, the targets of reduced complexity and costs can also be reached. Despite the positive results up to now, final proof of robustness still has to be furnished by field tests. The field tests started in September 2010. The design of the injector offers the possibility to retrofit CR engines in the field without having to replace the whole system. The potential of pressure increase to 1800 bar already considered in design and testing lay the best possible foundations for the further development of the combustion process in order to reach emission stage IMO Tier 3 in connection with additional modifications inside the engine.

REFERENCES

[1] Senghaas, C.; Schneider; H.; Reinhard, S.; Jay, D.; Ehrström, K.: Second generation of HFO injection system for medium speed engines to fulfil future requirements. CIMAC Congress 2010, Bergen
[2] International Maritime Organization (IMO): Protocol of 1997 to amend Marpol 73/78, Annex VI of MARPOL 73/78 Regulations for the Prevention of Air Pollution from Ships and Final Act of the 1997
[3] Senghaas, C.; Altmann, O.; Schwalbe, M.; Jay, D.; Lehtonen, K.: Advanced technology for HFO injection systems developed for medium speed engines. CIMAC Congress 2007, Vienna
[4] Jorach, R. W.; Schneider, H.; Kerckhoff, A. J.; Altmann, O.: From high speed diesel to medium speed HFO engines – L'Orange platform based common rail pumps fulfill future demands. CIMAC Congress 2004, Kyoto

WWW.VIEWEGTEUBNER.DE

Gasoline Engines are the answer to the challenges of future

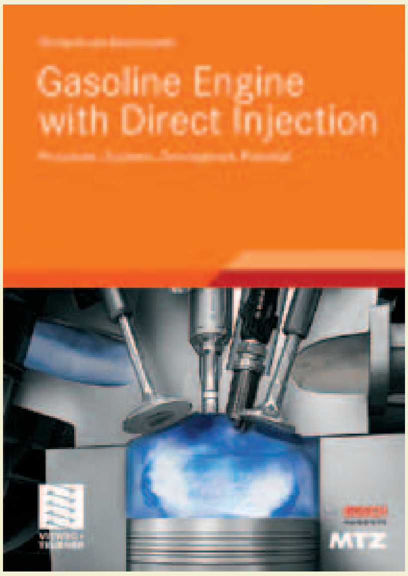

Richard van Basshuysen

Gasoline Engine with Direct Injection

Processes, Systems, Development, Potential

2009. xviii, 437 pp. With 399 Fig. Hardc. EUR 49,00
ISBN 978-3-8348-0670-3

Direct injection spark-ignition engines are becoming increasingly important, and their potential is still to be fully exploited. Increased power and torque coupled with further reductions in fuel consumption and emissions will be the clear trend for future developments. From today's perspective, the key technologies driving this development will be new fuel injection and combustion processes. The book presents the latest developments, illustrates and evaluates engine concepts such as downsizing and describes the requirements that have to be met by materials and operating fluids. The outlook at the end of the book discusses whether future spark-ignition engines will achieve the same level as diesel engines.

authors | editors

Dr.-Ing. E. h. Richard van Basshuysen was Head of Development for premium class vehicles and for engine and transmission development at Audi. Today, he is editor of the magazines ATZ and MTZ. The editor was supported by a distinguished team of authors consisting of 22 experts and scientists from industry and universities.

Please send me

____ Copies
Gasoline Engine with Direct Injection
ISBN 978-3-8348-0670-3
EUR 49,00
(+ shipping and handling)

Fax +49(0)611.7878-420

Company	Last name | First name	321 09 001
Department		
Street name	Postcode/Zip | City, Country	
Date | Signature		

TECHNIK BEWEGT.

VIEWEG+TEUBNER

SIMULATION OF THE COMPRESSOR PERFORMANCE OF EXHAUST GAS TURBOCHARGERS

Turbocharging is an important component of modern downsizing concepts. As an application example from BMW shows, the use of efficient CFD simulation already allows the steady-state performance of a compressor to be examined at an early stage of development.

AUTHORS

DIPL.-ING. (FH) THOMAS SAILER
is CFD Engineer in the Area of SI Engine Powertrain Development at the BMW Group in Munich (Germany).

DIPL.-ING. SAMUEL BUCHER
is CFD Engineer in the Area of SI Engine Powertrain Development at the BMW Group in Munich (Germany).

DR.-ING. BODO DURST
is Manager CAE Combustion in the Area of SI Engine Powertrain Development at the BMW Group in Munich (Germany).

DR.-ING. CHRISTIAN SCHWARZ
is Department Manager Thermodynamics, Turbocharging and Exhaust System in the Area of SI Engine Powertrain Development at the BMW Group in Munich (Germany).

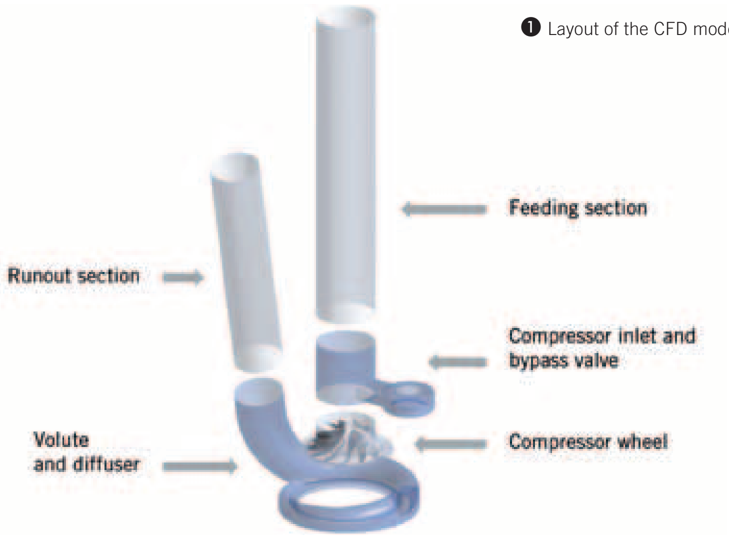

❶ Layout of the CFD model (exploded view)

EFFICIENTLY PERFORM THE SIMULATIONS REQUIRED

In view of the continuing discussion around the production of anthropogeneous CO_2, the concept of downsizing internal combustion engines promises a sustainable solution for closing the gap between consumption and performance. The optimisation of radial compressors – as the main components of turbochargers and co-determinants of Efficient Dynamics – is thus becoming increasingly important.

In this context, 3D CFD calculation represents a suitable tool for compressor development by virtue of the fact that internal flow structures can be visually represented in order to obtain a fundamental understanding of the process of compression and to determine the performance capability over the entire characteristic map. Thus, using 3D simulation it is possible, for example, to produce characteristic data maps for 1D gas exchange simulation before the turbocharger is available for real testing on the hot gas test bench.

The quality of the calculation results achievable with 3D CFD is on one hand mainly depending on the amount of work put into the simulation in order to produce the most accurate representation of reality by the model. On the other hand, the development loops necessary within a development process for volume production and the restricted time available only permit a limited degree of detail. Consequently, careful consideration is required as to how much time and effort is reasonable to efficiently perform the simulations required.

GEOMETRICAL LAYOUT OF THE CFD MODEL

A CFD model for a radial compressor can basically be divided into two sections, a static and a rotating section. The first of those includes the housing, which is made up of the compressor inlet, bypass valve, volute and diffuser. The housing geometry is extended by what are referred to as feeding and runout section by which, on the inlet side, an even flow rate can be achieved before entry into the compressor housing and, on the outlet side, the highly turbulent flow can settle on exit from the housing. This ensures that the parameters are not defined too close to the compressor, thereby influencing the solution too greatly. The rotating section comprises the compressor wheel, ❶.

The static section is computed in an absolute co-ordinate system and the rotating section in a relative co-ordinate system. At the interfaces between static and rotating computation sections, transfer of the flow variables is modelled by means of a “multiple frames of reference” approach. Most commercially available CFD programs offer a variety of options for this [1]. In this particular application, a frozen rotor interface has proved to be the most useful for the purpose of static analyses. With this definition, the position of the compressor wheel relative to the housing remains fixed/frozen and the rotational motion of the compressor wheel is taken into account by the co-rotating relative co-ordinate system. The advantages of this methodology are in its numerical robustness and speed of calculation. The disadvantage of the method is that the simulation results can be dependent on the position of the compressor wheel. However, for the variables of interest in the calculations performed in this case, the effect is negligible.

The geometrical position of the interfaces should be defined in such a way that they are not located in a vortex area created by flow detachment, as this would negatively affect the stability of the simulation.

COMPUTATIONAL GRID, BOUNDARY CONDITIONS AND SETTINGS

The reliability of a numerical simulation is strongly dependent on the existing mesh quality, i.e. on parameters such as grid angle, expansion ratio or aspect ratio of the control volumes. Another important feature for mesh generation is the resolution of the boundary layer. The resolution required varies according to the turbulence and wall function model applied. The results presented here are based on completely block-structured hexahedral meshes that produce good mesh quality combined with high computation efficiency and resolve the layers close to the wall well.

The aim of the boundary conditions and settings to be produced is to obtain a simulation set-up with which calculations can be performed across the entire characteristic map and the results produced correspond well with the test bench results. Herby, the aim is to determine the position and characteristic of

BOUNDARY CONDITIONS	
Model inlet	Pressure and temperature
Model outlet	Mass flow rate
Rotating domain	Turbocharger speed
SETTINGS	
Fluid	Air ideal gas
Turbulence	Shear-stress-transport (SST)
Advection scheme	High resolution
Heat transfer	Total energy

❷ Boundary conditions and settings for steady-state compressor simulation

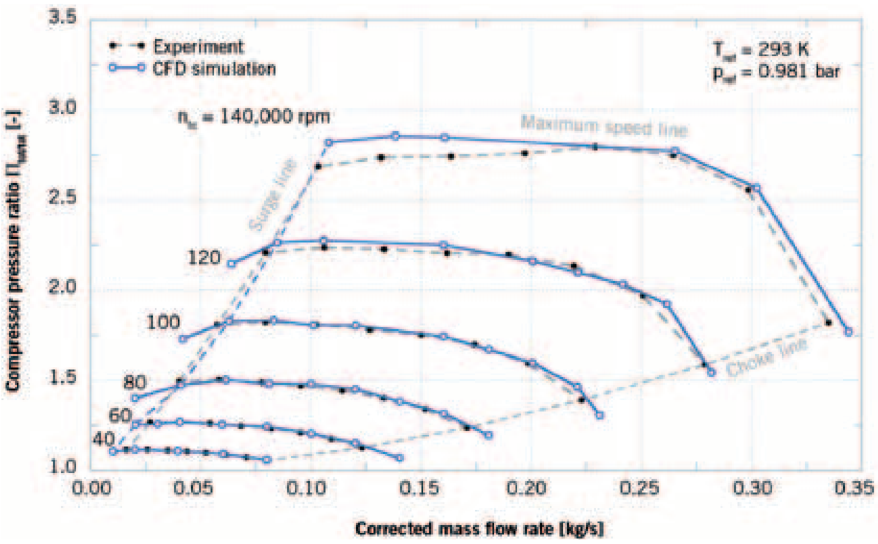

❸ Comparison of simulation and test-bench results for pressure ratios

the rotational speed curves, as well as the surge and choke lines.

The compressor housing temperature on the test bench is, firstly, affected by heat conductivity and radiation on the part of the turbine. Furthermore, there is a non-homogeneous temperature distribution pattern over the housing which can only be determined and subsequently specified as a parameter for the simulation with considerable time and effort. For this reason, the walls of the volute and the diffuser are defined as adiabatic.

The other boundary conditions and settings chosen for the steady-state compressor simulation are summarised in ❷ [2]. The numerical analyses are carried out with the CFD software package Ansys CFX 12.1.

COMPARISON WITH TEST BENCH DATA

❸ and ❹ show a comparison between experimental results and the results obtained from static 3D CFD computations. In them, the compressor mass flow corrected by reference quantities $\dot{m}_{kor}$, Eq. 1, is applied to the abscissa, and the total pressure ratio $\Pi_{tot/tot}$, Eq. 2, or the isentropic efficiency $\eta_{is,tot/tot}$, Eq. 3, applied to the ordinate. For the efficiency calculation based on simulation data, the definition independent of the temperature T_{t2} is used, as this is strongly dependent on the housing wall temperature and thus significantly complicates comparison with measured data.

Determination of the compressor characteristics based on test-bench results is generally subject to a variety of influencing factors. Thus, the attachment of the turbocharger to the test-bench peripherals, the measurement systems used and the nature and method of measurement have a significant effect [3]. Furthermore, CFD simulations are based on theoretical CAD data that does not necessarily perfectly match the real component produced.

POSITION AND CHARACTERISTIC OF ROTATIONAL SPEED CURVES

As is evident from ③, the pressure ratios produced by simulation and bench tests nevertheless match well in the lower and middle sections of the data map. Only at maximum speed there is a maximum deviation of approximately 5 % near the surge line and outside the area of relevance to the engine. This is attributable to the decline in the speed curve towards lower mass flow rates observed in the measurements, as consequently not every pressure ratio is definitely determined by a single mass flow and the CFD code thus has difficulty finding a steady state solution [4].

In the case of the efficiency levels in ④ as well, very good agreement is evident across broad areas of the data map despite the influencing factors previously referred to. The maximum deviation is around 5 % points in this case. Only in the lowest speed band around 40,000 rpm do the differences between simulation and bench tests rise to as much as 15 % points. It is, however,

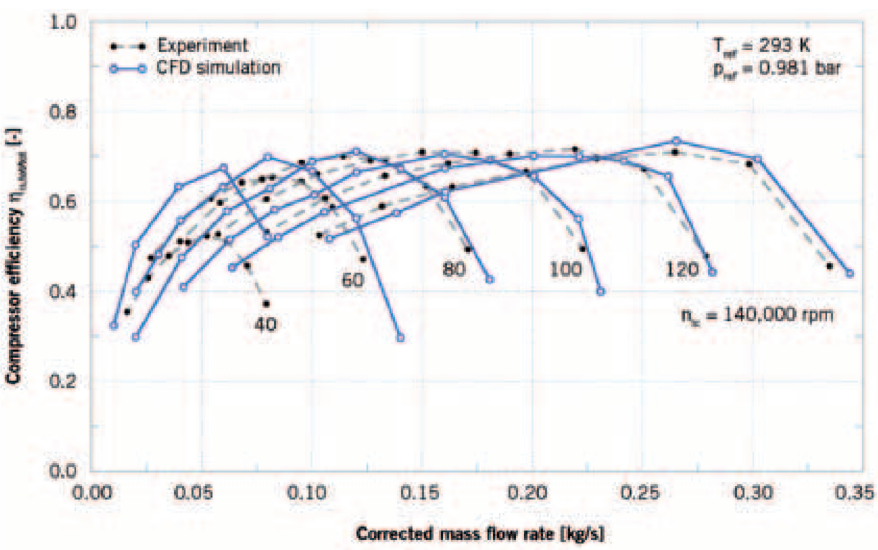

❹ Comparison of isentropic efficiency levels between CFD simulation and physical measurement

EQ. 1

$$\dot{m}_{kor} = \dot{m} \cdot \frac{p_{ref}}{p_1} \cdot \sqrt{\frac{T_1}{T_{ref}}}$$

EQ. 2

$$\Pi_{tot/tot} = \frac{p_{t2}}{p_{t1}}$$

EQ. 3

$$\eta_{is,tot/tot} = \frac{\Pi_{tot/tot}^{\frac{\kappa-1}{\kappa}} - 1}{\frac{T_{t2}}{T_{t1}} - 1} = \frac{\dot{m} \cdot c_p \cdot T_{t1} \cdot (\Pi_{tot/tot}^{\frac{\kappa-1}{\kappa}} - 1)}{Md \cdot \omega}$$

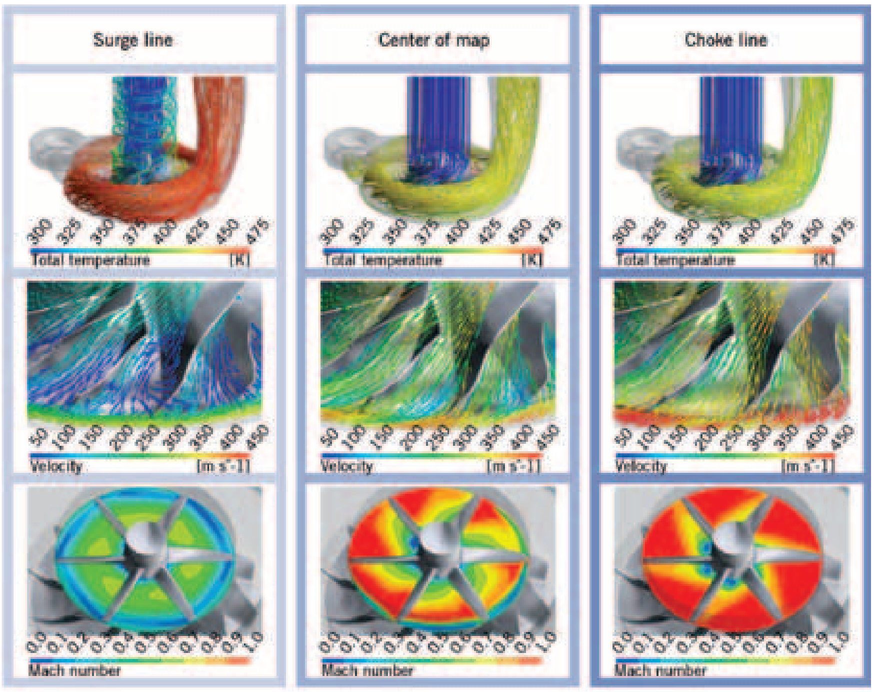

❺ Visual representation of compressor behaviour at different mass flow rates for a constant turbocharger speed (n_{TC} = 140,000 rpm)

sufficiently well known that in this area, the heat flux from turbine to compressor results in substantially lower isentropic compressor efficiency levels on the test bench and, therefore, should not be ignored [5, 6].

SURGE LINE

The surge line at the left-hand end of the speed curves, ③, is virtually identical with the pattern determined by measurement. The simulation results shown here are entirely based on steady state analyses which were terminated as soon as the solution started to show periodic convergence or the pressure ratio significantly dropped. Surging is a substantially transient phenomenon which results from the interaction between compressor and air ducting. The transient simulations actually required here are, however, extremely time-intensive, which is why the described pragmatic procedure is very attractive.

❺ visually illustrates the flow processes inside the radial compressor at different mass flow rates for a constant turbocharger speed n_{TC} of 140,000 rpm. Looking at the left hand side of the top row it can be seen from the streamlines shown that, adjacent to the wall, back-flow of already compressed and consequently heated air takes place near the surge line and manifests itself in a temperature rise at the compressor inlet. In addition, the generally higher temperature level in the outlet housing due to the greater compression at lower mass flow rates is noticeable. In the center of the data map and at the choke line, the inflow is more homogeneous.

The speed vectors in the middle row reveal the flow detachment in the compressor wheel caused by imperfect inflow at low throughput rates. Ultimately, this leads to the back-flow effects at the compressor wheel inlet already described, while at the other two load points, virtually constant through-flow and the increasing velocity level as the mass flow rises are identifiable.

CHOKE LINE

With regard to the position of the choke line it should be pointed out that its characteristic in the central and lower areas of the load map is not physically defined but rather determined by the efficiency level falling below a certain value. For that reason, a representation based on simulation data is dispensed with. The greatest possible throughput rate at the maximum turbocharger speed also corresponds very well with the figure measured.

In the bottom row of ⑤ the Mach number distribution in the compressor wheel's narrowest flow cross-section is shown in the form of a contour plot. It can be clearly seen that at the choke line the Mach number adopts a value of one across virtually the entire cross-section and thus the throughput rate cannot be further increased. If a higher mass flow rate is specified as a parameter, the simulation is aborted due to non-compliance with the continuity equation. The Mach number level of the operating points at reduced throughput rates is correspondingly lower.

SUMMARY AND OUTLOOK

The results shown clearly demonstrate the capabilities of present-day CFD codes and their potential for shortening development times. It is possible with the aid of CFD to obtain reproducible, robust and, above all, comparable data on the static performance capability of a compressor at a very early stage of development on the basis of CAD data before hardware is available for physical measurement.

However, the future aim in 3D computation of turbochargers must be to be able to adequately represent the transient behaviour as well. Thus, it would be desirable attempting, for example, to simulate the interaction between turbine and compressor during the speeding-up phase in order to be able to draw conclusions as to the turbocharger's subsequent response characteristics when fitted to an engine.

REFERENCES

[1] Ansys, Inc.: Ansys CFX-Solver Modeling Guide. Release 12.1, 2009
[2] Sailer, T.: Numerische Analyse des Verdichterverhaltens eines Abgasturboladersystems. Hochschule München, Graduation Thesis, 2008
[3] Mai, H.; Sens, M.; Pucher, H.: Parameterstudie zur Turbolader-Kennfeldvermessung. Informationstagung Motoren, Heft R549 (2010)
[4] Skopil, M. A.: Turboladerverdichterkennfelder interpretieren und simulieren. 10. Tagung Der Arbeitsprozess des Verbrennungsmotors, Graz, 2005
[5] Pucher, H.: Nickel, J.: Vermessung erweiterter Kennfeldbereiche von Fahrzeugmotoren-Turboladern. 8th Supercharging Conference, Dresden, 2002
[6] Smiljanovski, V.; Schorn, N.; Scharf, J.: Messung des Turbinenwirkungsgrades bei niedrigen Turboladerdrehzahlen. 13th Supercharging Conference, Dresden, 2008

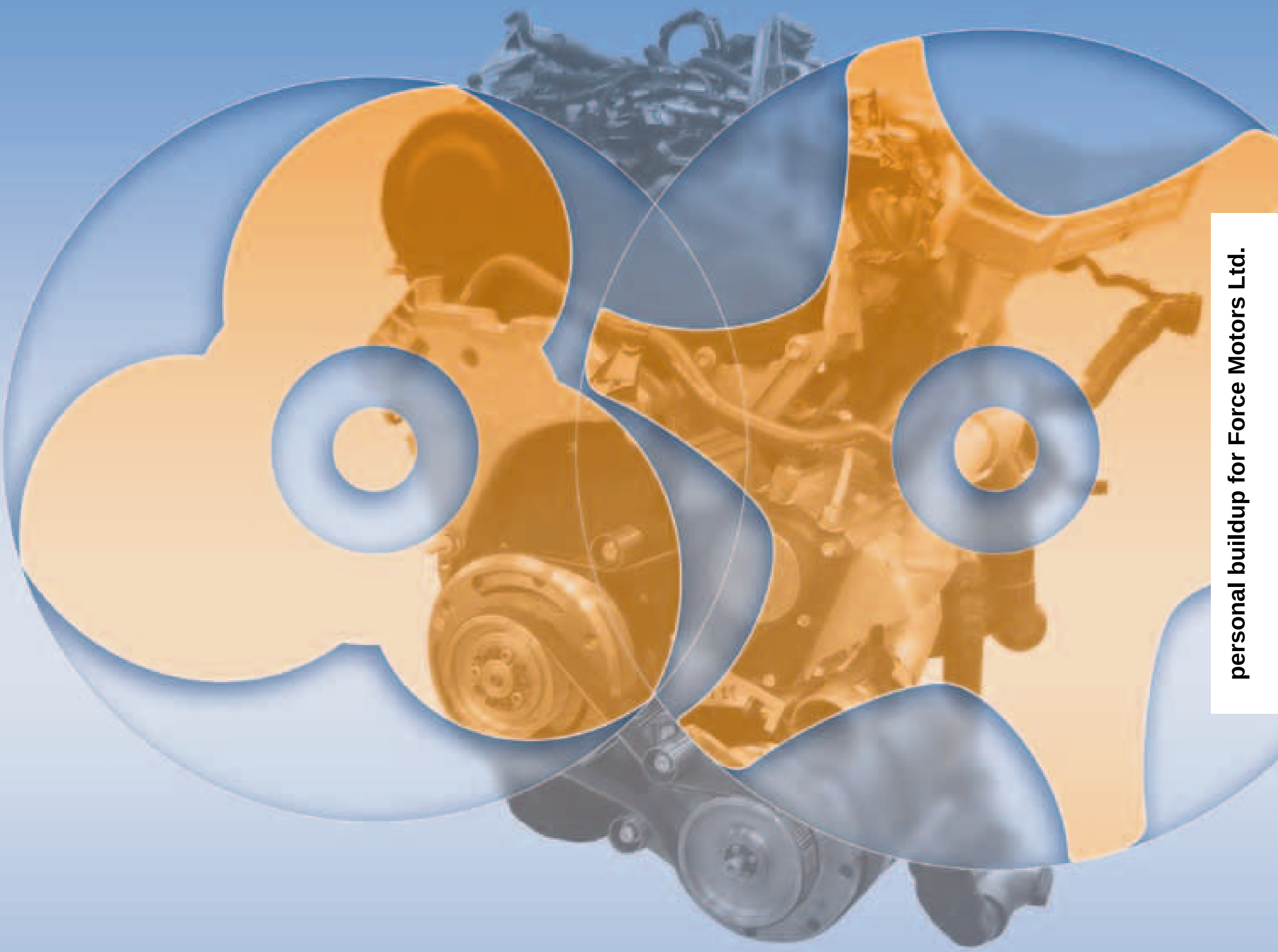

THE IAV ACTIVE HIGH-EGR CONCEPT

Exhaust gas recirculation (EGR) is a proven method of emissions reduction in diesel engines. The higher the exhaust gas rates in the combustion air, the more nitrogen oxide emissions are reduced. To meet always higher demands, IAV has developed the active High-EGR concept where a twin screw compressor with a newly developed rotary slide control has been placed between the exhaust-gas turbocharger and the motor. Driven by a pulley drive planetary gear with power split, the charger is able to actively compress fresh air and exhaust gas and to to mix the two elements to the desired ratio.

AUTHORS

DIPL.-ING. KARSTEN ROHRSSEN
is Team Manager within Diesel Engines Division, Business Area Powertrain Mechatronics, responsible for Combustion and Concepts of Four Cylinder Engines, at IAV GmbH in Gifhorn (Germany).

DIPL.-ING. GERD HÖFFELER
is Head of Department within Diesel Engines Division, Business Area Powertrain Mechatronics, responsible for Combustion and Concepts, at IAV GmbH in Gifhorn (Germany).

EXTENSION OF THE ENGINE CALIBRATION SPACE

The recognition that three components determine the reduction of emissions by exhaust gas recirculation motivated to develop an active EGR feeding. These are the specific power of the motor, the charge density in the cylinder and the exhaust gas ratio in the combustion air. These three variables create a space in which the calibration of the exhaust gas recirculation is ranged. In an aspirated engine, the charge density is determined by the ambient pressure and is consequently limited. With small loads it is still possible to re-circulate exhaust gas to the cylinder but when the specific power increases, thus causing a greater need of air, the ability to re-circulate the exhaust gas is reduced. The engine calibration space is declining. With a charged motor the charge density can be increased. The extra fresh air can be used to achieve a greater power and also in order to re-circulate more exhaust gas. Since the engine calibration space is increasing, there is a larger scope for designing the calibration, ❶. Thus, it is not possible to look at the exhaust gas recirculation without considering the charging. These considerations have led to the High-EGR concept discussed here. The use of a screw compressor also permits a low-pressure exhaust gas recirculation without a particle filter and the application of an air cooled exhaust gas cooler.

STRUCTURE OF THE ACTIVE EGR DELIVERY

The new High-EGR concept uses a lysholm screw machine for an active feeding of the exhaust gas. The structure, ❷, corresponds initially to the classical arrangement of a charged diesel engine. In the new EGR concept, the exhaust gas for the recirculation is taken out from a point behind the oxidation catalyst, cooled down in a separate air cooled exhaust gas cooler and aspirated by the modified screw compressor. The screw compressor with two inlets is the heart of the new concept. Through one of these inlets, the pre-compressed air flows from the charge air cooler into the

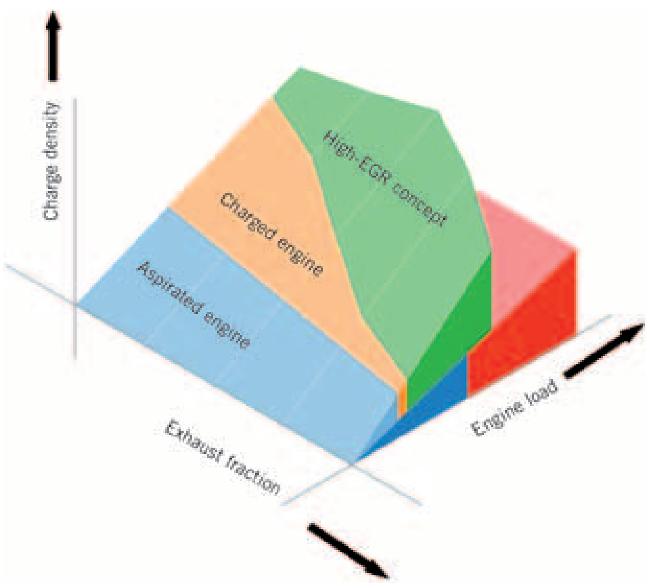

❶ The active High-EGR concept increases the charge density and the EGR rate, thus creating a larger scope for designing the calibration

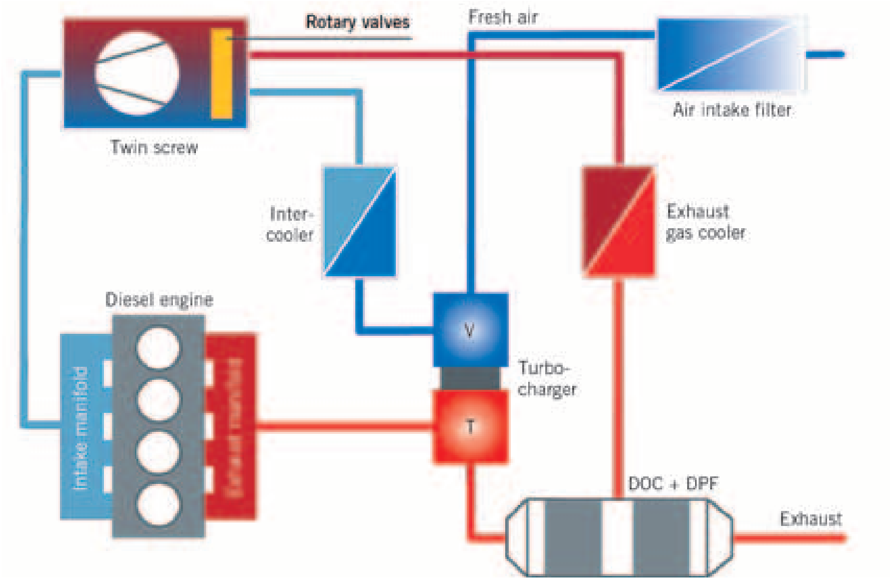

❷ The new High-EGR concept uses a lysholm screw machine for an active feeding and mixing of the exhaust gas

twin screw charger. The exhaust gas flows through the other inlet into the screw compressor. By means of a rotary valve control, the EGR rate – that is the exhaust gas element in the combustion gas – is set here. The re-circulated exhaust gas and the charger air are either compressed or decompressed, depending on the flow rate of the screw machine. The gas is transported from the compressor directly to the engine.

This results in a simple construction with the following advantages. In spite of the low-pressure exhaust gas recirculation, the exhaust gas can be cooled in a separate EGR cooler. As the screw machine can actively compress the gas mixture, it is possible to choose the exhaust gas recirculation ratio very freely at all operation points. Hence is it feasible to create the exhaust gas recirculation even at high loads. Through coupling the screw compressor with the combustion engine, the EGR ratio can be kept at a constant level even at changing revolution speed without any problems. Since the screw charger compared to a flow charger is more insensitive to dirt, deposit and condensation water, the exhaust gas temperature can actually fall below the dew-point, for which reason the system works even without a particle filter. The system with mechanical charging provides a high pressure ratio even at low revolution speeds and loads. With this combined EGR and charging system a good cold engine idling can be achieved.

QUANTITY CONTROL

During the development of the EGR concept, different options for the quantity control were tested and evaluated using the engine process simulation program “Themos”. To use concepts with rotary valves and bypasses for quantity control purposes as in [1] and [2] did not lead to the desired results due to a deterioration of the efficiency. A rotation speed control of the screw compressor provided the best results. Since an electric machine is always placed in the belt drive of the combustion engine, namely as generator, it also lends itself to be used as a rotation speed regulated drive unit. A planetary drive was developed as a coupling to the engine. The planetary drive splits the power requirement of the screw machine to the combustion engine and the electric motor. The gear is dimensioned in a way that approximately two thirds of the power for the screw charger is produced by the combustion engine and only one third by the electric engine. Thus, a rather small electric engine at only 3 kW is sufficient.

Inside the planetary gear a one-way clutch is arranged in such a way that it is impossible for the rotation speed to fall below the engine rpm. Hence, the electric machine can be used as a generator to charge the batteries and the screw com-

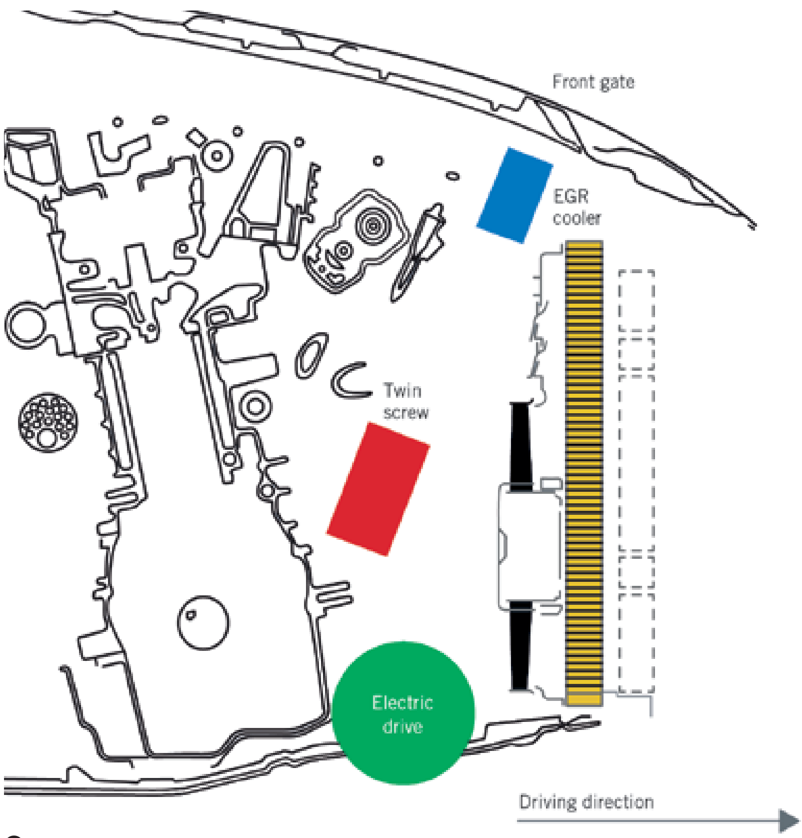

❸ The EGR cooler is located above the charger air-cooler in the vehicle

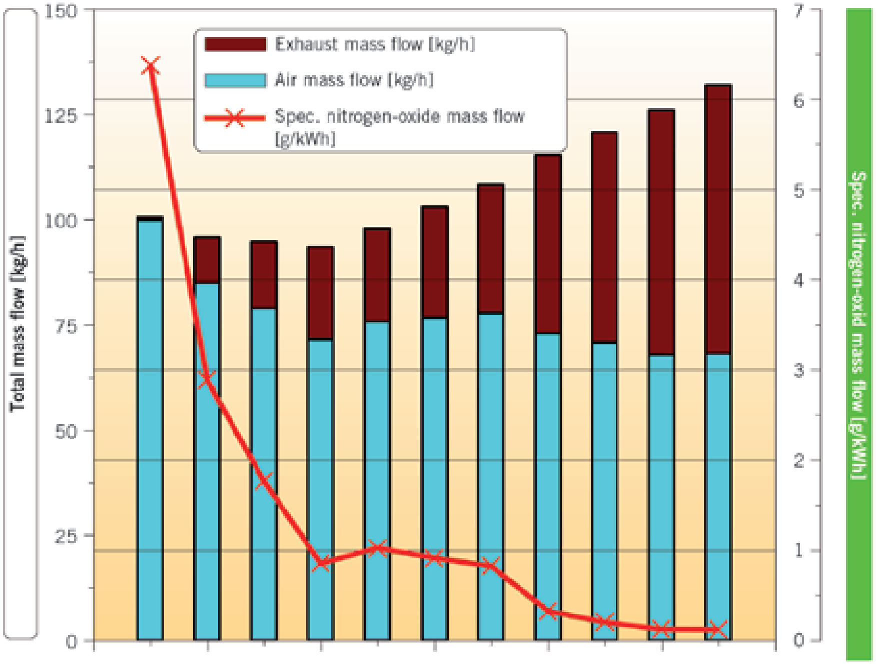

❹ The EGR variation shows that very high EGR rates are only reachable with a constant air-fuel mixture ratio

pressor is always rotating at minimum revolution speed and thus does not require an additional bypass or a coupling.

MIXTURE CONTROL

The control unit for the EGR ratio comprises two rotary valves placed in front of the both inlets on the screw compressor. They divide the inlet area into two – one section for the exhaust gas and one for the fresh air. As described in [3], each of them covers the screw rotators in such a way that no transverse flow of the charger air is created in the EGR flow course or the other way around. The rotary valves are pivoted attached to the drive shaft and can thus enlarge or reduce either the exhaust gas part or the fresh air element. This arrangement allows to compress the exhaust gas in the screw machine up to the charging pressure and to mix it with the fresh air. As charging air and exhaust gas are always transported simultaneously, there is no risk of the motor suddenly being overfilled with exhaust gas when – as the load changes – the exhaust gas turbocharger does not deliver a charging pressure but the mechanical charger is already feeding exhaust gas. This is the major advantage of this arrangement compared to a plain exhaust gas feeding pump.

PROGRAMMING THE CONTROL ALGORITHM

The control of the EGR is preformed by a program written in Matlab/Simulink. The electric motor rotation speed control and the rotary valve control actuators are controlled via an UNI-CAN interface developed by IAV. The sensor signals, for example pressure, rotation speed and temperature are also imported via the CAN messages. As with known EGR concepts, the quality control dependent on the engine rpm and the injection quantity ensures a minimum quantity of fresh air. The correcting variables for this control system are the signal of the air mass gauge and the position of the rotary valves. The input value for the quantity control is the pressure and the temperature in the intake tube of the combustion engine and the correction value for the quantity control is the rotation speed of the electric engine.

EGR COOLER

As the analysis of [4] has confirmed, there are two possibilities to reduce deposits in exhaust gas cooler. One way is to avoid the EGR temperature falling below the dew-point temperature in order to prevent condensation. The other alternative is to cool down the exhaust gas as far as possible below the dew-point temperature and thus make use of the cleaning effect of the condensation water. Due to the importance of a low temperature in the intake tube for low NO_x emissions, an air cooled exhaust gas cooler has been developed which by means of the low temperature of the cooling agent can cool down the exhaust gas as far as possible. The thermal inertia is low, caused by the thin walls of the cooler and due to the fact that no cooling water must be heated. Thus, the temperature behaviour is very positive after a cold start. By using a cool air flap in the vehicles air inlet, an exhaust gas bypass is no longer necessary. However, when cooling down the exhaust gas below the dew-point it is imperative that the cooler is the highest point in the EGR line and that all pipes have a continuous gradient. Arranging the EGR cooler above the charger air cooler, ❸, ensures this.

TEST IN ENGINE TEST BENCH

The most important parameters of the concept were determined during an extensive simulation phase using the program system Themos A model of the modified screw compressor calculated by the department for screw machines at the University in Dortmund was integrated in THEMOS and extensive parameter studies were performed. These led to the choice of the Opcon OA 1040 with a capacity of 400 ccm per revolution as the most suitable charging aggregate for a 2.0 l diesel engine.

ENGINE TEST RESULTS

The concept was mounted and tested on the test bench. Using the described construction, the revolution speed range from 800 to 4000 rpm and the power range from idle speed up to full load could be described. As the flow rate of the screw machine rises with increasing gas inlet pressure, it does not function as a throttle even at a high revolution speed and high charging pressure and thus does not need a bypass. By choosing a suitable drive transmission ratio it can even be used as a second charging step. So far the tests have only been performed up to a pressure ratio of 1.2 via the screw compressor.

❹ shows the concept's mode of operation. Starting with a pure fresh air charging, the exhaust gas element was con-

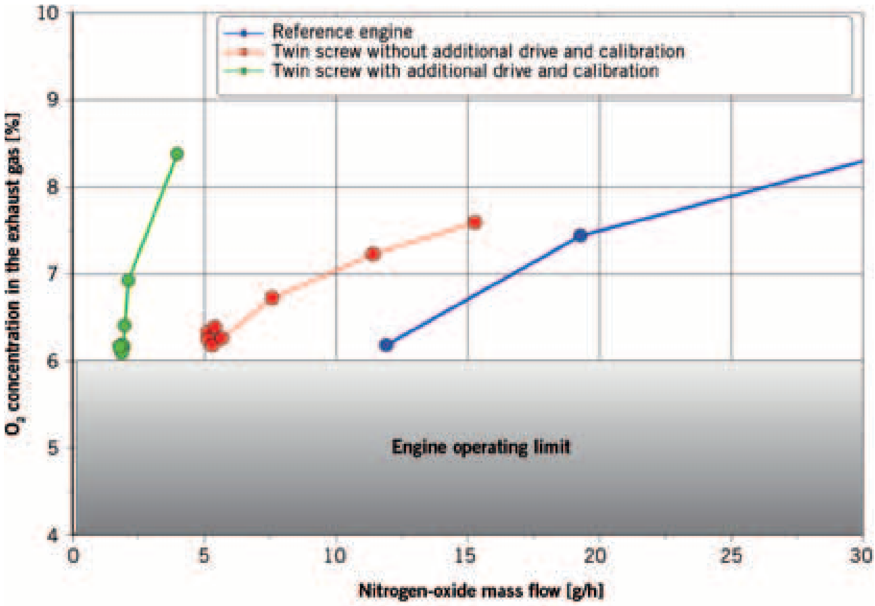

❺ With an increased EGR ratio the remaining oxygen content should not fall under a critical limitation value for stable engine running; the case is 1500 rpm and 80 Nm

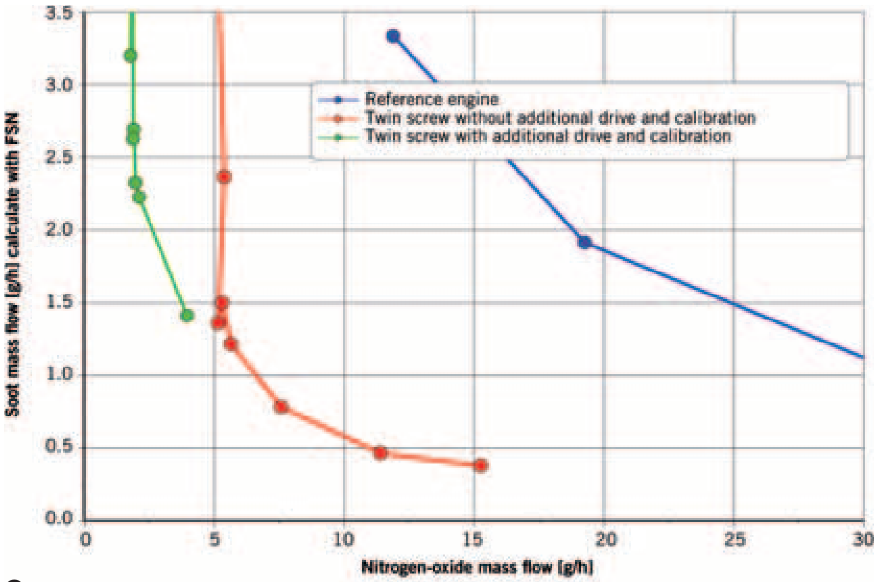

❻ Decreasing the NO_x emission the particle emission can be kept constant by means of engine calibration

stantly increased. However, the fresh air portion must not fall below a critical value to make sure that the carbon hydride and carbon monoxide emissions do not increase too much. Therefore the oxygen mass in the cylinder was held at a constant level by increasing the charge density, [5]. Even with an increased EGR ratio the remaining oxygen content does not fall under a critical limitation value and the particle emission can be kept constant by means of engine calibration, ❺ and ❻.

SUMMARY AND PROSPECTS

The previously executed studies show that the IAV High-EGR concept is suitable for reducing NO_x emissions of a diesel engine. The twin screw compressor has proven itself as an aggregate for transport of high exhaust gas rates. The possibility to change the EGR rate and the filling of the cylinder extensively independent from each other creates extra scope for development in the engine calibration in order to meet future requirements. The next development stage will be the validation of the promising measurements from the engine test bench in a real vehicle.

REFERENCES

[1] Frambourg, M.; Rohrssen, K.: Ein neues Schraubenverdichterkonzept zur Realisierung sehr hoher Abgasrückführraten beim Dieselmotor. VDI-Tagung Schraubenmaschinen Dortmund 10/2010

[2] Wachtmeister, G.: Untersuchung der Ablagerungsmechanismen auf der gasseitigen Oberfläche von Abgaswärmeaustauschern und die Entwicklung von Lösungsansätzen zu ihrer Vermeidung und zum Ablösen der Ablagerung. FVV-Frühjahrstagung April 2010 Bad Neuenahr, 04/2010

[3] Oscarsson, J.: Regulation device for a screw rotor maschine for supercharging internal combustion engines. Patent WO 95/02766,1995

[4] Rüden, K. von: Beitrag zum Downsizing von Fahrzeug-Ottomotoren. TU Berlin Diss. 2004

[5] McTaggart-Cowan, G.; Bushe; W. K., Hill, P. G. and Munshi, S. R.: NO_x reduction from a heavy-duty diesel engine with direct injection of natural gas and cooled exhaust gas recirculation. 191 Int. J. Engine Res.; Vol. 5; No. 2

THANKS

The authors would like to thank Mr. Michael Frambourg for his valuable support during the development of the presented High-EGR concept.

FULLY VARIABLE MECHANICAL COOLANT PUMP FOR COMMERCIAL VEHICLES

For a long time, development work in the field of coolant pumps has focused on improving performance and durability as well as reducing operating noise. However, the increasingly tough fuel efficiency and emission standards of recent years now make the introduction of more flexible systems unavoidable. Pierburg Pump Technology presents a concept of a fully variable coolant pump featuring an adjustable guide vane that regulates the coolant flow in line with the needs of the engine.

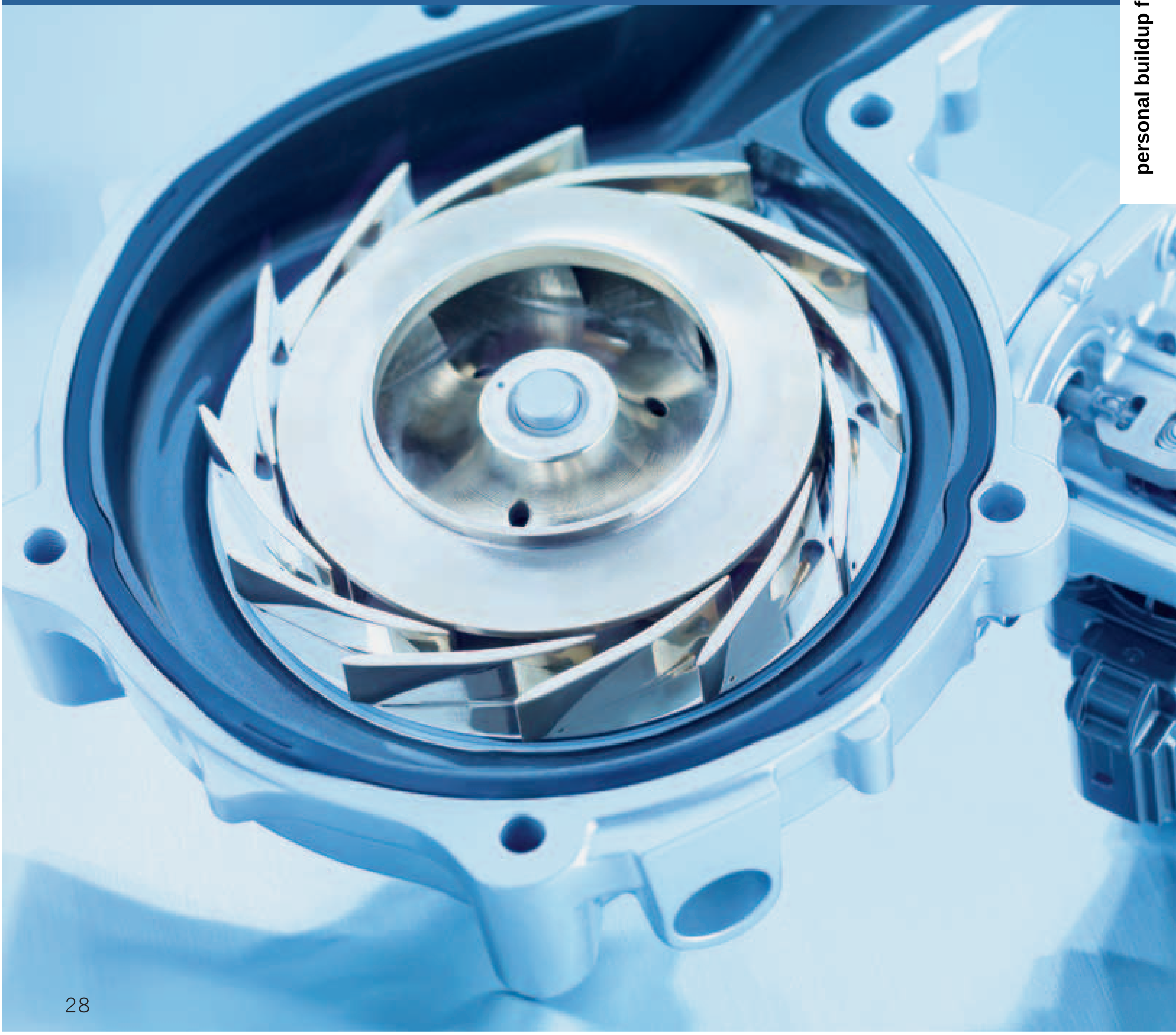

AUTHORS

DR.-ING. BERND WICKERATH
is Technical Expert Fluid Dynamics at Pierburg Pump Technology GmbH in Neuss (Germany).

DIPL.-ING. ARNAUD FOURNIER
is Project Manager Development Mechanical Water Pumps at Pierburg Pump Technology France S.à.r.l. in Thionville (France).

DIPL.-ING. JEAN-MICHEL DURAND
is Senior Manager Product Engineering Mechanical Water Pumps at Pierburg Pump Technology France S.à.r.l. in Thionville (France).

DIPL.-ING. ACHIM BRÖMMEL
is Vice President Engineering and Manufacturing Processes at Pierburg Pump Technology GmbH in Neuss (Germany).

OBJECTIVE AND MOTIVATION

The hydraulic design of a coolant pump relates directly to the adverse thermal stress in the engine. Full load, maximum rated speed and a extremely high ambient temperature characterize this "worst case" situation and dictate the pump's design point. Owing to these design criteria and the fixed transmission ratio between the engine and the pump, in most operating situations the engine receives too much coolant, which also means the pump consumes more power than necessary. In addition, for several minutes following a cold start of a combustion engine, the coolant pump is not supposed to supply any coolant at all, thus shortening the warm-up phase of the engine as well as reducing exhaust emissions.

Due to the issues explained above, Pierburg Pump Technology has developed a fully variable mechanical coolant pump which, via a continuous adaptation mechanism, assures improved regulation of cooling output in line with the actual requirements of the engine. Optimizing the cold start of the combustion engine and reduced power consumption for the coolant pump were key objectives in developing this innovative pump. A further parameter was the need for a fail-safe system, ensuring that the variable pump would continue to function as a conventional pump in that case.

LAYOUT AND FUNCTION

Conventional radial pumps commonly used in cars and commercial vehicles are the basis for development of the fully variable coolant pump. In these pumps, pressure build-up derives primarily from the centrifugal acceleration of the medium to be conveyed. Fluid entering the pump is seized by the rotating impeller and forced outwards in a circular path. Subsequently, the medium must be decelerated with as little loss as possible in order to exploit the kinetic energy present at the impeller outlet as a means of augmenting the static pressure. For this reason, in conventional pumps, a volute is directly connected to the impeller. This fully variable pump features an additional guide vane, ❶, located between the impeller and the volute which decelerates the medium to be conveyed, just as in a diffusor. In pump engineering, bladed diffusors of this type are primarily employed in multi-stage pumps in order to eliminate the swirl of the flow before entering the next stage. In the fully variable coolant pump, the diffusor blades

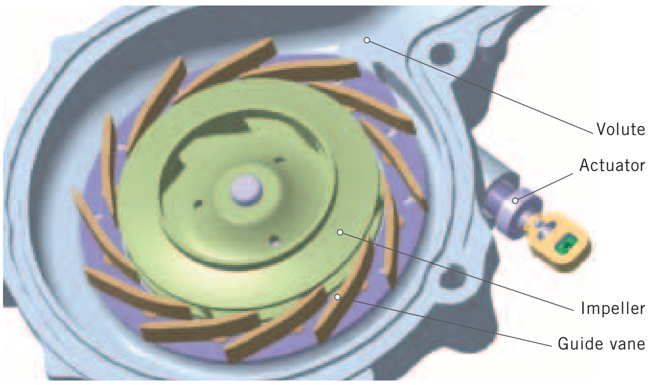

❶ Layout of the fully variable mechanical coolant pump

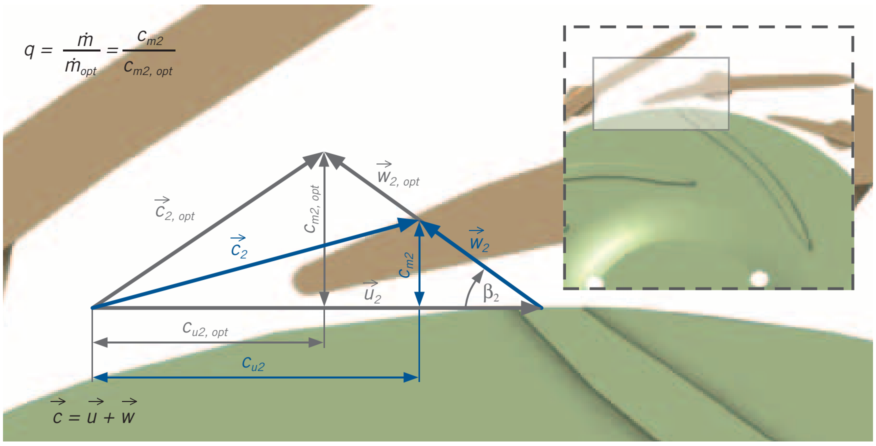

❷ Velocity triangle at the impeller outlet

are designed to be adaptable, enabling them to regulate the flow of medium to meet the cooling requirements of the combustion engine.

Adjustment of the blades results in a reduction in the flow of coolant, which in turn diminishes the drive torque acting on the impeller shaft as well as reducing the pump's power consumption. Since this may not be readily evident, the theoretical power consumption is deduced below with the aid of the velocity triangle at the impeller outlet, ❷, and Euler's Turbine Equation, Eq. 1:

EQ. 1	$Y = \frac{P_i}{\dot m} = u_2 \cdot c_{u2}\,(-u_1 \cdot c_{u1})$

The equation describes the mass flow-specific work Y transmitted by the impeller to the fluid, subject to the circumferential velocities (u_1, u_2) and the circumferential components of the absolute flow velocities (c_{u1}, c_{u2}) at the inlet and outlet of the impeller. In the case of swirl-free inflow, the final term of Eq. 1 is not applicable. In order to determine net output, Eq. 2, however, the dissipation loss caused by bearing friction has to be taken into account, as well as the friction moment acting on the exterior wall of the impeller:

EQ. 2	$\frac{P}{\dot m} = \frac{P_i + P_a}{\dot m} = u_2 \cdot c_{u2} + \frac{P_a}{\dot m}$

These power dissipations, summarized in the external losses P_a, depend primarily on the number of revolutions per minute and are essentially unaffected by the volume of medium conveyed. Conversely, the circumferential component of the flow velocity c_{u2} changes materially with the flow rate. This is evident in the velocity triangle, ②. The relative flow angle β_2 at the impeller outlet is essentially determined by the geometric characteristics of the impeller, such as the number and angle of the blades, and thus remains constant in the event of a reduction in the meridian velocity c_{m2}. Here, the meridian component of the flow velocity signifies the flow of medium through the impeller, Eq. 3:

EQ. 3	$\dot m = \rho \cdot c_{m2} \cdot A_2$

It follows that the circumferential components of the absolute velocity c_{u2} must increase, which can be expressed with the aid of the velocity triangle as a function of the relative flow rate $q = \dot m / \dot m_{opt}$, Eq. 4:

EQ. 4	$c_{u2} = u_2 - \frac{c_{m2}}{\tan \beta_2} = u_2 - \frac{c_{m2,opt}}{\tan \beta_2} \cdot q$

Here, the index "opt" signifies variables in the design point, i.e. the best efficiency point. Deriving from the equations stated above, the power consumption of the impeller may be expressed by a quadratic equation in q, which apart from the relative flow rate q contains solely those variables that are independent of the mass flow rate, Eq. 5:

EQ. 5	$P = \dot m_{opt} \cdot u_2 \cdot q \cdot \left(u_2 - \frac{c_{m2,\,opt}}{\tan \beta_2} \cdot q\right) + P_a$

❸ Power consumption with a reduction in flow rate

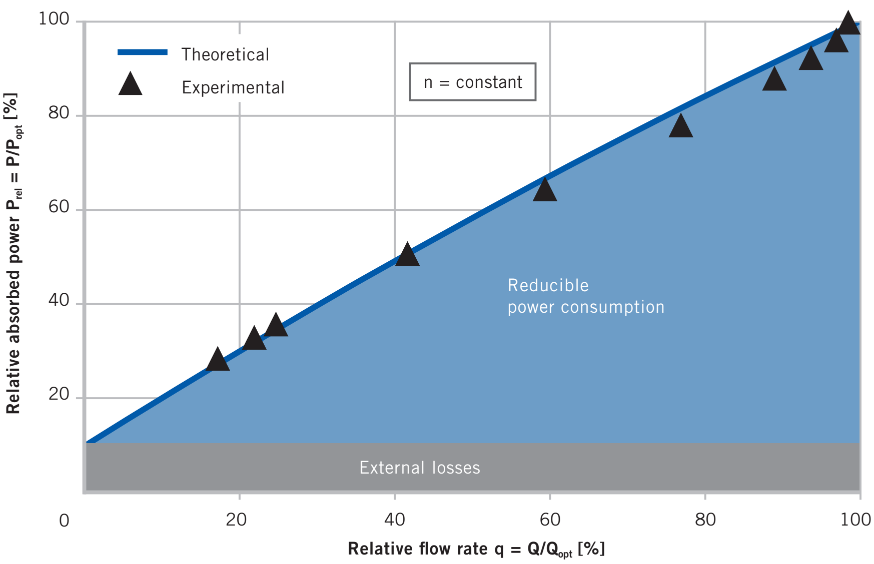

❸ depicts the theoretically derived progression of the power consumption, Eq. 5, for an executed pump (Q_{opt} = 450 l/min, Δp = 2.5 bar) in comparison to existing measurement readings. Accordingly, a reduction in the mass flow rate leads to a steady decline in the pump's power consumption, until at zero delivery only the external losses P_a apply.

HYDRAULIC DESIGN

The impeller shape and the type of pump result from requirements deriving from the volumetric flow rate Q, hydraulic head H and the rotational speed n, which characterize the conveyance requirements via the specific speed, Eq. 6:

EQ. 6	$n_q = n\ [\text{min}^{-1}] \cdot \frac{\sqrt{Q\ [\text{m}^3/\text{s}]}}{(H\ [\text{m}])^{3/4}}$

In both the passenger car and commercial vehicle segments, small to medium specific speeds result, implying the use of the radial impellers. To obtain maximum efficiencies, moreover, the impeller diameter and the specific speed must be harmonized. Furthermore, in order to keep the dimensions of the variable pump small, the impeller's external diameter has been reduced compared to the conventional design, in turn increasing the number of rotations. The necessary adjustment in the number of rotations is achieved by means of a corresponding transmission ratio between the combustion engine and the pump.

Drawing on standard design criteria, the impeller layout is intended to obtain optimum hydrodynamic blade load so as to achieve the maximum degree of efficiency. Furthermore, the number of the impeller blades and guide vanes must be harmonized in order to reduce pressure pulsations and hydraulic excitation forces.

The guide vanes are engineered to operate without flow control in the design point until the narrowest cross-section is reached; as such, the flow is not redirected. To do this, the blade angle at leading edge is designed in accordance with the flow angle (zero incidence) and the mean camber line represents a logarithmic spiral in case of constant channel height. As a result, the guide vanes allow the fluid to flow into the stator as freely as possible in accordance with the principle of conservation of angular momentum. The subsequent diffusor section is a compromise between optimum diffusor length and the smallest possible external diameter, resulting in minimal flow losses and a compact design. The experimental results confirm the high quality of the stator's hydraulic design. Compared to the conventional variant, the fully variable coolant pump displays somewhat lower power consumption even with a completely opened stator.

ACTUATOR SYSTEM

A further challenge in implementing the fully variable concept involves development of an adaptation mechanism, ❹. Owing to the very limited space available in passenger car and commercial vehicle applications, the most package-neutral solutions possible are necessary for new developments. Therefore, the smallest possible actuator system for proportional control of the guide vane position is required. Consequently, minimizing the forces necessary for adjusting the blades is a central design objective for the adaptation mechanism. Owing to the large number of influencing factors, optimizing the geometry requires a mathematical model that allows prediction and analysis of the anticipated adjustment forces. Besides the blade pressure distribution of the respective operating point, the primary influencing parameters are the geometric characteristics of the adjusting mechanism, such as the position of the rotating axis and guide pin, as well as the incline angle of the guide groove. Simultaneously, the adjusting mechanism determines the flow-through of the stator, particularly with medium guide vane positions, and thus influences the hydraulic behaviour of the pump. Thus, besides the use of a tool specially developed for this application for calculating the blade adjustment forces, numerical flow simulations are indispensable.

CHARACTERISTIC DIAGRAM MEASUREMENTS AND SAVINGS POTENTIAL

Based on the optimization process described above, a prototype was developed and measured in a pump test rig with various guide vane positions. ❺ shows the relative flow rate q measured for this pump as a function of the relative rotational speed N. The guide vane position here is quantified by means of the actuator's PWM signal, corresponding approximately to the narrowest flow cross-section in the stator. The fully variable pump displays the hydraulic behaviour necessary to enable effective control of pump performance. For every speed of the pump, the volumetric flow rate drops continuously with increasing guide vane adjustment, i.e. diminishing flow cross-

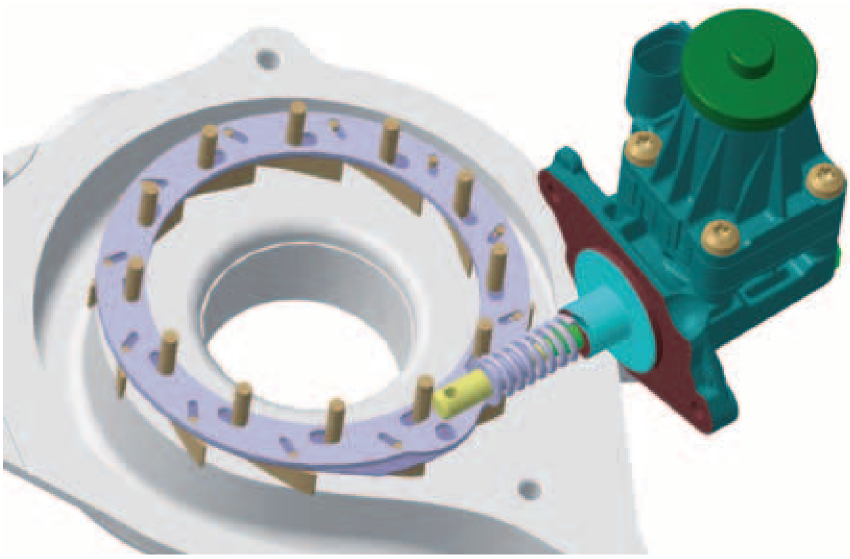

❹ Adaptation mechanism of the fully variable coolant pump

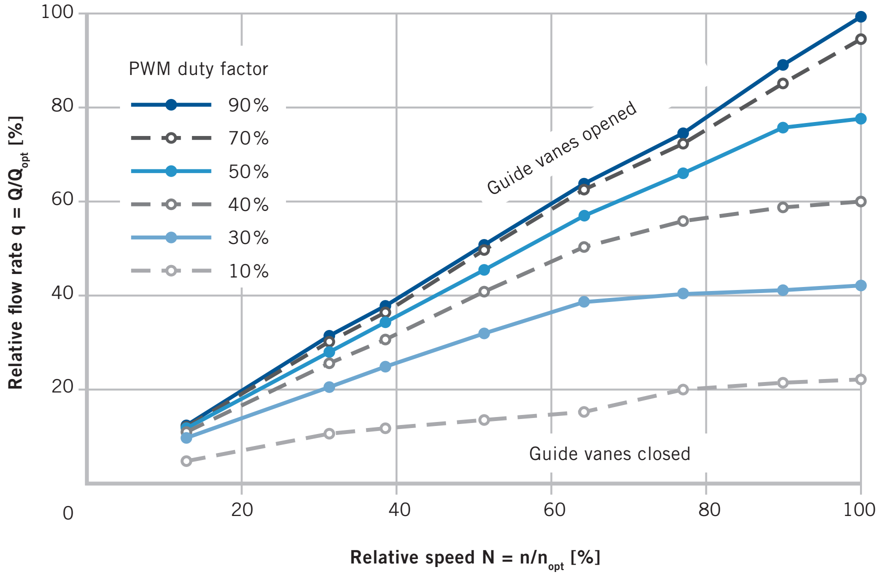

❺ Influence of guide vane adjustment on flow rate

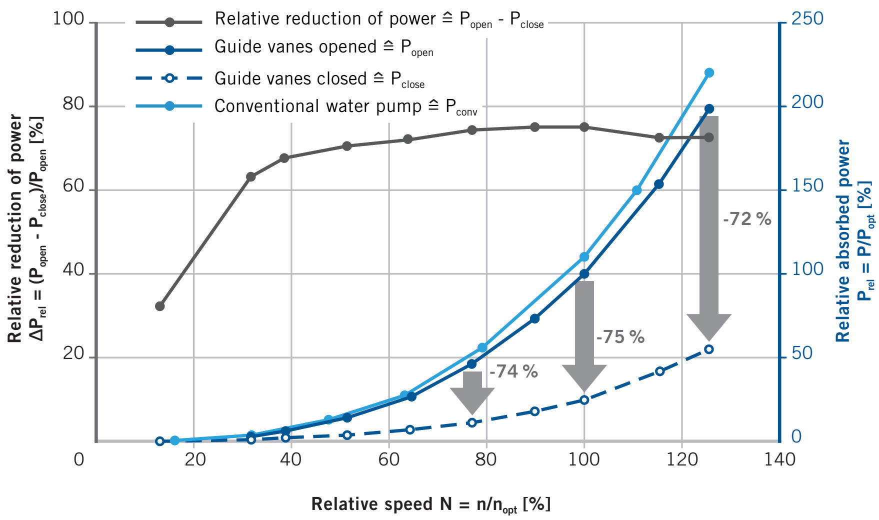

❻ Power-saving potential of the fully variable coolant pump

section, whereas when the guide vane position remains constant, the flow rate rises with the number of rotations.

At the rated speed of the pump, the reduction in power consumption depicted in ③ can be achieved depending on the reduced flow rate with respect to the design point. ❻ shows the power consumption at various speeds for a conventional pump (P_{conv}) compared to a pump from Pierburg Pump Technology with a completely opened (P_{open}) and completely closed stator (P_{close}).

Owing to a slight improvement in the efficiency, the fully variable pump displays slightly lower power consumption than the conventional pump, even with a completely opened stator. Even though most operating points of the combustion engine do not permit complete closure of the guide vanes, the significant reduction in power consumption ($P_{open} - P_{close}$) nevertheless shows the high power-saving potential of the fully variable coolant pump throughout a large spectrum of rotational speeds.

SUMMARY

Via the use of an adjustable control mechanism, the fully variable coolant pump developed by Pierburg Pump Technology makes it possible to regulate the flow of coolant to meet the needs of the engine. In addition to optimizing the cooling process of the combustion engine, the pump's variability results in lower fuel consumption and emission levels, since the diminishing flow of coolant simultaneously reduces the power absorbed by the pump. Achieving the power-saving potential in a driving cycle, such as the European Transient Cycle (ETC), depends primarily on the cooling requirement of the combustion engine with respect to the operating point. Based on previous studies, the fully variable coolant pump will result in fuel savings of approximately 2 % under realistic conditions.

EVAPORATORS FOR MOBILE WASTE HEAT RECOVERY SYSTEMS

Thesys develops evaporators for waste heat recovery systems for mobile and stationary applications. These evaporators utilize the enthalpy availability of hot exhaust gas both in the cooled exhaust gas recirculation duct as well as in the main exhaust gas for example in the muffler. At present there are three different designs for evaporators under development. Prototype measurements have already partially proved their function and performance.

AUTHORS

DR.-ING. PETER AMBROS
is Managing Director of the Thesys GmbH in Kirchentellinsfurt (Germany).

PROF. DR.-ING. JOCHEN ORSO
teaches CAD Design and CAD Layout Planning at ESB Business School Reutlingen and is Freelancer for Thesys GmbH in Kirchentellinsfurt (Germany).

DIPL.-MATH. TECHN. AXEL FEZER
is Managing Director of the Thesys GmbH in Kirchentellinsfurt (Germany).

HARALD NECKER
is responsible for Prototyping and Manufacturing Process Enhancement at the Thesys GmbH in Kirchentellinsfurt (Germany).

BASICS

The utilization of the waste heat of combustion engines on the basis on a Rankine process is a promising technology to reduce the CO_2 emissions of future vehicles and for e.g. trucks provides a fuel consumption saving potential of app. 5 to 8 % [1, 2, 3, 4, 5].

In a Rankine waste heat recovery process, a working fluid is being compressed in a feeding pump to a high pressure level, vaporized and overheated in an evaporator. The overheated steam will then be expanded in an expander providing mechanical energy. The expanded fluid will then be condensed in a condenser and by passing a collecting tank be led back to the pump.

For the series application of a mobile waste heat recovery system the necessary components have to be developed, meeting the high requirements regarding power, packaging, weight, reliability and price. In addition to the expander, key components are the evaporators, which have a dominant impact on the efficiency of the waste heat recovery system. In this paper, evaporators are described using the enthalpy supply of the hot exhaust gas of the engine. For integrating these evaporators into the vehicle, two locations are prioritized:

: Exhaust gas recirculation evaporators (EGR evaporator): as a substitute of today's series exhaust gas recirculation cooler (EGRC), the EGR evaporator is provided with exhaust gas on a maximum temperature level. Additionally the engine cooling system is relieved by outsourcing of the EGRC heat load.
: Main exhaust gas evaporator (MEG evaporator): integrating the MEG evaporator into the exhaust gas duct down flow of the aftertreatment system provides the MEG evaporator with a high exhaust gas flow rate but on a lower temperature level.

MALFUNCTION RISKS OF EVAPORATORS

The concept finding and design of evaporators needs over and above the challenging performance requirements to meet significant structural mechanical challenges and also faces the risk of instable operation. Due to the gas-to-gas-heat transfer, evaporators are exposed to material temperatures of up to 550 °C. In parallel, there are pressures up to 60 bar with the additional risk of corrosion and blockages in the working fluid duct. Other than conventional heat exchangers without phase change, evaporators face the risk of instable operation, e.g. [6]:

: statical instability
: aperiodic instability
: periodic instability
: pressure drop instability induced by large steam bubbles (slug flow)
: oscillatoric instability of parallel evaporation ducts.

THERMODYNAMIC SIMULATION OF EVAPORATORS

The thermodynamic dimensioning of evaporators is done with the home made simulation tool TheSim. In detailed thermodynamic models the geometry-specific heat transfer coefficients and the heat transfer resistance in the separation walls as well as the efficiency of primary and secondary heat transfer surfaces and surface heat losses are taken into consideration. Furthermore, the pressure drop characteristics of the flow ducts and the characteristics of fluids and materials are implemented. The resulting thermodynnamic models allow reliable dimensioning as well as variation and optimization of heat exchangers.

In TheSim an evaporator is divided into a minimum of three zones. This allows the modelling and simulation of different geometrical structures inside the evaporator by using the correlating heat transfer characteristics, ❶.

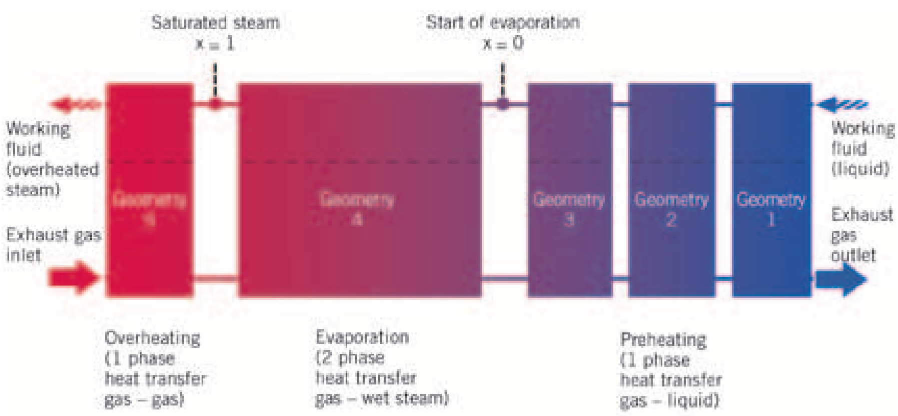

❶ Thermodynamic model of an evaporator using Thesim

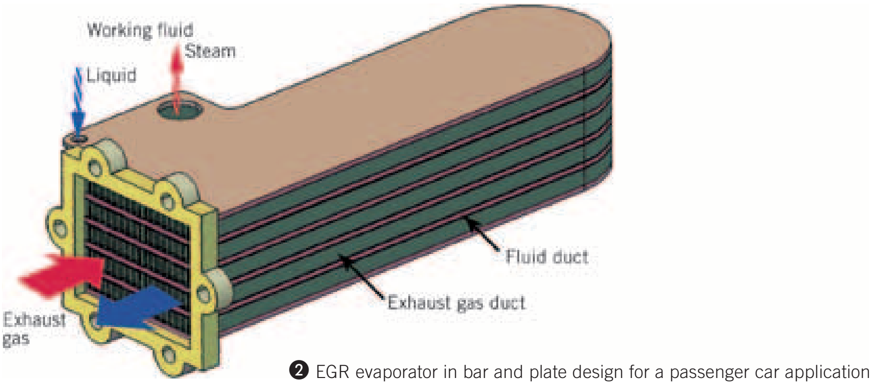

❷ EGR evaporator in bar and plate design for a passenger car application

The thermodynamic correlations are specifically defined for every zone of the evaporator and are gained by regression of the measurement results. The evaporator-specific two-phase heat transfer correlations are based on modified Shah-correlations with regressed parameters.

BAR AND PLATE EVAPORATOR

The principle design of a bar and plate evaporator for a passenger car series application is shown in ❷. Scope for the development is a design being compatible in terms of packaging as well as media connection positions to replace the series EGR cooler.

A bar and plate design enables maximum flexibility in the geometrical design of the fluid ducts. Therefore, the evaporator can be optimally designed to meet the hydraulic and thermodynamic requirements leading to good stability of evaporation and to a high performance density. Nevertheless this design requires a higher material usage and high volume automation is limited due to the quantity of different parts. For high series volumes this design will therefore be transferred into a layered cooler design.

For an offroad application two prototypes of EGR evaporators were built up showing differences in the design of the working fluid ducts (P1, P2). For both prototypes thermodynamic performance measurements were done on an evaporator test bench, ❸.

For the measurements, the exhaust gas flow rate was kept constant at 150 g/s and the fluid side working pressure at 40 bar. For different exhaust gas inlet temperatures, the fluid flow rate was controlled to a constant steam outlet temperature.

The measurement results show a stable evaporation and overheating of both evaporator designs P1, P2. The measured performance increases significantly with the exhaust gas inlet temperature and meets 40 kW at inlet temperatures of 500 °C. The thermodynamic performance simulation using Thesim for the specification indicates values of 62 kW at 650 °C. With the available test bench, it was not possible to validate this prognosis.

TWIN ROUND TUBE EVAPORATOR (TRT)

To serve as an alternative for the bar and plate design for high production volumes a new twin round tube evaporator design is under development. This evaporator is built up as a tube bundle with twin tubes as shown in ❹. Each twin tube consists of two concentric round tubes with the hot exhaust gas inside the inner tube. The annular gap between inner and outer tube serves as the working fluid duct.

The geometry of the working fluid duct is designed to cope with different local fluid densities and velocities. One or both tubes will be manufactured as twisted tubes, similar as they have been in series for EGR coolers for years. A twist of the inner tube provides the additional advantage of inducing turbulence and therefore increasing the heat transfer performance on the exhaust gas side. Enhanced capabilities in working fluid duct design provide twisted outer tubes. The usage of twisted tubes provides the additional benefit of reducing material stresses, especially under the demands of temperature cycle operation due to the elasticity of the tubes.

To validate the performance of a TRT evaporator, a single twin tube prototype was built up and measured on a calorimeter. The comparison of the measurement results with the thermodynamic simulation are shown in ❺ [7].

The measured heat flows on the exhaust gas and working fluid side show a deviation of 16 to 20 %, mainly caused by a non-optimized insulation on the test bench. There is a heat flow output of 2.3/2.9 kW from the hot exhaust gas and a heat flow input into the working fluid of 1.9/2.4 kW.

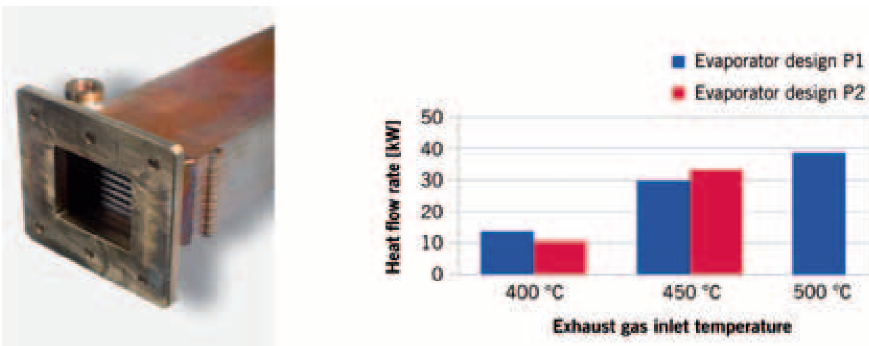

❸ Performance measurement results of EGR evaporators in bar and plate design for an offroad application

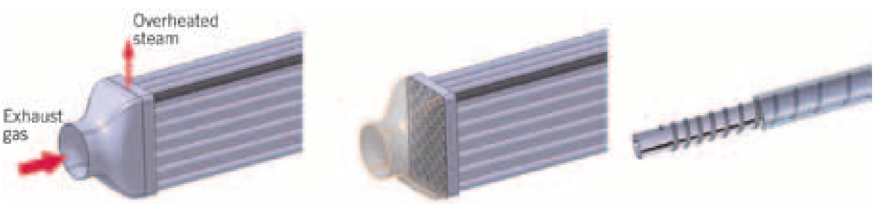

❹ EGR evaporator in twin round tube design and evaporator tube assembly

Substituting the offroad EGR evaporator in ③ with a package-compatible TRT evaporator with 33 twin tubes, the thermodynamic simulation with Thesim predicts a performance of 48 kW.

Due to the usage of standardized parts and manufacturing processes, this design is applicable for higher production volumes. Additionally, the TRT evaporator is a very robust design for the high inner pressure, pressure cycle, and thermal cycle loads are handled by round tubes which can be provided with the required pressure strength and elasticity by appropriate dimensioning of material gage and twist geometry.

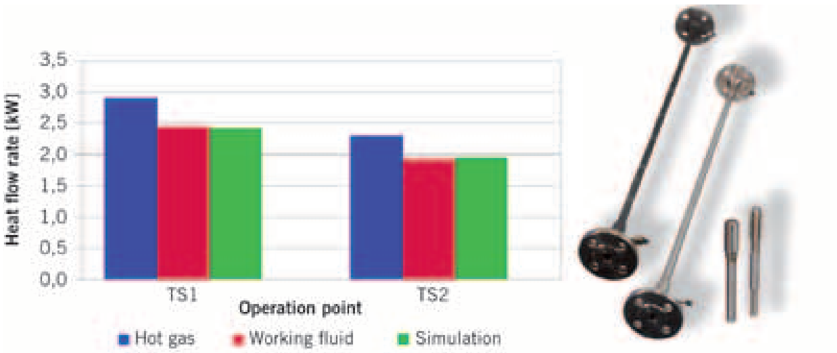

❺ Comparison of measurement and thermodynamic simulation results of a twin round tube evaporator

❻ Twin flat tube evaporator

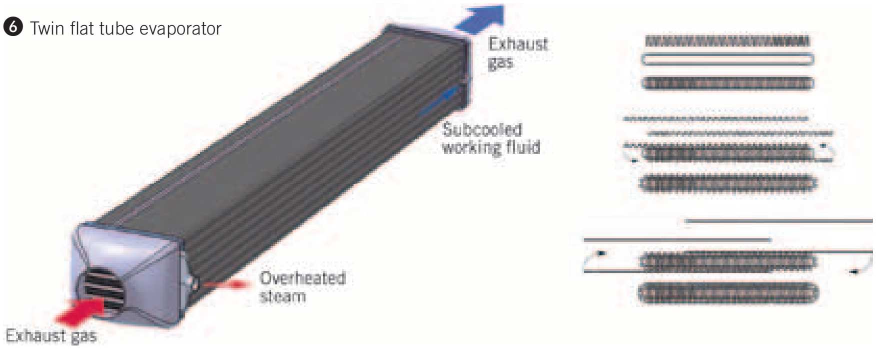

TWIN FLAT TUBE EVAPORATOR (TFT)

Motivation for the development of the twin flat tube evaporator is the creation of a design which is capable of a high volume series production and meets the high performance density of a plate and bar design by using turbulators or fins on the exhaust gas and working fluid side. Here flat tubes are stapled to a flat tube bundle, provided with fluid headers, and brazed, ❻.

Design base is the usage of flat tubes with fins being used in series EGR coolers. These flat tubes are wrapped by fins and finally by one or two bended metal sheets. The result is a double wall flat tube ducting the hot exhaust gas inside and the working fluid in the annular gap channel. The main manufacturing risks result from the bending of the working fluid fin and the requirement of a leak-proof brazing between adjacent tubes. For evaluation of these risks there are ongoing manufacturing tests.

SUMMARY

Thesys develops evaporators for waste heat recovery systems for mobile and stationary applications. These evaporators utilize the enthalpy availability of hot exhaust gas both in the cooled exhaust gas recirculation duct as well as in the main exhaust gas e.g. in the muffler. At present there are three different designs for evaporators under development. Prototype measurements have already partially proved their function and performance.

For utilization of the exhaust gas recirculation heat and series volumes higher than app. 1000 pc/a, the designs of twin round tube evaporators or twin flat tube evaporators are appropriate. These designs are applicable for high series production and provide a high performance density. Nevertheless, for a series application a high investment in development and series production equipment is needed. For lower production volumes the bar and plate design is preferable, as a robust design providing high manufacturing flexibility.

For utilization of energy in the main exhaust gas in the muffler, the twin round tube design is appropriate as it provides a high packaging flexibility due to flexible design of the outer tube bundle surface. Additionally, due to the existing muffler housing, the exhaust gas flow can be divided into an inner and outer flow, providing an energy input into the working fluid inside and outside the tubes. Furthermore the exhaust gas side pressure drop will be significantly reduced.

Prototype evaporators in bar and plate design and twin round tube design were built up and successfully measured on test benches. For evaporators in twin flat tube design, manufacturing tests are ongoing.

REFERENCES

[1] Berger, J.: Umsetzung und Erprobung eines thermischen Rekuperationssystems mittels Rankine Cycles in einem Schienenfahrzeug. Tagung “Thermische Rekuperation im Kraftfahrzeug”, Haus der Technik, München, 05./06.11.2009

[2] Banzhaf, M.; Edwards, S.; Pantow, E.: Thermomanagement für künftige Nutzfahrzeuge. In: ATZ 112 (2010), Nr. 9

[3] Höttger, M.: Abwärmenutzung mittels Dampfkraftprozessen. Tagung “Thermische Rekuperation im Kraftfahrzeug”, Haus der Technik, München, 05./06.11.2009

[4] Freymann, R.; Strobl, W.; Obieglo, A.: Der Turbosteamer, ein System zur Kraft-Wärme-Kopplung im Automobil. In: ATZ 110 (2008), Nr. 5

[5] Schaller, K.: Nutzfahrzeuge für die Zukunft. In: ATZ 112 (2010), Nr. 9

[6] Ngoma, D.; Loth, R.: Sensitivitätsstudien zu Strömungsstabilität von Abhitzedampferzeugern. Veröffentlichung Technische Universität Darmstadt, 2002

[7] Maul, R.: Thermodynamische Untersuchungen an mobilen Verdampfern. Bachelorthesis Hochschule Esslingen, 07/2010

THANKS

The authors would like to thank Voith Turbo GmbH & Co. KG in Heidenheim for their support and the permission to publish development results.

FIGURE © KGG1951 / Wikipedia

BIOGENIC VEHICLE FUELS IN GENERAL AVIATION AIRCRAFTS

Numerous small piston engine powered aircraft may use the cheaper and lead-free vehicle gasoline as fuel instead of dedicated aircraft gasoline. In a comprehensive study for the European Aviation Safety Agency (EASA) the Aachen University of Applied Sciences (FH Aachen), in cooperation with several industrial partners, investigated the implications of elevated ethanol shares of up to 15 % (v/v) in gasoline with respect to the airworthiness of small aircraft.

AUTHORS

PROF. DR.-ING. THOMAS ESCH
is Head of the Subject and Research Area Applied Thermodynamics and Combustion Technology at the Aachen University of Applied Sciences (Germany).

PROF. DR.-ING. HARALD FUNKE
is Head of the Institute of Gas Turbines and Aircraft Engines at the Aachen University of Applied Sciences (Germany).

DR.-ING. PETER ROOSEN
is Director of g.o.e.the GmbH in Aachen (Germany) and a Physicist and Thermodynamics Specialist for System Modeling and Opimisation.

DIPL.-ING. ULRICH JAROLIMEK
ist Director of the ISP GmbH in Aachen (Germany).

MOTIVATION AND STATISTICAL BASIS

The respective licensing is presently coupled to an obligatory content limit of 1 % of free ethanol in the fuel to which most of the Super Plus grade fuels are presently conforming. Due to the politically induced admixture of up to 5 % ethanol this value tends to be surpassed more and more frequently even in this grade level. The extensive introduction of even higher doted fuels (E10) is to be expected soon.

The European Nations fulfil their obligations on a CO_2 emission reduction partly by requesting a mandatory admixture of biogenic, renewable fuel components to conventional fossil vehicle fuels. Due to technical and economic reasons only an admixture of ethanol is a viable industrial scale alternative in the case of Otto engine fuels. Ethanol differs considerably from the fossil fuel components, though, both in its physical and chemical properties. A former alternative, ETBE (ethyle tert butyle ether) that may be won partially from ethanol as well, is no alternative as it is counted only partially as biogenic.

A small amount of the Otto engine fuels produced for vehicle operation has been branched for the operation of small Otto engine equipped aircraft that comply to respective regulations. Not only for economic reasons a growing number of pilots makes use of this vehicle fuel, being frequently titulated as Mogas. Even though a larger number of small aircraft continues to operate on Avgas (aviation gasoline) this aviation oriented fuel is increasingly incriminated for its relatively high lead content. Accordingly a technically viable and at the same time affordable alternative is sought.

The potential endangerment of aircraft operation imposed by ethanol containing Otto fuels was first elicited by a FMEA (on the production and distribution of fuel, its warehousing, its utilization in the aircraft, and its effect on constructive parts). A detailed exemplaric investigation of the recognized high priority issues followed for two typical small aircraft engines: a Rotax 9120 ULS, being cleared for vehicle gasoline usage complying to DIN EN 228, and an Avgas only Lycoming O 360 A1A engine. After respective tests the Rotax engine was even allowed to use up to 10 % (v/v) ethanol admixed gasolines. The engine experiments were flanked by long-term storaging tests, laboratory investigations on temperature-induced demixing of water-stained fuels, dynamic vapour pressure measurements under aircraft-like conditions, flight tests with an experimental aircraft, and a comprehensive material compatibility check.

❶ shows the number of actually or potentially Mogas using aircraft in Europe, derived from respective numbers available for the United Kingdom and Germany. Since the aircraft fleet of these two countries already accounts for about 40 % of Europe's total, the derived statistic may be regarded as practically relevant. All in all a number of nearly 20,000 affected aircraft may be assumed.

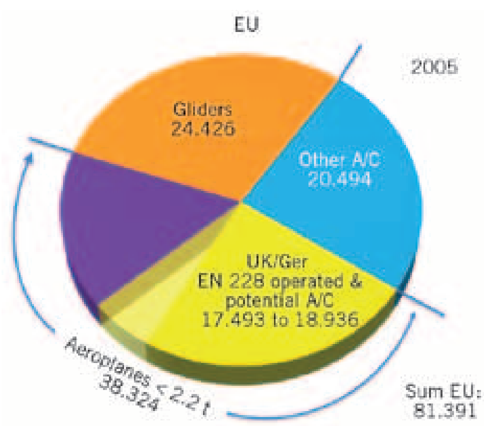

❶ Number of actually or potentially Mogas using aircraft in Europe (statistic data 2005)

DIFFERENCES OF MOGAS AND AVGAS

Dedicated aircraft fuel addresses different operation conditions than vehicle fuel: Due to the temperature decrease at altitudes of partially several kilometers the tank content temperature decreases also significantly. In thermal equilibrium temperatures of -35 °C and less are possible. All engine parts are also aircooled and hence dependent on the propeller induced air throughput that differs substantially for different flight conditions. The engine layouts and the combustion design, hence the materials choice of the engine and fuel system parts date back usually several decades and originate from eras when nobody would consider admixing free ethanol to fossil fuel.

PARAMETER	MOGAS	AVGAS 100LL
Distillation end point	210 °C	170 °C
Residue	< 2 % v/v	< 1,5 % v/v
Oxygen content	2,7 % m/m	not permitted
Methanol content	< 3 % (in vehicle grade "Super")	not permitted
Isopropyle alcohol	< 10 % (in vehicle grade "Super")	not permitted
Isobutyle alcohol	< 10 % (in vehicle grade "Super")	not permitted
Tert-butyle alcohol	< 7 % (in vehicle grade "Super")	not permitted
Total alcohol content	< 1% (if used as MoGas)	not permitted
Ether	< 15 %	not permitted
Water	no normative limit	free of water
Vapour pressure (DVPE)	winter 60…90 kPa summer 45…60 kPa	always 38…49 kPa
Freezing point	undefined	freezing point < -60 °C
Additives	various and differing	limited number
Quality compliance	DIN EN 228	ASTM D 910-02
Octane number	MOZ min 88	MOZ min 100
Lead content	< 0,005 g/l	< 0,56 g/l
Electr. conductivity	no specification	specified
Handling	custom defined quality management for storage and transport	comprehensive definition of handling, storaging requirements and logistics
Warehousing	random sampling	test of every delivery
Distribution control	control by lorry driver	loading under surveillance
Sulphur	< 50 ppm	< 500 ppm
Storage control	occasional tank control and water detachment, as habitual in branch and market	daily control, regular tank maintenance and water detachment

❷ Comparison of selected properties of Avgas and Mogas

Since a sudden engine stop is much more critical, not to say life-threatening, to an aircraft compared to a vehicle, dedicated aircraft fuels underly a very strict production surveillance concerning the specification of their composition, their technical properties, and the distribution chain including the warehousing on the airfield and the storaging in the individual aircraft tank.

❷ compares the most important properties of Avgas and Mogas. Remarkable and important with respect to potential effects of ethanol admixtures is the difference in vapour pressures, even though the given numbers are not appropriate to describe the differing shapes of the boiling curves of the multicomponent substance "fuel".

While Avgas is distributed with identical physical properties over the course of the year, vehicle gasolines fluctuate seasonally, especially with respect to the vapour pressure.

HAZARD POTENTIALS

From the remarkably higher vapour pressure the first hazard potential can be immediately derived for ethanol-admixed fuels even though it may be the least comprehensible one to most of the pilots. Admixtures of rather small amounts of ethanol to conventional fossil fuel increase the vapour pressure of the mixture remarkably [1]. This is caused by a changed environment of the individual ethanol molecules compared to the pure bulk substance: The individual molecules are lacking hydrogen bonding partners if they are immersed in non-polar, hydrophobic base fuels in small percentages. This effect is a non-linear one, though: With an increasing ethanol admixture the vapour pressure of a fossil fuel with unchanged base composition steeply rises until a share of 2 to 3 % is reached. Surpassing this value the vapour pressure decreases slowly and drops, at high ethanol content values above 40 %, even below that of the base fuel.

❸ Test rig for examination of the influence of dynamic vapour pressure drop on vapour bubble generation

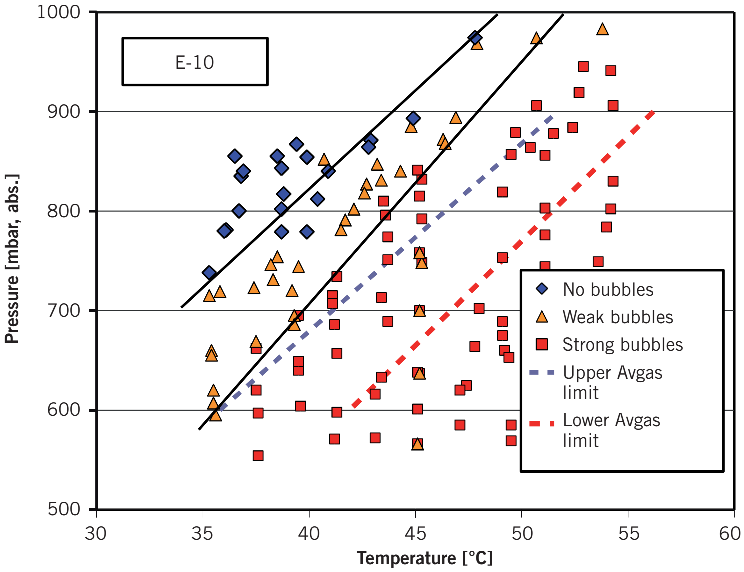

❹ Occurrence of vapour bubbles in an E10 mixture compared to Avgas

❺ Test-rigged Rotax 912 ULS engine

Taken separately, any marketed gasoline brand will comply to the DIN EN 228 norm, regardless of its individual ethanol share. The selection of an appropriate fossil fuel basestock will take care of that. The situation becomes problematic, though, if different brands of gasoline with differing ethanol shares are mixed, e.g. by refilling an aircraft tank with a significant amount of residual fuel. Here the vapour pressure of the emerging mixture may rise by several percents compared to the values for the individual original brands. In conjunction with the inherently higher vapour pressures of vehicle gasolines this may lead to increased vapour bubble generation in the hot vicinity of an aircraft's engine. This effect was scrutinized in the sense of a worst case simulation in a custom test rig, ❸, simulating the components of an aircraft fuel system. Ethanol was admixed to conventional fossil fuel in varying amounts. The nascence of vapour bubbles induced by increased temperatures and at the same time lowered ambient pressures was detected optically. ❹ depicts the occurrence of vapour bubbles in an E10 mixture compared to Avgas. Two boundary lines derived from the readout of an optical bubble detector define a range of increasing bubble intensities in which the pilot is likely to notice first glitches up to severe impairments of the engine operation. These lines are rendered as solid lines in the diagram. For comparison the same limiting lines observed in Avgas are drawn dashed into the same diagram. They show that in Mogas a bubble nascence of comparable intensity is observed by markedly lower temperatures and higher ambient pressures compared to Avgas.

Especially after a longer descent phase with reduced propeller speed and during re-entry into warmer, lower atmospheric strata the fuel system adjacent to hot engine parts may heat up significantly. Respective experiments have been performed with FH Aachen's laboratory plane, yielding temperatures partially even above 60 °C. The occurrence of vapour bubbles is to be expected under these conditions, would the aircraft have been flown on Mogas. At the end of the descent during the landing phase the availability of the full engine power is mandatory as a touch-and-go may be necessary in a critical situation. Should the vapour bubble production have been to strong this may not be the case, and the engine may even starve at the attempt of a stronger acceleration. This effect is called "vapour locking" since the formed bubbles may cut the delivery of liquid fuel to the carburettor.

Caused by the significantly increased enthalpy of evaporation an exactly contrary effect may be experienced as well: Practically all Otto fuel consuming aircraft engines are still equipped with carburettors. The heat required for the at least partial evaporation of the fuel must be drawn from a cooling of the created fuel/air mixture. If condensable humidity is present in the carburettor this may lead to a deposition of ice in the delicate fluid-dynamically optimized geometries and may severely deteriorate their properties. Since this effect is depending non-linearly on several factors (water content of the air and the fuel, temperature of the air, parasitical heat coupling to the engine, etc.) the occurrence of the so called carburettor icing is near to impossible to predict on a theoretical basis. Experiments on an ethanol-caused temperature drawdown have been performed both with a test-rigged Rotax 912 ULS engine, ❺, and FH Aachen's grounded experimental aircraft Morane, equipped with a Lycoming O 360 A1A engine. In order to monitor the temperature drop as a function of ethanol share the engines were operated on respective differently admixed fuels. The resultant fuel/air mixture temperature was measured in the intake manifold after the carburettor. Depending on the actual fuel/air ratio that must be set manually to a value appropriate for the given flight condition in many small aircraft, additional temperature decreases of up to 4 °C were observed, ❻, compared to an operation on standard fossil fuel.

Ethanol containing fuels exhibit the principally pleasant property of binding water. With increasing ethanol share the so-called water bearing capability increases as well. It correlates positively to the temperature of the liquid. This creates a problem in the case of avionic usage, though: The low ambient temperatures in greater heights

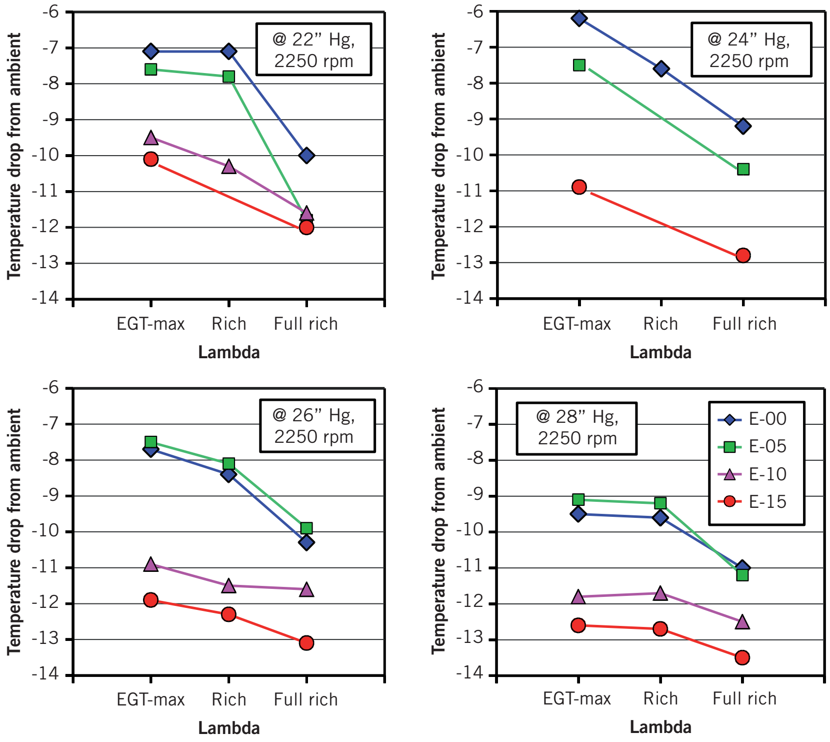

❻ Temperature decreases in the intake manifold for varying load states (given as absolute manifold pressures in inch mercury column) for a Lycoming O 360 A1A engine; „EGT-max" = maximum of exhaust gas temperature

and the usually high fuselage flow cause a significant temperature decrease in the aircraft's tanks that are usually also exposed to a strong venting. Temperature development experiments performed on the hull and the interior of a rather well covered aircraft tank showed decreases of some 20 °C relative to ground conditions. As long as the fuel contains only low amounts of water this drop does not cause any harm. If larger amounts of water have been absorbed by the fuel, for example by leaking filler caps, logistic errors, absorption of ambient humidity etc., they may not show up while on the ground if their abundancy does not suffice to form a second phase that the pilot is usually looking for before a flight. Due to the positive correlation of the water bearing with temperature such a second phase may form spontaneously during a flight when the fuel cools out, ❼, splitting the once homogeneous fuel into two phases vertically segregated by gravity: The upper phase contains mostly fuel components but exhibits a slightly deteriorated knocking property. The lower phase consists almost completely of ethanol and water. Since the

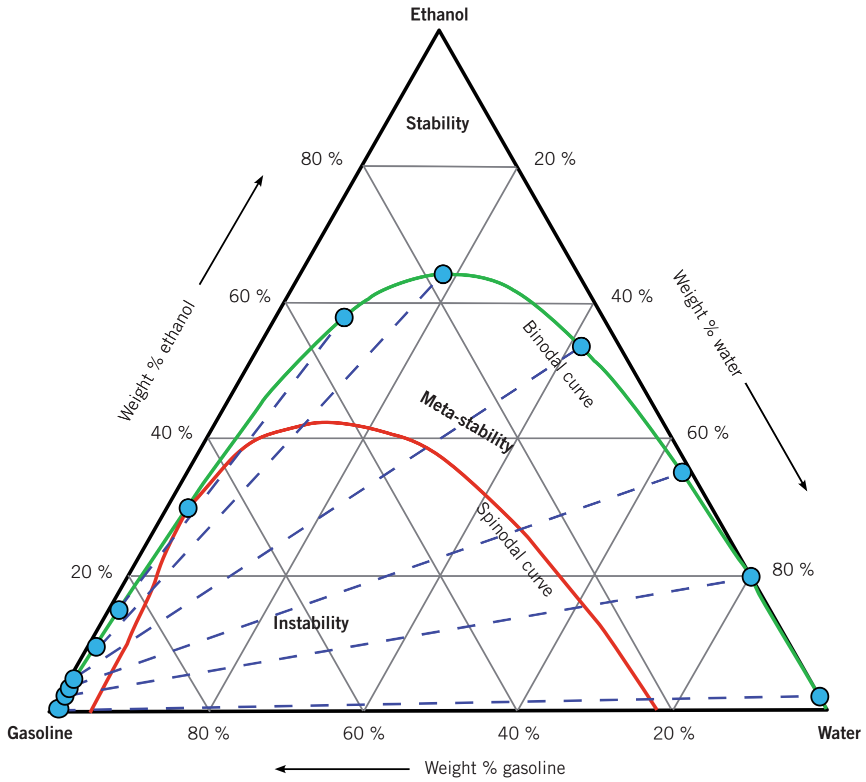

❼ Ternary diagram of fossil fuel/ethanol/water mixture with qualitative decomposition boundary; normal fuel compositions at lower left diagram edge depending on ethanol content; instabilities by water input lead to unmixing into two phases along dashed lines outlet of most aircraft tanks is situated at the bottom unburnable "fuel" is sucked into the fuel system and causes a starvation of the engine. The particular danger of this effect is based on the fact that a pilot cannot detect the looming malfunction in advance, as there is no identifiable second phase at the time of take-off and no practical device is at hand for detecting solved water in the fuel. Respective measurement devices are currently in development but not yet available as of today.

Apart from some material incompatibilities in older vehicles the new ethanol containing gasoline mix imposes only minor nuisances for the ground traffic. The average age of the German vehicle fleet is some eight years. With about 20 years in average the European air fleet is of distinctly higher age. Accordingly, many materials of aircraft fuel systems exhibit a constructive age of more than 30 years and are not ready for ethanol admixtures. They are prone to a variety of failures: Brittling and swelling, both leading to a stability loss may occur; detached flakes of old depositions resolved by the ethanol may clog filters or narrow flow cross-sections.

In the material compatibility researches the area of elastomers surfaced as the most problematic one. In many aircraft NBR based "rubber" variants are put to work that do not withstand ethanol at higher temperatures, as they are encountered in the proximity of the engine. There exist perfluoro rubbers that present viable alternatives. But due to economic reasons – the base material is about a hundredfold more expensive – no respective replacements or exchange parts have been produced and certified for avionic usage so far. Although the relatively small amounts of needed material would increase the price just by some to some ten Euros there has been no reason for the manufacturers to develop them.

SUMMARY

Air traffic would in general also be possible with ethanol admixed fuels. This includes older aircraft types as well if they are refurbished carefully and in compliance with a larger number of modifications to counteract potential hazards. Even in that case they should switch the used fuel for good and should not been flown with changing mixes of differently composed fuel brands. The hazards to be taken care of strongly depend on the individual aircraft model, its construction and its usage history, though. Another essential aspect is the necessity of a very thorough, regular maintenance of all fuel exposed components as potential deficiencies can create much greater adverse effects in the presence of ethanol containing fuels in comparison to former, purely fossil fuels. The full report of the study is available for free public electronic download on the EASA website [2].

REFERENCES

[1] Ludzay, J.; Terschek, R.: DGMK-Forschungsbericht 645, S. 19f. Deutsche Wissenschaftliche Gesellschaft für Erdöl, Erdgas und Kohle, 2005
[2] http://easa.europa.eu/safety-and-research/research-projects/miscellaneous.php

PEER REVIEW ATZ | MTZ

PEER REVIEW PROCESS FOR RESEARCH ARTICLES IN ATZ AND MTZ

Scientific articles of universities in ATZ Automobiltechnische Zeitschrift and MTZ Motortechnische Zeitschrift are subject to a proofing method, the so-called peer review process. Articles accepted by the editors are reviewed by experts from research and industry before publication. For the reader, the peer review process further enhances the quality of the magazines' content on a national and international level. For authors in the institutes, it provides a scientifically recognised publication platform.

In the ATZ | MTZ Peer Review Process, once the editors has received an article, it is reviewed by two experts from the Advisory Board. If these experts do not reach a unanimous agreement, a member of the Steering Committee acts as an arbitrator. Following the experts' recommended corrections and subsequent editing by the author, the article is accepted.

In 2008, the peer review process utilized by ATZ and MTZ was presented by the WKM (Wissenschaftliche Gesellschaft für Kraftfahrzeug- und Motorentechnik e. V. / German Professional Association for Automotive and Motor Engineering) to the DFG (Deutsche Forschungsgemeinschaft / German Research Foundation) for official recognition.

THE SEAL OF APPROVAL FOR SCIENTIFIC ARTICLES IN MTZ.
MTZ
PEER REVIEW
REVIEWED BY EXPERTS FROM RESEARCH AND INDUSTRY.

IMPRINT

MTZ WORLDWIDE

www.MTZonline.com

Founded 1939 by Prof. Dr.-Ing. E. h. Heinrich Buschmann and Dr.-Ing. E. h. Prosper L'Orange

Organ of the Fachverband Motoren und Systeme im VDMA, Verband Deutscher Maschinen- und Anlagenbau e.V., Frankfurt/Main, for the areas combustion engines and gas turbines
Organ of the Forschungsvereinigung Verbrennungskraftmaschinen e.V. (FVV)
Organ of the Wissenschaftliche Gesellschaft für Kraftfahrzeug- und Motorentechnik e.V. (WKM)
Organ of the Österreichischer Verein für Kraftfahrzeugtechnik (ÖVK)
Cooperation with the STG, Schiffbautechnische Gesellschaft e.V., Hamburg, in the area of ship drives by combustion engine

01 I 2011 _ January 2011 _ Volume 72
Springer Automotive Media I Springer Fachmedien Wiesbaden GmbH
P. O. Box 15 46 · 65173 Wiesbaden · Germany I Abraham-Lincoln-Straße 46 · 65189 Wiesbaden · Germany
Amtsgericht Wiesbaden, HRB 9754, USt-IdNr. DE811148419

Managing Directors Dr. Ralf Birkelbach (Chairman), Armin Gross, Albrecht Schirmacher I **Senior Advertising** Armin Gross I **Senior Marketing** Rolf-Günther Hobbeling
Senior Production Christian Staral I **Sales Director** Gabriel Göttlinger

EDITOR-IN-CHARGE
Wolfgang Siebenpfeiffer#

EDITORIAL STAFF

EDITOR-IN-CHIEF
Johannes Winterhagen (win)
phone +49 611 7878-342 · fax +49 611 7878-462
johannes.winterhagen@springer.com

VICE-EDITOR-IN-CHIEF
Ruben Danisch (rd)
phone +49 611 7878-393 · fax +49 611 7878-462
ruben.danisch@springer.com

CHIEF-ON-DUTY
Kirsten Beckmann M. A. (kb)
phone +49 611 7878-343 · fax +49 611 7878-462
kirsten.beckmann@springer.com

SECTIONS
Electrics, Electronics
Markus Schöttle (scho)
phone +49 611 7878-257 · fax +49 611 7878-462
markus.schoettle@springer.com
Engine
Ruben Danisch (rd)
phone +49 611 7878-393 · fax +49 611 7878-462
ruben.danisch@springer.com
Online
Katrin Pudenz M. A. (pu)
phone +49 6172 301-288 · fax +49 6172 301-299
redaktion@kpz-publishing.com
Production, Materials
Stefan Schlott (hlo)
phone +49 8191 70845 · fax +49 8191 66002
Redaktion_Schlott@gmx.net
Research
Dipl.-Ing. (FH) Moritz-York von Hohenthal (mvh)
phone +49 611 7878-278 · fax +49 611 7878-462
moritz.von.hohenthal@springer.com
Service, Event Calendar
Martina Schraad (mas)
phone +49 611 7878-276 · fax +49 611 7878-462
martina.schraad@springer.com
Transmission
Dipl.-Ing. Michael Reichenbach (rei)
phone +49 611 7878-341 · fax +49 611 7878-462
michael.reichenbach@springer.com

PERMANENT CONTRIBUTORS
Richard Backhaus (rb),
Dipl.-Reg.-Wiss. Caroline Behle (beh),
Prof. Dr.-Ing. Stefan Breuer (sb),
Jürgen Grandel (gl), Ulrich Knorra (kno),
Prof. Dr.-Ing. Fred Schäfer (fs),
Roland Schedel (rs)

ENGLISH LANGUAGE CONSULTANT
Paul Willin (pw)

ADDRESS
P. O. Box 15 46, 65173 Wiesbaden, Germany
redaktion@ATZonline.de

MARKETING I OFFPRINTS

PRODUCT MANAGEMENT AUTOMOTIVE MEDIA
Sabrina Brokopp
phone +49 611 7878-192 · fax +49 611 7878-407
sabrina.brokopp@springer.com

OFFPRINTS
Martin Leopold
phone +49 2642 9075-96 · fax +49 2642 9075-97
leopold@medien-kontor.de

ADVERTISING

HEAD OF SALES MANAGEMENT
Britta Dolch
phone +49 611 7878-323 · fax +49 611 7878-140
britta.dolch@best-ad-media.de

KEY ACCOUNT MANAGEMENT
Elisabeth Maßfeller
phone +49 611 7878-399 · fax +49 611 7878-140
elisabeth.massfeller@best-ad-media.de

SALES MANAGEMENT
Sabine Röck
phone +49 611 7878-269 · fax +49 611 7878-140
sabine.roeck@best-ad-media.de

MEDIA SALES
Frank Nagel
phone +49 611 7878-395 · fax +49 611 7878-140
frank.nagel@best-ad-media.de

DISPLAY AD MANAGER
Petra Steffen-Munsberg
tel +49 611 7878-164 · fax +49 611 7878-443
petra.steffen-munsberg@best-ad-media.de

AD PRICES
Price List No. 54 (10/2010)

PRODUCTION I LAYOUT
Heiko Köllner
phone +49 611 7878-177 · fax +49 611 7878-464
heiko.koellner@springer.com

SUBSCRIPTIONS
VVA-Zeitschriftenservice, Abt. D6 F6, MTZworldwide
P. O. Box 77 77, 33310 Gütersloh, Germany
Renate Vies
phone +49 5241 80-1692 · fax +49 5241 80-9620
SpringerAutomotive@abo-service.info

YOUR HOTLINE TO MTZ
Editorial Staff
☎ +49 611 7878-393
Reader's Service
☎ +49 611 7878-151
Advertising
☎ +49 611 7878-395

SUBSCRIPTION CONDITIONS
The eMagazine appears 11 times a year at an annual subscription rate 199 Euro for private persons and 299 Euro for companies. Special rate for students on proof of status in the form of current registration certificate 98 €. Special rate for VDI/ÖVK/VKS members on proof of status in the form of current member certificate 172 €. Special rate for studying VDI members on proof of status in the form of current registration and member certificate 71 €. Annual subscription rate for combination MTZworldwide (eMagazine) and MTZ (print) 398 €. The subscription can be cancelled in written form at any time with effect from the next available issue.

HINTS FOR AUTHORS
All manuscripts should be sent directly to the editors. By submitting photographs and drawings the sender releases the publishers from claims by third parties. Only works not yet published in Germany or abroad can generally be accepted for publication. The manuscripts must not be offered for publication to other journals simultaneously. In accepting the manuscript the publisher acquires the right to produce royalty-free offprints. The journal and all articles and figures are protected by copyright. Any utilisation beyond the strict limits of the copyright law without permission of the publisher is illegal. This applies particularly to duplications, translations, microfilming and storage and processing in electronic systems.

Springer Automotive Media is a brand of Springer Fachmedien. Springer Fachmedien is part of the specialist publishing group Springer Science+Business Media.

AUTHORS

DIPL.-ING. MATTHIAS BUDDE
is Research Assistant at the Institute for Combustion Engines at RWTH Aachen University (Germany).

DIPL.-ING. SVEN BRANDT
is Research Assistant at the Institute for Machine Elements and Tribology at University of Kassel (Germany).

DR.-ING. SVEN KRAUSE
is Research Assistant at the Institute of Measurement Technology at the Hamburg University of Technology (Germany).

DR.-ING. MARCUS GOHL
is Head of the Research and Engineering Team at APL Automobil-Prüftechnik Landau GmbH (Germany).

INFLUENCE OF THE MIXTURE FORMATION ON THE LUBRICATING OIL EMISSIONS OF COMBUSTION ENGINES

Due to diminishing resources, reduced design periods and cycles of life, the knowledge about mechanisms leading to oil emissions plays a major role in today's combustion engine design. During the FVV research project No. 933 "Lubricating Oil Emissions and Mixture Formation" the influence of mixture formation on the fuel wall film formation and the oil emissions of a single-cylinder research engine have been investigated. The research was performed at the Institute for Combustion Engines (VKA) at RWTH Aachen University, at the Institute of Measurement Technology at Technical University Hamburg-Harburg (TUHH) and at the Institute for Machine Elements and Tribology IMK at University of Kassel.

THE SEAL OF APPROVAL FOR SCIENTIFIC ARTICLES IN MTZ.
MTZ
PEER REVIEW
RECEIVED 2010-08-16
REVIEWED 2010-09-30
ACCEPTED 2010-11-02
REVIEWED BY EXPERTS FROM RESEARCH AND INDUSTRY.

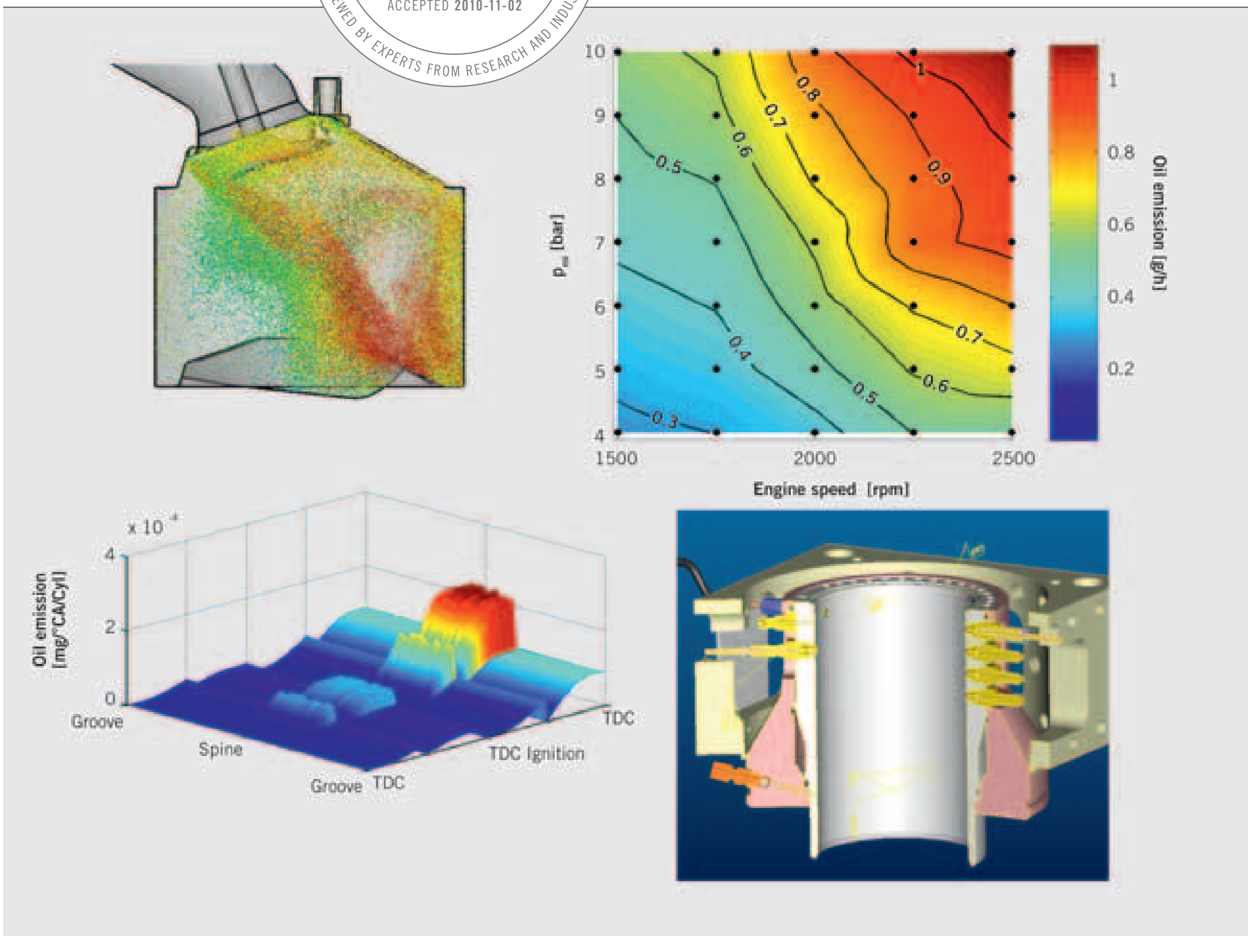

1 INTRODUCTION

The purpose of the research project is to investigate the influence of the mixture formation on the oil emissions and thus on the oil balance of SI engines [1]. The cylinder liner wall film is of great importance for the analysis of such correlations and therefore its composition is analyzed in detail. ❶ shows the mechanisms such as parameters of injection and charge motion that have an impact on the oil emissions of direct injection SI engines by influencing the mixture formation and the fuel entrainment into the wall film.

A measurement technique on the basis of laser-induced-fluorescence (LIF) has been used to analyze the oil and fuel wall film thickness during engine operation. The fuel content in the wall film has been analyzed using a probe sampling technique and an analysis by mass spectrometry afterwards. Iso-octane and a RON95-fuel have been used as fuels due to their characteristics of fluorescence.

The engine investigations have been accompanied by the simulation of mixture formation in the combustion chamber and the wall film formation on the cylinder liner. Using those results and the design data of the engine, the oil emissions have been calculated using the software tools KORI3D [3] and PRO [4]. By doing so, this method of simulation has been expanded to the usage for DI SI engines and the effects of mixture formation on the oil emissions.

2 EXPERIMENTAL SETUP AND PROCEDURE

For the investigation of the influence of fuel on the oil evaporation in a mixture of oil and fuel, a fundamental experiment has been conducted first. The results from this fundamental experiment are used for the calculation of oil emissions. The location of LIF probes and sampling probes have been determined by simulations of mixture formation on the basis of existing data prior to test bench initial operation. ❷ shows the positions of probes for LIF and sampling on the unwound cylinder liner wall. The focus is on the region of the injector target at 180 ° circumferential angle; here four LIF probes and two sampling probes have been placed.

In the following the work packages of measurement are presented. The investigations excluding the fundamental experiment have been conducted using a single-cylinder research engine with a compression ratio for both, direct injection (DI) and port fuel injection (PFI), of ε = 12.0, a bore of 85 mm and a stroke of 85 mm. The investigations of film thickness, oil emissions and the wall film sampling were conducted at four operating points at n = 2000 rpm and IMEP = 10 bar with changing parameters of mixture formation:

- port fuel injection (PFI), λ = 0.8, w/o tumble
- direct injection (DI), λ = 0.8, w/o tumble
- direct injection (DI), λ = 1.1, w/o tumble
- direct injection (DI), λ = 1.1, w/ tumble.

2.1 FUNDAMENTAL EXPERIMENT ON OIL EVAPORATION

The purpose of the fundamental experiment is to analyze the influence of fuel on the oil evaporation in a mixture of oil and fuel. Thereby, the incidents of oil evaporation are to be reproduced that are also supposed to happen in the cylinder liner wall film. The focus and the challenge of this experiment are to demonstrate the highly dynamic heat introduction via non-equilibria states during engine combustion

The investigation is conducted in a nitrogen-filled pressure chamber with a volume of 55 cm^3. There is a sample carrier in the chamber with a diameter of 45 mm and an oil-fuel-mixture of 5 mm thickness. The energy entrainment happens via a pulsed laser beam through a silica window. The laser is a donut-laser with a Gaussian distribution of intensity in the beam profile.

After the energy entrainment the evaporated oil-fuel-mixture is evacuated from the chamber and analyzed for oil contents by quadrupole mass spectrometry (MS) of the type "Lubrisense 1200" [5] using the "Selected Ion Monitoring" operating mode. The filter width of the mass filter is therefore set to m/z = 100. The filter centres are at M = {100; 200; 300} m/z. This results in one filter for fuel in the range of $50 < m/z_1 < 150$ and two filters for oil in the ranges of $150 < m/z_2 < 250$ and $250 < m/z_3 < 350$ for the used combination of media (Iso-octane as fuel and Texaco

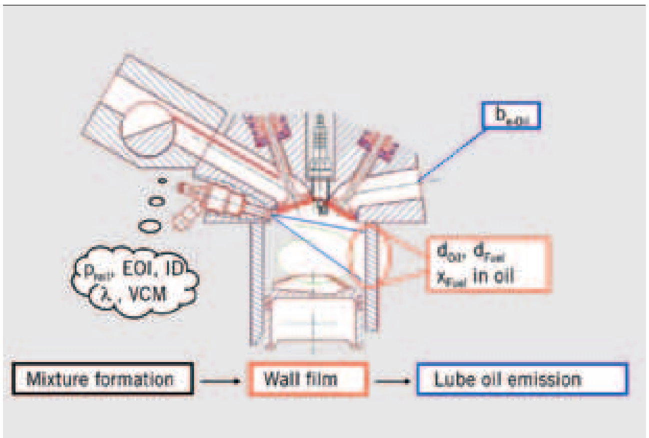

❶ Parameters of mixture formation and oil emissions

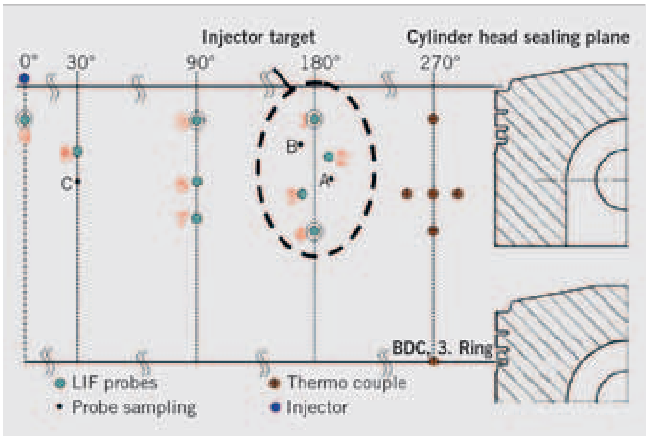

❷ Positions of LIF probes and sampling probes on the unwound cylinder liner wall

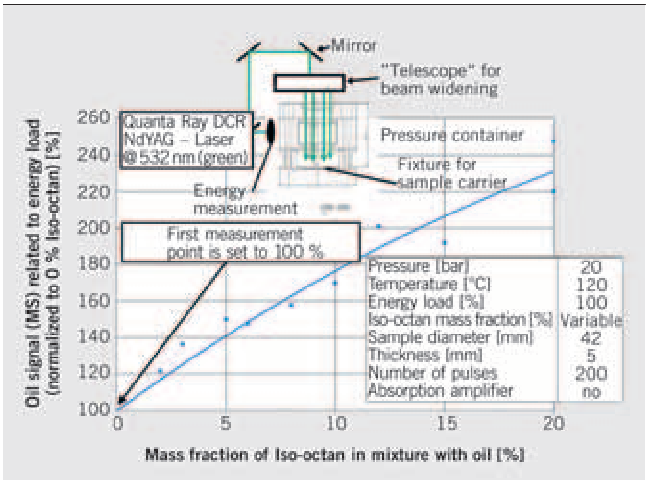

❸ Results of fundamental experiment: influence of fuel concentration on oil evaporation

MEASUREMENT STEP/ORDER	FUEL	LUBRICATING OIL
1. Engine preparation	Iso-octane (ASTM) 99,75 %	Texaco Havoline Energy 5W30
2. Measurement of fuel film thickness	RON95 + 0,1 % Lumilux	PAO (Poly-Alpha-Olefin)
3. Measurement of oil film thickness	Iso-octane (ASTM) 99,75 %	Texaco Havoline Energy 5W30 + 0,05 % Lumilux

❹ Operating media and tracer

Havoline 5W30 as lubricating oil). For this configuration a sampling rate of f = 100 Hz per filter can be realized.

❸ shows the MS oil signal calibrated to a reference value. Due to the shot-to-shot divergence the oil signals a referenced to the introduced laser energy. As reference value the measurement of a pure oil sample (0% Iso-octane content) is used. With 20% Iso-octane content in the mixture, the amount of evaporated oil is already doubled. On the other side, chamber pressure and film thickness show almost no effect on the oil evaporation. The results are used as boundary conditions and validation data for the simulation of oil emissions. This fundamental experiment already shows the significant influence of the fuel content in the wall film on the oil evaporation.

2.2 OPTICAL MEASUREMENT OF FILM THICKNESS

For the measurement of film thickness a new measurement technique on the basis of laser-induced-fluorescence (LIF) has been developed allowing for the measurement of wall film thickness at full load operation conditions.

Due to the wall film wetting by fuel, the operating media fuel and oil are present at the LIF probe at the same time. Therefore, a serial procedure for the measurement of film thickness is used. In using only one tracer for both media, all of the optical components have to be calibrated for only one wavelength. The operating media are selected so that the medium to be analyzed does fluoresce very intensely, whereas the other does not, thus avoiding interference and securing a clear distinction. ❹ shows the operating media and tracer Lumilux CD 345 chosen for each measurement step (white: no fluorescence, green: fluorescence, brown: auto fluorescence of the oil). This tracer has been used for both, fuel and lubricating oil. The spectrum of absorption is in the range of 250 to 520 nm with a maximum at 465 nm.

As an example for the signal curve of a LIF probe during film thickness measurement. ❺ shows the curve during one engine

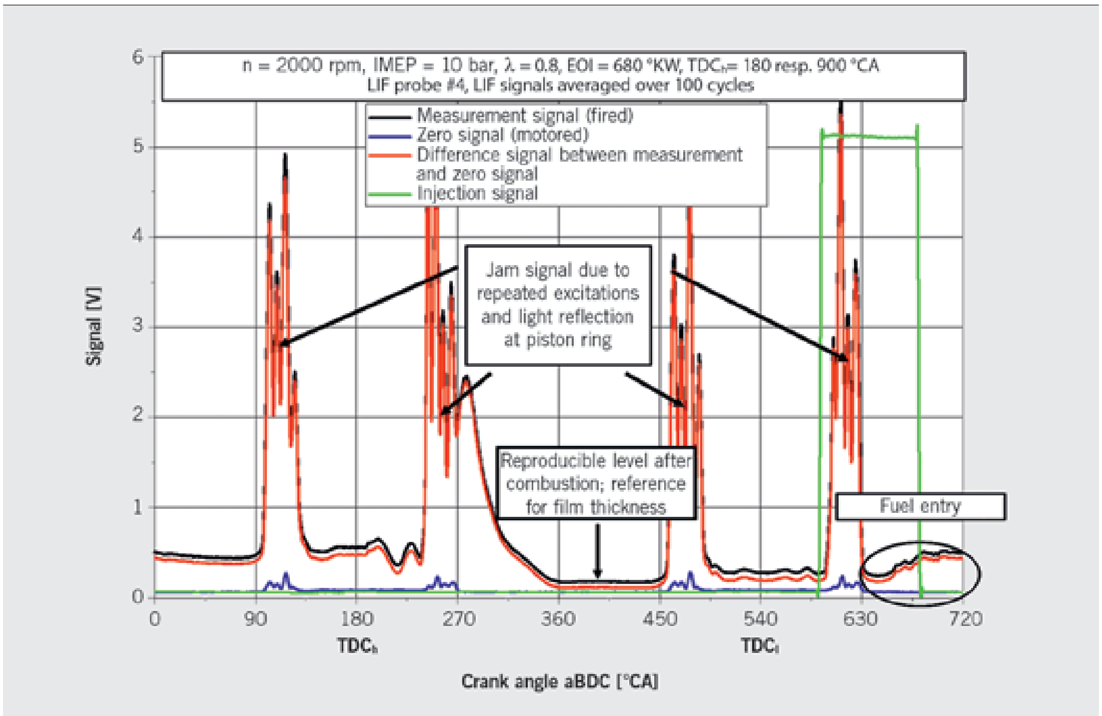

❺ Signal curve of fuel film measurement at LIF probe #4

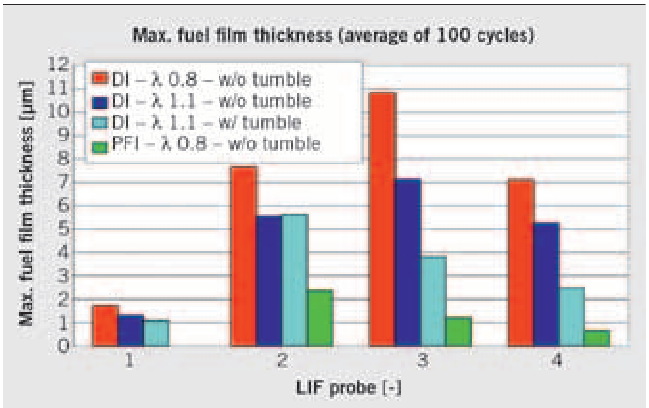

❻ Maximum fuel film thickness at LIF probes 1 to 4 (n = 2000 rpm and IMEP = 10 bar)

cycle at probe 4. The blue curve represents the signal from the motored engine without fuel injection. Due to reflexions of the piston rings while passing the probe there are small amplitudes in the signal curve. Those amplitudes are increased significantly with the presence of the tracer Lumilux during fired engine operation (red and black curve). After the combustion and destruction of the fluorescence characteristics, a reproducible reference level is reached between 360 and 450 °CA. After the beginning of the injection a significant ascent can be seen in the measurement signal after 630 °CA. The film thickness can be determined as the difference to the reference level.

❻ shows a comparison of max. values of fuel film thickness at LIF-Probes 1 to 4 in the injector target area (for exact probe positions see ②). Max. values of fuel film thickness are below 1 µm for all other probes beyond the injector target area. Therefore it can be concluded that the influence of fuel entrainment into the wall film is limited to this region. For DI operating points the fuel entrainment decreases by 30 % with a leaner mixture from $\lambda = 0.8$ to $\lambda = 1.1$ and shrinks to half of the original value with increased charge motion. The port fuel injection (PFI) shows a significantly lower level of fuel entrainment into the wall film. The oil film thickness was measured with 1.5 to 2.5 µm at half stroke.

2.3 WALL FILM SAMPLING

The concentration of fuel in the wall film on the cylinder liner wall is determined by mass spectrometry (MS) in a quasi-online procedure. A small amount of the oil is sucked in from the liner film on a capillary, evaporated and directed to the mass spectrometer for analysis. The time-accurate allocation of the probe sampling is achieved by a fast-acting dose valve that connects the capillary to a pressure controlled vacuum. The crank angle for dose valve opening is set to $\varphi = 670$ °CA to $\varphi = 690$ °CA during engine operations. With this configuration the highest fuel concentrations have been measured. The discrete packages of liquid taken from the wall film are separated by gas pads within the sample capillary. The single volumes of oil in the capillary can be optically determined. A significant accumulation around the average of $V_{Sample} \approx 0.25$ nl can be observed.

The wall film probe sampling has been used during engine test bench run. Main focus of interest was the fuel content in the oil film in dependence of the mixture formation parameters. Three sampling probes have been placed at different positions at the cylinder liner wall (see ②). The comparison of fuel content at those sampling positions can be seen in ❼.

The same trend as with the optical measurement of film thickness is visible: The fuel content in the wall film reaches highest values in the injector target region and decreases with a leaner mixture and increasing charge motion.

2.4 MEASUREMENT OF OIL EMISSIONS

The measurement of oil emissions uses the quadrupole mass spectrometer "Lubrisense 1200" [9]. The advantage of the used measurement system is the high power of detection on the one hand and on the other hand the direct detection of evaporated oil molecules. This is of great importance for the validation as the usage of tracer methods poses a risk of failure. The system dynamics allow for measurements in high speed ranges with resolution of single cycles.

❽ shows a schematic diagram of the system's setup for the detection of lubricating oil emissions behind the exhaust valve. Gas is taken from the exhaust manifold through a heated intake system with pressure stages and transferred to a fore vacuum. From there a defined, constant part of the gas reaches the ion source and the molecules are ionized. Through lenses and a hexapole the molecules are transported into the high vacuum area. Only ions with a mass-to-load-ratio indicating oil are led to the

FUEL MASS CONCENTRATION AT POSITION	DI $\lambda = 0.8$ W/O TUMBLE	DI $\lambda = 1.1$ W/O TUMBLE	DI $\lambda = 1.1$ W/ TUMBLE	PFI $\lambda = 0.8$ W/O TUMBLE
A	66.9 %	38.6 %	17.3 %	1.2 %
B	26.9 %	1.9 %	1.8 %	2.7 %
C	0.6 %	0.7 %	0.9 %	1 %

❼ Results of probe sampling (n = 2000 rpm and IMEP = 10 bar)

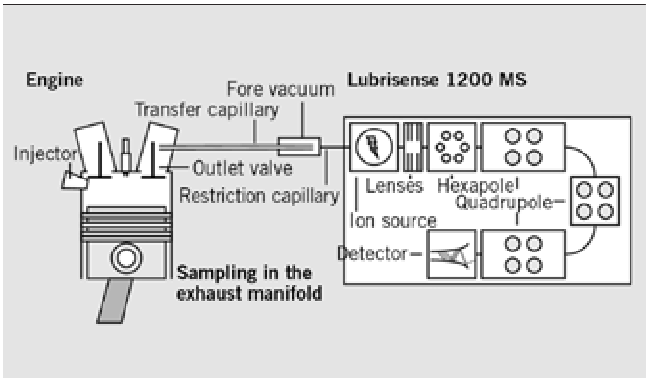

❽ Schematic diagram of the test set-up for determining the oil emission behind the exhaust valve

detector by a quadrupole mass filter with special filter characteristics. Therefore, the mass filter is run in "Selected Ion Monitoring" mode (SIM) in combination with a highpass filter method (HPM). Lubricating oil molecules are clearly visible in the detected spectrum as they are in low concentration in the exhaust gas and have higher numbers of carbon atoms as gasoline fuel.

The results of the measurement of oil emissions are compared to the results of the simulation of oil emissions in the following chapter.

3 SIMULATION OF MIXTURE FORMATION AND OIL EMISSIONS

The simulations consist of CFD injection simulations for the determination of fuel entrainment into the wall film and simulations of oil emissions. Furthermore, injection simulations on the basis of existing data are used to determine the location of probes for LIF and sampling in the injector target region.

The cylinder geometry of the research engine has been meshed as moving mesh using the software ES-ICE v2.02.054 in order to simulate the mixture formation and the fuel wall film formation. Measured pressure and temperature date from test bench runs for film thickness measurements have been used as boundary conditions. The simulation of in-cylinder charge motion and mixture formation is performed using the software STAR-CD v3.26. The injection is simulated with a primary break-up model for a swirl injector according to Han [6]. The wall film formation of droplets interacting with the liner wall is modelled by the STAR-CD built-in model of Bai [7] for the droplet-wall interaction in CI and SI engines. ❾ shows the integrated fuel film masses for one cycle of the DI operating points on the unwound cylinder liner wall and the position of the LIF probes as black crosses. The distribution of the wall film is obviously dependant on the operating point. The results agree with the LIF results in terms of spatial distribution and temporally sequence from start of injection to start of wall film formation at the probes' positions. The differences in absolute values of film thickness result from the evaporation behaviour of the tracer used in the LIF measurements.

The simulation of oil emissions uses the mixture viscosities of fuel and lubricating oil in the wall film as boundary conditions. Those viscosities are calculated according to an approach by Teja and Rice [8] on the basis of the oil film heights from the simulation of piston ring movement (KORI3D) and the fuel wall film thickness from the simulation of mixture formation.

The simulation of oil emissions with PRO uses both, mixture viscosities and the fuel mass content in the oil wall film. Furthermore, in the case of local fuel entrainment into the wall film oil evaporation considers the dependence of fuel content as demonstrated in the fundamental experiment. Besides the fuel entrainment into the wall film straight from injection, the measurements

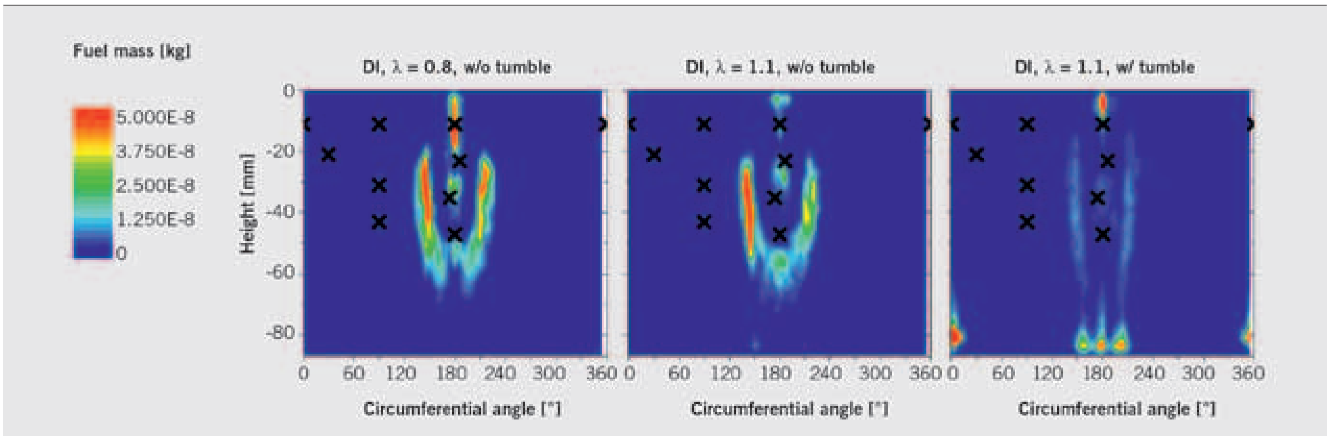

❾ Integrated fuel wall film masses of the simulated operating points on the unwound cylinder liner wall (n = 2000 rpm and IMEP = 10 bar)

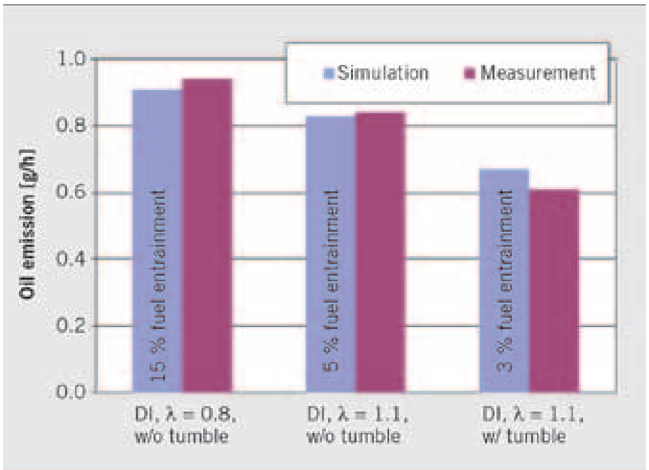

⓾ Results of oil emission measurement and simulation (n = 2000 rpm and IMEP = 10 bar)

at the probes in the injector target area indicated a non-complete evaporation of fuel. For consideration of this effect a constant fuel entrainment in the injector target area (+/- 40 ° around ring spine) over the complete height of the cylinder liner is assumed in the simulation. The amount of fuel entrainment bases on measured data and depends on the operating point.

The simulation and the measurement of oil emissions are in good agreement with the consideration of an operating-point-dependant constant fuel entrainment in the injector target area. ⓾ shows a comparison of measured and simulated oil emissions of the DI operating points.

4 SUMMARY

During this research project the influence of the mixture formation on the oil emission has been proven as it occurred with the change from port fuel injection to direct injection with lateral injector position in modern SI engines. The fundamental experiment proved higher oil evaporation with higher fuel contents in the mixture. The measurements at the single-cylinder research engine showed lower fuel entrainment by leaning the mixture from λ = 0.8 to λ = 1.1 by approx. 30 %, while at the same time the oil emission decreases about 11 %. With an additional tumble charge motion the fuel entrainment decreases once more about approx. 35 % and at the same time the oil emission decreases another 27 %. Fuel concentration (fuel rich) and the flow intensity as part of the mixture formation have the strongest influence on the oil emission. These trends have been proven with the simulation method in using the results of the fundamental experiment and the information about the fuel entrainment into the wall film.

REFERENCES

[1] Pischinger, S.; Stein, C.; Budde, M.; Matz, G.; Krause, S.; Knoll, G.; Brandt, S.; Schlerege, F.: Beeinflussung der Schmierölemission durch die Gemischbildung im Brennraum von Verbrennungsmotoren. FVV-Abschlussbericht zum Vorhaben Nr. 933, 2010

[2] Stein, C.; Budde, M.; Wittler, M.; Pischinger, S.; Krause, S.; Matz, G.; Brandt, S.; Schlerege, F.; Knoll, G.; Gohl, M.; Adomeit, P.: Influence of the Mixture Formation on the Lubrication Oil Emission of Combustion Engines. SAE Paper, 2010-01-1275, 2010

[3] Knoll, G.; Lechtape-Grüter, R.: Kolbenringreibung II. FVV-Forschungsheft 570-1, 1994 und 570-2, 1995

[4] Knoll, G.; Lechtape-Grüter, R.: Ölverbrauchssimulation. FVV-Forschungsheft 707, 2001

[5] Gohl, M.; Ollesch, T.; Matz, G.: Massenspektrometrische Bestimmung der Ölemission im Abgas von Otto- und Dieselmotoren. FVV-Abschlussbericht zum Vorhaben Nr. 758, 2002

[6] Han, Z.; Fan, L.; Reitz, R. D.: Multidimensional Modeling of Spray Atomization and Air-Fuel Mixing in a Direct-Injection Spark-Ignition Engine. SAE-Paper 970884 (1997)

[7] Bai, C.; Gosman, A. D.: Development of Methodology for Spray impingement simulation. SAE-Paper 950283 (1995)

[8] Teja, A. S.; Rice, P.: The measurement an prediction of the viscosities of some binary liquid mixtures containing n-hexane. Chem. Eng.Tech., Vol. 62, 1981

[9] Knoll, G.; Schlerege, F.; Matz, G.; Krause, S.; Thiemann, W.; von Hollen, P.; Robota, A.: Ölemissionen eines Ottomotors, Verfahrensentwicklung zur Messung und Simulation. In: MTZ Motortechnische Zeitschrift 70(2009)2, S. 166-173

THANKS

This work was performed within the scope of a research project sponsored by the BMWi (through AiF under sponsoring number 15075N) in Germany and accompanied and supported by a research group of the Research Association for Internal Combustion Engines (Forschungsvereinigung Verbrennungskraftmaschinen e. V., consisting of industry representatives). The coauthors would like to express their sincere gratitude to the research group led by Dr. Ing. M. Gohl, APL Automobil-Prüftechnik Landau GmbH, for their significant support.

AUTHORS

PROF. DR.-ING. DR. H. C. HELMUT TSCHÖKE
is Head of Chair for Reciprocating Machines at the Institute for Mobile Systems of the University Magdeburg (Germany).

DIPL.-ING. MATTHIAS SCHULTALBERS
is Vice President for Gasoline Engine Systems of IAV GmbH in Gifhorn (Germany).

DR.-ING. WOLFRAM GOTTSCHALK
is Senior Technical Consultant for Gasoline Engine Systems of IAV GmbH in Gifhorn (Germany).

DIPL.-MATH. TECH. EVA-MARIA HUTHÖFER
is Research Engineer for Gasoline Engine Systems of IAV GmbH in Gifhorn (Germany).

DIPL.-ING. ANDREAS JORDAN
is Research Engineer for Gasoline Engine Systems of IAV GmbH in Gifhorn (Germany).

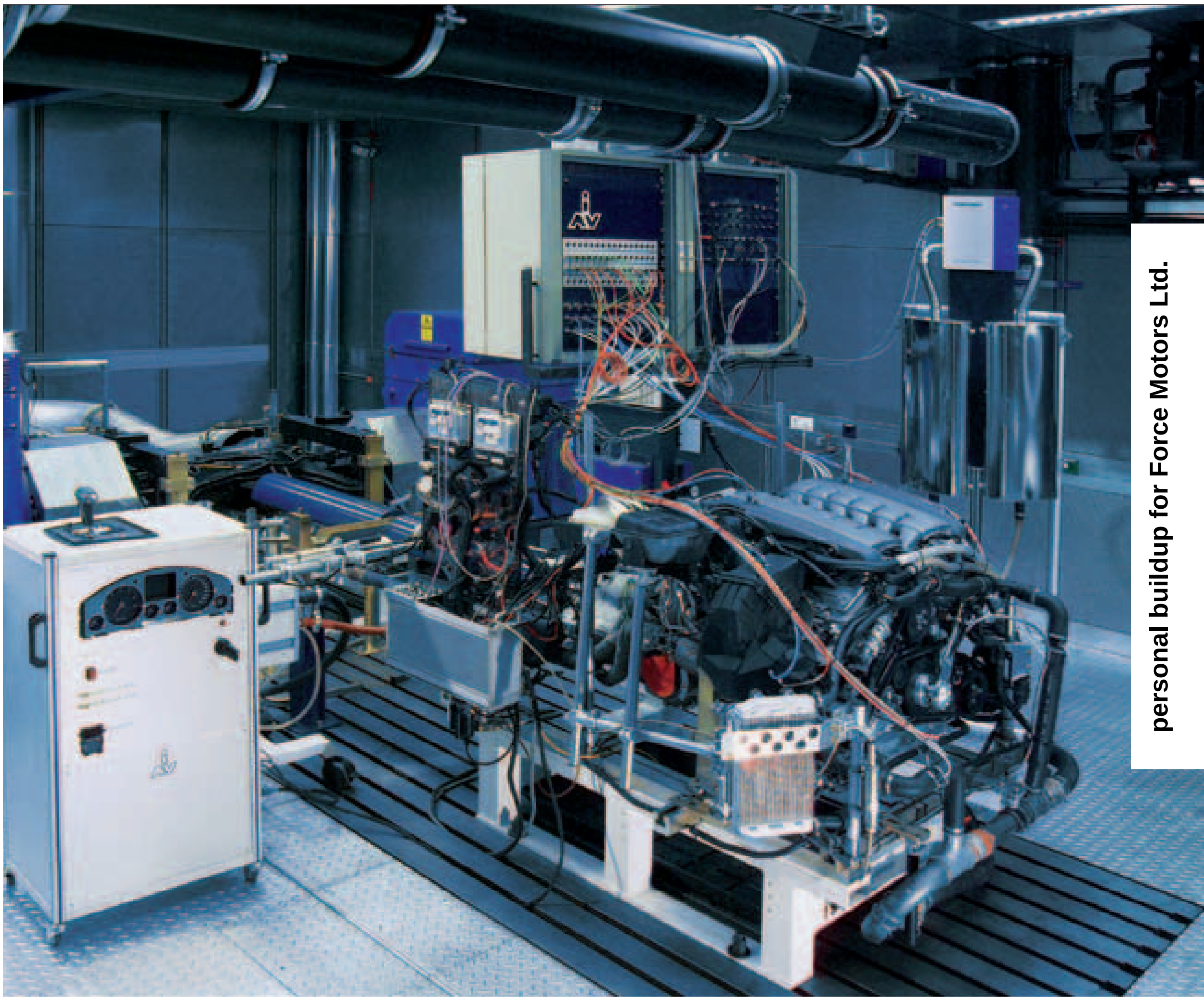

THERMODYNAMIC OPTIMIZATION CRITERIA FOR IGNITION TIMING CALIBRATION OF ADVANCED SI ENGINES

Engine developers always try to adjust the ignition timing to the most efficiency-effective value in respect to the point of operation and the boundary conditions. In cooperation of IAV (Ingenieurgesellschaft Auto und Verkehr) with the Otto-von-Guericke University Magdeburg a promising method for the simultaneous improvement of calibration quality along with a decreased test bench effort was developed.

1 MOTIVATION

The permanent aim during the development of advanced direct-injecting SI engines is the improvement of brake specific fuel consumption. This goal results in the motivation to always adjust the ignition timing to the most efficiency-effective value in respect to the point of operation and the boundary conditions. Therefore a methodically suitable procedure for test bench measurements and engine ECU calibration is necessary.

2 THERMODYNAMIC OPTIMIZATION CRITERIA FOR THE CALIBRATION OF IGNITION TIMING

There is exactly one efficiency-optimum ignition timing for each operational point of a SI engine. An efficiency loss at non-optimum ignition timing is mainly related due to the change of three basic sources of losses. These are

- the loss due to exhaust gas enthalpy
- the loss due to wall heat transfer and
- the loss due to non-ideal gross heat release.

In terms of wall heat transfer loss the integral amount of heat is not decisive, but the progress of heat flux. If the spark event occurs earlier than the optimum an intensive heat transfer to the cylinder walls takes place as a result of high peak temperatures and pressures. At retarded ignition timing the wall heat transfer is decreasing but the exhaust gas enthalpy loss is elevated. The optimum ignition timing can be finally seen as the best compromise of all losses.

Several thermodynamic optimization criteria can be applied for the calibration of the optimum ignition timing. The most popular in practice and technical publications are

- the crank angle position of specific points of net or gross heat release and
- the peak pressure crank angle position.

2.1 CENTRE OF HEAT RELEASE CRITERION

The most popular optimization criterion is the so-called centre of heat release criterion by Bargende [1] that is referring to the position of 50 % net or gross heat release. This optimization criterion was presented by a publication referring to a fully automatic optimization method for generating a spark timing map based on thermodynamic criteria [1].

The starting point was the statement based on the investigation of several production engines that the crank angle position of 50 % gross heat release is nearly α_{50} = ~8 °CA after TDC at efficiency-optimum ignition timing. Additionally it was reported that the crank angle position of 50 % net heat release can also be used because these two characteristic points differ at maximum only 1 °CA for SI engines with homogeneous charge. The major benefit by using the net heat release criterion is the real-time capability with low demands to the computation performance. Bargende pointed out that the efficiency-optimum crank angle positions of 50 % net or gross heat release is depending on engine speed, load, combustion duration and EGR rate which is deriving from a varying wall heat transfer.

2.2 PEAK PRESSURE POSITION CRITERION

The determination of the optimum ignition timing based on the peak pressure position is evaluated in different ways by technical publications. Scientific publications seldom use this optimization criterion; almost exclusively the center of heat release criterion is applied which became highly important for the ignition timing optimization of SI engines – mainly due to its advantage of fast and simple determination. The optimum peak pressure crank angle position is given by α_{pmax} = 14 .. 20 °CA after TDC [2, 3].

3 COMPARISON OF OPTIMIZATION CRITERIA

3.1 FREQUENCY DISTRIBUTION

In ❶ the frequency distribution of the optimization criteria are represented to evaluate the positions of 50 % net heat release and peak pressure at minimum fuel consumption of present SI engine concepts. The basis of this comparison is measurement data from several direct-injecting SI engine layouts for the validation of

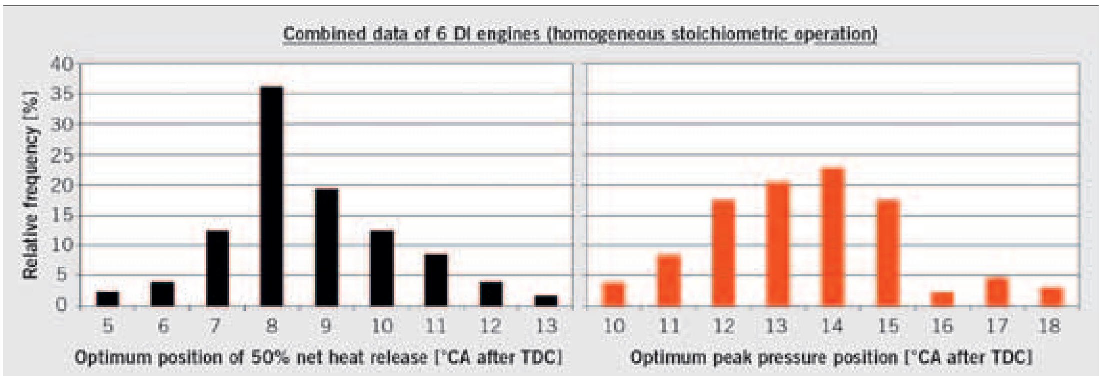

❶ Relative frequency distribution of 50 % net heat release and peak pressure positions at optimum ignition

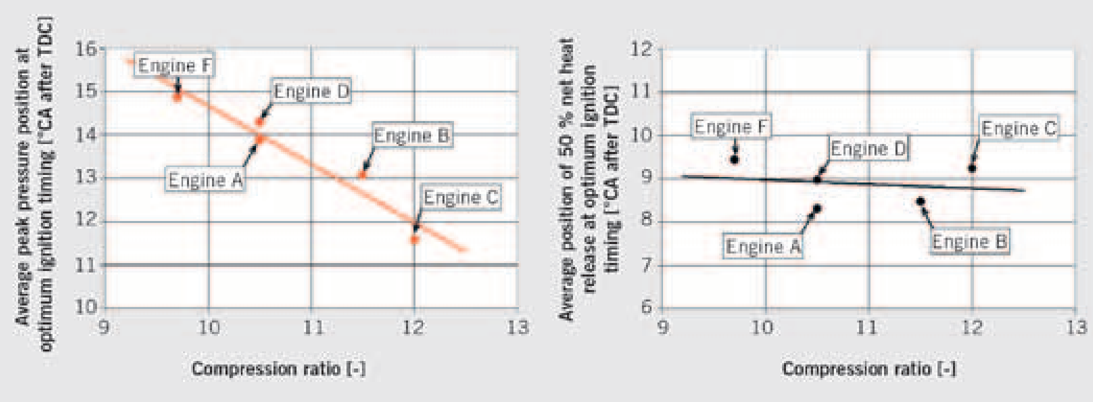

❷ Average position of 50 % net heat release and average peak pressure position at optimum ignition timing in respect to the compression ratio

engine ECU torque structure at optimum ignition timing. Certain operational points of high engine load, e. g. when the ignition timing had to be retarded to non-optimum conditions because of knocking, have not been taken into this consideration

Based on these data the average of optimum crank angle positions of 50 % net heat release for the investigated engines is α_{50} = 8,65 °CA after TDC. In ① it is shown that the crank angle position of α_{50} = 8 °CA was observed most frequently, which is preferred in technical publications. In contrast the peak pressure position is distributed less distinct. The peak pressure position α_{pmax} = 14 °CA after TDC was observed most frequently but it is not clearly separating from the other categories.

The comparison of these optimization criteria might suggest that the peak pressure position is more sensible to varying operational conditions like engine speed, load, turbulence intensity, EGR rate or geometrical dimensions of the engine like e. g. cylinder displacement, compression ratio or stroke-to-bore-ratio.

3.2 DEPENDENCY ON THE ENGINE LAYOUT BY APPLICATION OF OPTIMIZATION CRITERIA

In order to investigate the dependency on the engine layout ❷ is representing the average peak pressure position and average 50 % net heat release position for the investigated engines at optimum ignition timing in respect to the compression ratio. Again, operational points with knock limitation are not included. It can clearly be seen that the peak pressure position at optimum ignition timing is advancing with increasing compression ratios. The comparison of engines A and D is illustrating that other factors are still influencing the average peak pressure position because its values differ slightly despite their equal compression ratio.

As for the optimization criterion "50 % net heat release position" no major dependency on the compression ratio could be observed it can be evaluated to be more independent from the engine layout in contradiction to the peak pressure position.

3.3 DEPENDENCY ON THE OPERATIONAL POINT BY APPLICATION OF OPTIMIZATION CRITERIA

In order to investigate the effects of varying boundary conditions in the combustion chamber on the thermodynamic optimization criteria like e. g. EGR rate, charge motion intensity or volumetric efficiency ❸ is illustrating the trends of 50 % net heat release position and peak pressure position in respect to the engine speed and brake mean effective pressure. The isolines are determined to represent a certain histogram category of ① by the areas in between.

Both thermodynamic optimization criteria show a dependency of the crank angle position on the point of operation. Especially

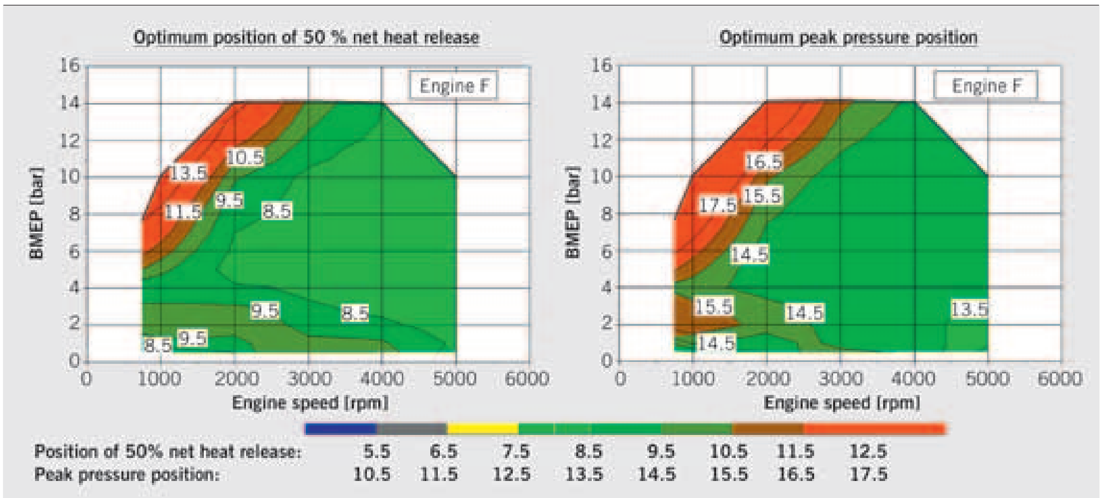

❸ Distribution of 50 % net heat release position and peak pressure position at optimum ignition the dependency on the engine speed is remarkable. The engine speed dependency is deriving from the dependency of the optimization criteria on the wall heat transfer loss as already mentioned. The share of wall heat transfer loss is decreasing with increasing speed and thus decreasing time for the heat transfer. The optimum crank angle position is advancing due to this effect. This can be observed for both the optimum crank angle position of 50 % net heat release and optimum peak pressure position.

The optimum crank angle positions for both optimization criteria show a qualitatively comparable behaviour over the entire map area for all investigated engines. Substantial differences among the engines can be observed even for low engine speeds and brake mean effective pressures. This can be linked to the fact that the individual engine characteristics like e. g. charge motion, EGR rate or cylinder surface-cylinder displacement-ratio have a significant influence on the net heat release and wall heat transfer.

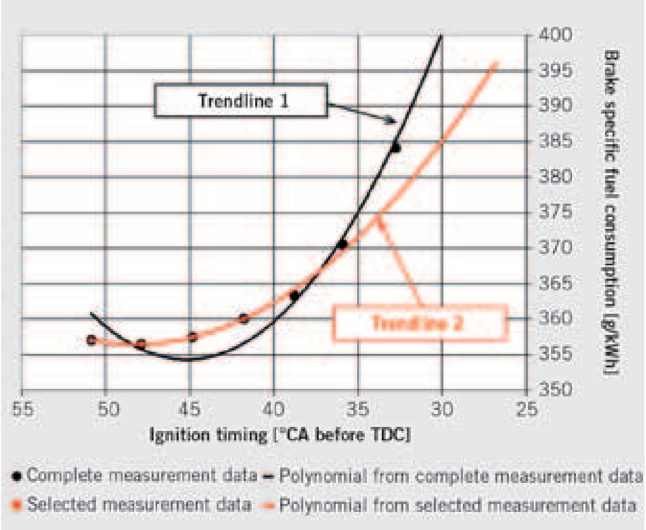

❹ Description of ignition timing sweeps by 2nd order polynomials

4 ADDITIONAL FUEL CONSUMPTION BY APPLICATION OF OPTIMIZATION CRITERIA

As mentioned above, the actual optimum positions of the thermodynamic optimization criteria differ from the crank angle positions mentioned in the technical publication in several map areas. Because of this reason, an increased fuel consumption has to be expected if α_{50} is adjusted to 8 °CA after TDC for the entire map area.

In order to be able to estimate this additional fuel consumption at non-optimum ignition timing for all investigated engines and points of operation a mathematical description of their dependency on the ignition timing is given for

- brake specific fuel consumption
- 50 % net heat release position α_{50} and
- peak pressure position α_{pmax}

Because of their simple applicability and high accuracy 2nd order polynomials are applied [4].

For a detailed explanation ❹ is representing a measured ignition timing sweep with two trend lines. The entire measurement data have been used for trend line 1 (black). Only selected data have been used for trend line 2 (red).

Trend line 1 is representing the entire data mathematically reasonably well but there are quite large differences in the area of optimum ignition timing. For this reason the data which have to be used for each ignition timing sweep have been selected in a way that the area of the optimum ignition timing is best represented by trend line 2. It has been shown that, depending on the operational point, no measurement data should be taken into account if the 50 % net heat release position is later than α_{50} = 20 °CA after TDC.

By means of these 2nd order polynomials it is possible to calculate additional virtual measurement data by interpolation. Therefore the expected additional fuel consumption can be calculated for every engine at every operational point if a constant crank angle position of an optimization criterion was applied over the entire engine map.

❺ is representing this situation for various direct-injecting SI engines. The displayed curves show the average additional fuel consumption to be expected if the ignition timing is set for the entire engine map area without knock limitation in a way that a constant crank angle position of the optimization criterion is given. Point of operation for a break mean effective pressure p_e = 0 bar have not been taken into account.

It can be seen that there is no crank angle position for an average additional break specific fuel consumption of 0 %. When strictly implementing one of the optimization criteria with a constant

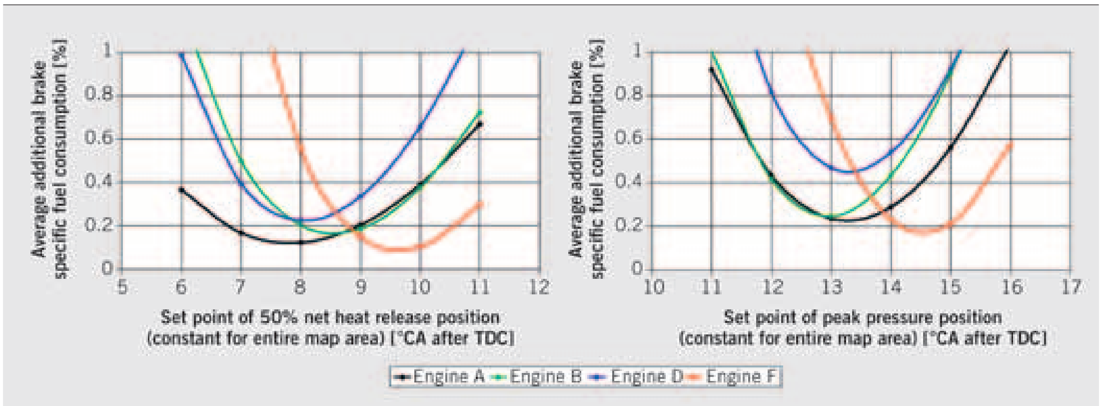

❺ Average additional break specific fuel consumption at various optimization crank angle positions

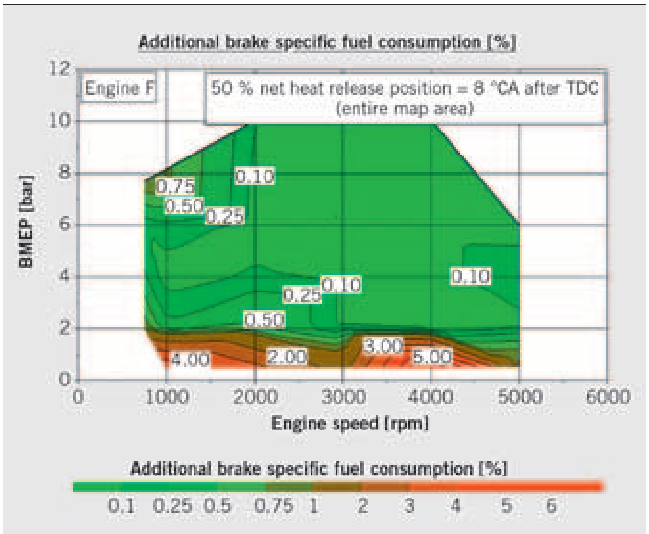

❻ Distribution of additional brake specific fuel consumption at a 50 % net heat release crank angle position of α_{50} = 8 °CA after TDC for engine F

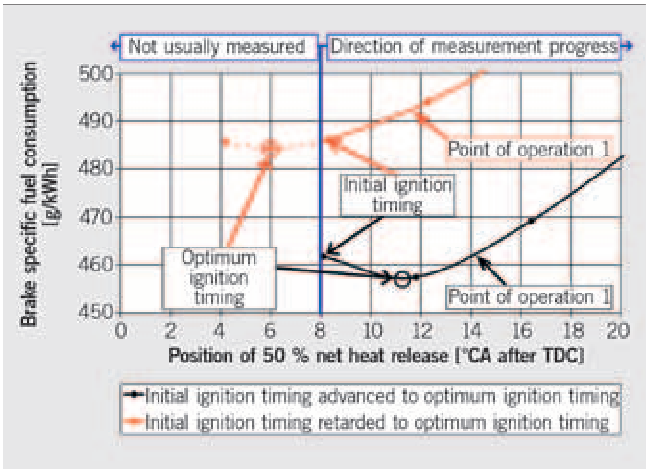

❼ Trend of brake specific fuel consumption at various optimum 50 % net heat release crank angle positions

set point over the entire engine map generally an additional fuel consumption is to be expected.

For the engines A, B and D the "50 % net heat release crank angle position" optimization criteria is a suitable compromise when aiming for α_{50} = 8 °CA after TDC suggested by the technical publications. The additional fuel consumption is around 0.2 % within the given engine map area. Remarkable additional fuel consumption was observed for engine F. Additionally a tendency to retarded crank angle positions can be found. One of the reasons is the increased wall heat transfer loss by its large cylinder surface-cylinder displacement-ratio.

❻ is representing how the calculated additional fuel consumption is distributed in the engine map for the example of engine F. A retarded ignition timing caused by engine knocking has been corrected within this calculation. It shall be demonstrated for which engine map areas the optimization criterion can be applied to determine the optimum ignition timing.

It can be observed that even at low engine speeds and low engine loads remarkable additional fuel consumption has to be expected if the optimum ignition timing is determined by the application of the center of heat release criterion. This optimization criterion can be applied without restrictions in the central map area.

5 AUTOMATED ENGINE MAP MEASUREMENT FOR THE ECU CALIBRATION

It has been demonstrated that an increased fuel consumption has to be expected if only a constant set point of 50 % net heat release or peak pressure crank angle position is utilised to define the optimum ignition timing. It can be stated that these two criteria are suitable to determine the optimum ignition timing quite accurately.

The application of the 50 % net heat release crank angle position is to be preferred if one of these two criteria has to be selected. As represented in ⑤ the 50 % net heat release crank angle position criterion is more independent from the engine layout. Only a slightly increased brake specific fuel consumption has to be expected.

Retarded ignition timing set points starting at the optimum value are measured for selected operational points to calibrate and validate the engine ECU torque structure. The partial tasks "Calibration of optimum ignition timing" and "Validation of engine ECU torque structure" can be combined to one single measurement unit to optimize the demand for resources. If the center of heat release crank angle position criterion (α_{50} = 8 °CA after TDC) is applied to determine the initial ignition timing for the ignition timing sweeps it can be expected that this selected initial ignition timing is

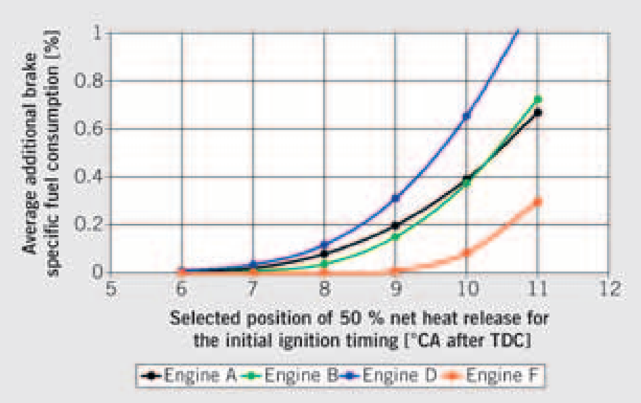

❽ Average additional brake specific fuel consumption at selected 50 % net heat release crank angle positions for initial ignition timing

differing from the actual optimum ignition timing for several operational points. The actual optimum ignition timing can be earlier or later than the selected initial ignition timing as it is represented exemplary in ❼ based on measurement data of engine F from two different operational points.

At a retarded optimum 50 % net heat release crank angle position ($\alpha_{50} > 8$ °CA after TDC) this will not cause difficulties because the area of actual optimum ignition timing will be passed. The optimum ignition timing can be calculated afterwards between two measurement points via interpolation by a polynomial.

At advanced optimum 50 % net heat release crank angle position ($\alpha_{50} > 8$ °CA after TDC) the area of actual optimum ignition timing will not be passed. An operational point is not adjusted in an efficiency-optimum way concerning the ignition timing if the initial ignition timing of the sweep is calibrated in the engine ECU.

For this reason the initial ignition timing should not be defined by the 50 % net heat release crank angle position of $\alpha_{50} = 8$ °CA after TDC but by an advanced position of this criterion.

In ❽ the relationship between the average additional brake specific fuel consumption and various 50 % net heat release crank angle positions for the definition of the initial ignition timing is presented. It can be observed that nearly no additional fuel consumption is to be expected at a selected 50 % net heat release crank angle position of $\alpha_{50} = 6$ °CA after TDC. Almost all operational points can be adjusted by its actual optimum ignition timing. It is guaranteed by the start of the ignition timing sweep at this advanced combustion that measurement points prior to the optimum ignition timing are taken into consideration and the actual optimum ignition timing will safely be determined as the peak value position of indicated efficiency.

It is possible that for operational points with high EGR rates and low combustion chamber turbulences an increased spark advance is necessary to adjust the 50 % net heat release crank angle position to $\alpha_{50} = 6$ °CA after TDC. Therefore an unacceptable engine roughness and a spark advance demand above a predefined limit should be set as an additional escape criteria.

6 SUMMARY AND FUTURE WORK

Within the scope of the described investigation a measurement and calibration methodology was developed which offers the possibility to both lower the brake specific fuel consumption of modern direct injecting gasoline engines and simultaneously reduce the required calibration and dyno time.

On the basis of experimental data gathered from six representative engines it can be shown how – based on thermodynamical optimization criteria – the determination of the optimum spark advance during specified operating conditions can be achieved using easily implementable mathematical methods. The determined reduction in brake specific fuel consumption of about 0.2 % shows the potential improvement in calibration quality. In future calibration projects the potential improvements regarding dyno time will be evaluated whereby the combination of the calibration tasks “spark advance optimization” and “validation of the torque structure” promises a clear time benefit.

REFERENCES

[1] Bargende, M.: Schwerpunkt-Kriterium und automatische Klingelerkennung. In: MTZ Motortechnische Zeitschrift 56, Nr. 10, 1995, S. 632-638
[2] Eriksson, L.: Spark Advance Modeling and Control. Linköping University, Department of Electrical Engineering, Dissertation, 1999
[3] Yoon, P.: Closed-Loop Control of Spark Advance and Air-Fuel Ratio in SI Engines Using Cylinder Pressure. SAE-Paper 2000-01-0933, 2000
[4] Röpke, K. et al.: DoE – Design of Experiments, Methoden und Anwendungen in der Motorenentwicklung. Verlag Moderne Industrie, 2005

THANKS

The authors like to thank Dipl.-Ing. Bernd Naumann, research engineer at the chair of reciprocating machines at the institute for mobile systems of the Otto-von-Guericke University Magdeburg, for his contribution and support of this publication.